9-15-2023 10:30 AM

Selective recruitment of cerebellum in cognition

Ladan Shahshahani, *Western University*

Supervisor: Diedrichsen, Jörn, *The University of Western Ontario*

A thesis submitted in partial fulfillment of the requirements for the Doctor of Philosophy degree in Neuroscience

Abstract

Previous studies of cerebellar function in humans have shown that it is activated by a myriad of tasks ranging from motor learning and language to working memory and more. These studies have prompted a deviation from the traditional view of the cerebellum as a purely motor structure. However, the precise contribution of the cerebellum to these tasks remains ambiguous.

A prevalent assumption in fMRI studies is interpreting BOLD activation as evidence of the cerebellum's involvement in specific tasks. However, this interpretation is potentially misleading, especially considering that the BOLD signal predominantly represents cerebellar input, with output activity largely absent. Consequently, observed activations in the cerebellum may merely reflect the transmission of signals via fixed anatomical connections with the neocortex, independent of any requisite cerebellar computations.

To circumvent this interpretative limitation, we present a novel framework. First, we take advantage of the diversity of tasks in a multi-domain task battery, proposing a **task-invariant model of cortico-cerebellar connectivity**. This model predicts cerebellar activation levels based on neocortical inputs. Building on this, we introduce the concept of **"selective recruitment"** to examine cerebellar-specific processes via functional MRI. Drawing insights from cerebellar patient studies, we validate this framework in the motor domain, demonstrating that the cerebellum's input is gated based on task requirements, with intensified activation at higher speeds.

Venturing into a more complex domain, we test the framework in a working memory task; A task with subtler deficits and inconclusive cerebellar patient study outcomes. We reveal that the cerebellum becomes selectively engaged during the encoding of substantial information loads, as demonstrated with six items in our task.

In sum, our approach of investigating selective cerebellar recruitment, particularly in

areas where patient studies offer limited clarity, paves the way for a more holistic comprehension of the cerebellum's nuanced roles, enriching our appreciation of this intricate "little brain."

Keywords: Cerebellum, cortico-cerebellar connectivity model, BOLD fMRI, selective recruitment, task-dependent gating

Summary for Lay Audience

Many think of the cerebellum, the so-called "little brain", as merely helping us move in a coordinated manner. But new studies suggest it is more versatile than we believed it to be, playing a role in understanding language, making decisions, social interactions, and even handling emotions. This revelation pushes us to rethink the myriad roles this small brain structure might hold in our daily lives. Yet, pinning down the exact role of cerebellum in these tasks has been a challenge.

In pursuit of finding cerebellar function, fMRI—a non-invasive imaging method to study brain activity—has shown that the cerebellum "lights up" in almost any tasks. However, the bright spots we see on fMRI images of the cerebellum might not always mean that the cerebellum is actively working on the task. It might light up simply because its connected neocortical areas are working. But does this mean that we had better abandon cerebellar imaging altogether? Are there tasks in which cerebellum specifically lights up, not reflecting activity in its connected neocortical regions?

In this thesis, we attempted to address these questions by reconsidering how we study cerebellar function using fMRI and see how it works in tandem with other brain regions, particularly the neocortex. To do this, we developed a tool to identify the neocortical regions that are sending input to the cerebellum. With this tool we can then investigate cerebellar activity in the context of its corresponding neocortical regions and ask which tasks engage the cerebellum specifically. We coined the term "selective recruitment" to discern when the cerebellum is uniquely involved.

Our results indicate distinct scenarios where the cerebellum takes the lead: like rapid alternating movements or encoding extensive information in memory. In essence, our work offers a fresh lens to understand the roles of this seemingly small brain structure.

Dedication

To the family I left behind and the family I met along the way!

Co-Authorship Statement

Chapter 2 is an shared effort with Maedbh B King, Rich Ivry, and Jörn Diedrichsen. Maedbh B King collected the data and along with Rich Ivry and Jörn Diedrichsen conceived the original idea. Maedbh King and I contributed equally to conceptualization and analysis. The citation is: King, M., Shahshahani, L., Ivry, R. B., & Diedrichsen, J. (2023). A task-general connectivity model reveals variation in convergence of cortical inputs to functional regions of the cerebellum. eLife, 12, e81511.

Chapter 3 is published on BioRxive. The experiment was conceptualized and designed by Jörn Diedrichsen and I. I collected the data and wrote the original manuscript with Jörn Diedrichsen and Rich Ivry. Maedbh King and Caroline Nettekoven provided feedback on the manuscript.

The citation is:

Shahshahani, L., King, M., Nettekoven, C., Ivry, R., & Diedrichsen, J. (2023). Selective recruitment: Evidence for task-dependent gating of inputs to the cerebellum. In bioRxiv (p. 2023.01.25.525395). https://doi.org/10.1101/2023.01.25.525395

Chapter 4 is not published yet. The experiment was conceptualized and designed by Jörn Diedrichsen and I. I collected the data and wrote the original manuscript with Jörn Diedrichsen.

The citation is:

Shahshahani, L., King, M., Nettekoven, C., Ivry, R., & Diedrichsen, J. (2023). Selective recruitment: Evidence for task-dependent gating of inputs to the cerebellum. In bioRxiv (p. 2023.01.25.525395). https://doi.org/10.1101/2023.01.25.525395

Acknowledgements

Thanks to my mentor, teacher, supervisor and colleague Dr. Jörn Diedrichsen. His profound knowledge and invaluable insights have been the compass for my PhD journey. His unwavering support has been indispensable, and without it reaching the finish line would have seemed unfathomable.

Thanks to Drs. Maedbh B King and Richard Ivry. Maedbh's determination, motivation, and integrity have been inspirational. And Rich for his incredible support and knowledge. Getting the chance to write with him has been one of the a highlight in my academic journey.

Thanks to Trevor Szekeres and Scott Charlton for all the help with the MRI data collection. Without them, this research would have been impossible.

Special thanks to Drs. Andrew Pruszynski and Ingrid Johnsrude for their incredible feedback throughout my PhD.

Thanks to the members of DiedrichsenLab, past and present. Each one has been an exemplary colleague. I am deeply grateful to Dr. Eva Berlot for her invaluable assistance in the early stages of my PhD. Especial thanks to my partner-in-crime, Dr. Caroline Nettekoven, for her steadfast support as I neared the end. Our shared enthusiasm for the CEREBELLUM, passion for art and culture, not to mention our mutual dark wit, has created a bond for life.

Thanks to my soul sisters, in no particular order, Farnoush, Nicky, Mohadese, and Roxana, and to my compadres, David, Omid, Ehsan, Masoud, Ramin, Alireza and Parham, without whom life in Canada seems unimaginable. I am grateful for all the sweat and bitter memories we made, all the deep discussions and the shenanigans.

Thanks to my grandmothers for being role models. Their courage and resilience in the face of oppression have deeply inspired me!

I owe immense gratitude to the most intelligent, compassionate, and principled

individuals I've ever met, my parents Roshanak and Majid, and my brother Milad. They instilled in me a strong sense of determination. The broad-mindedness of my parents greatly simplified life, while my sharp and clever brother added joy to my childhood.

Contents

List of Figures

List of Tables

List of Abbreviations

- **fMRI** Functional Magnetic Resonance Imaging
- **MDTB** Multi-Domain Task Battery
- **PET** Positron emission tomography
- **UCT** Universal Cerebellar transform
- **LTD** Long Term Depression
- **SNR** Signal to Noise Ratio
- **BOLD** Blood Oxygen Level Dependant
- **CSF** Cerebrospinal Fluid
- **NO** Nitric Oxide
- **SUIT** Spatially Unbiased Infra-tentorial template
- **MNI** Montreal Neurologic Institute
- **ROI** Region of interest
- **MDS** Multidimensional Scaling
- **CCAS** Cerebellar Cognitive Affective Syndrome
- **PCA** Principal Component Analysis

- **MDTB** Multi-domain task battery
- **DCN** Deep Cerebellar Nuclei
- **WTA** Winner-take-all

Chapter 1

Introduction

Throughout evolution, the cerebellum has undergone significant transformations. The presence of cerebellar-like structures can be traced back to early aquatic organisms, in which they played a role in coordinating movement as part of the vestibular system (Bell et al., 2008). As vertebrates evolved and became more complex, the cerebellum experienced a notable increase in size and peaked in humans and primates with an expansion rate estimated to surpass even that of the neocortex(Barton and Venditti, 2014).

Despite its relatively small size, the human cerebellum houses a remarkable number of neurons, approximately four times more than what is found in the neocortex (Azevedo et al., 2009; Herculano-Houzel, 2009). Most of these are densely packed granule cells. The cerebellum is a highly folded. In fact, the unfolded cerebellum occupies an area that is roughly equal to 80% of the entire neocortical surface (Sereno et al., 2020).

Based on the deficits observed after cerebellar damage (Holmes, 1939), the cerebellum has historically been associated with motor function. However, in recent decades, it has become evident that the cerebellum also plays a role in cognition. In humans, our understanding of cerebellar function comes from imaging studies. Functional magnetic resonance imaging (fMRI), in particular, has shown cerebellar activation in nearly all the tasks (King

et al., 2019). What the cerebellum contributes to different domains of cognition specifically, nevertheless, remains to be determined. But what has hindered our understanding of its specific function?

We posit that our failure to ascertain cerebellar function is tied to the way we currently study it. Traditionally, we have interpreted fMRI activation within brain structures, including the cerebellum, as an indication of their functional involvement. Nevertheless, two critical factors cast doubt on this interpretation. Firstly, fMRI activation observed in the cerebellum predominantly reflects its input (Gagliano et al., 2022; Mathiesen et al., 2000; Alahmadi et al., 2015, 2016). Secondly, the cerebellum and neocortex exhibit extensive interconnections (Kelly and Strick, 2003) and most of the input to the cerebellar cortex is provided by the neocortex. These factors raise the question of whether cerebellar activations merely reflect the activity within corresponding cortical regions. In light of these considerations, we argue in this thesis that we need to reconsider how we interpret cerebellar fMRI activations, and we propose a novel approach to investigate cerebellar function using fMRI.

To set the stage, this introductory chapter will cover the required background to understand our novel approach. First, we will focus on the micro-circuitry present within the cerebellar cortex and introduce one of the dominant models of cerebellar function based on this local circuitry. Secondly, to place cerebellar function within a broader context, we will examine findings from studies that examine the interconnections between the cerebellum and neocortex. Then, we will explore evidence from research conducted on healthy individuals and cerebellar patients, highlighting the role of the cerebellum in cognition. Furthermore, we will discuss the widely accepted concept of the universal cerebellar transform (UCT), which has implications for understanding cerebellar functionality across diverse tasks. Lastly, we will address challenges in the study of cerebellar function using magnetic resonance imaging (fMRI) and outline our attempt to overcome this challenge.

1.1 Functional neuroanatomy of the cerebellum

In this section, we will explore the fundamental components of the local circuitry in the cerebellum. Unlike the neocortex, this local circuitry is remarkably uniform throughout the entire cerebellar cortex. Following this, we will explore the connections between the cerebellum and the neocortex, which serve as the backbone for the cortico-cerebellar communication that underlies cognition.

1.1.1 Local circuitry of the cerebellum

Mossy fibers are one of two inputs to the cerebellum. Their primary targets in the cerebellar cortex are **granular cells** located in the granular layer. Upon entering the granular layer they excite multiple granular cells through a diffuse branching pattern. The synaptic sites where they connect with the granular cells are called **mossy rosettes**. On average, each mossy fiber can have 20-50 mossy rosettes (Marr, 1969).

Mossy fibers arise from various sources including the vestibular system, spinal cord, and Pontine nuclei. The **Pontine nuclei**, situated within the pons region of the brainstem, serve as the primary route for transmitting information from motor and associative regions of the neocortex to the cerebellum (Kelly and Strick, 2003). Unlike mossy fiber projections from the vestibular system or spinal cord, Pontine mossy fiber projections appear to be part of a closed loop network connecting the cerebellum and neocortex. Based on their physiological properties and their evolutionary development, Schwarz et al. (1997) suggested that the Pontine nuclei are not mere relay stations; rather, they modulate and gate the incoming neocortical information to ensure its appropriate representation in the cerebellum (Schwarz et al., 1997; Schwarz and Thier, 1999).

Granular cells are the most abundant type of neurons in the brain. A single granular

cell receives input from 4-5 mossy fibers (D'Angelo, 2018). Axons of a granular cell traverses the cerebellar folia and form a T-shape branch that travels longitudinally across folia called **parallel fiber**. Parallel fibers make excitatory synapses with Purkinje, Basket, Golgi, and Stellate cells(Figure 1.1**a**).

Purkinje cells, characterized by their distinct flat dendritic tree, are the output cells of the cerebellar cortex. They are aligned with each other, and the parallel fibers run perpendicular to the plane formed by their dendritic trees. These trees are arranged in a way such that there is minimum overlap among them. Axons of the Purkinje cells form the output of the cerebellar cortex, inhibiting cells within deep cerebellar nuclei(Figure 1.1**a**).

In addition to mossy fibers, **climbing fibers** also enter the cerebellar cortex. They originate in **inferior olive** and make contact with the Purkinje cells right at the base of the tree. They then ascend the dendritic tree, forming multiple synapses along the way. This unique synaptic pattern gives rise to what is known as a **complex spike**. Complex spikes are characterized by a single initial spike, followed by a series of spikes propagating through the dendritic tree, accompanied by intense depolarization. This sequence of events temporarily inhibits the activity of the Purkinje cell. Notably, each Purkinje cell receives input from a single climbing fiber. These fibers convey information from various sources, including the proprioceptive system and neocortical regions. Furthermore, the collaterals of climbing fibers target basket, stellate, and Golgi cells, contributing to the regulation of activity in granule cells as well(Figure 1.1**a**).

Output from the cerebellar cortex is projected to the **deep cerebellar nuclei (DCN)**. DCN comprises of 4 pairs of nuclei: Dentate, Fastigial, Emboliform, and Globose. Information from these nuclei is transmitted to neocortex through the thalamus. In humans, the most distinct Deep cerebellar nucleus is the Dentate nucleus with a tooth-shape structure visible in the middle of the cerebellar white matter(Figure 1.1**b**)

At least three different types of inter-neurons have been identified in the cerebellar

cortex. **Golgi cells** are inter-neurons with a wide dendritic tree that is excited by both mossy fibers in the granular layer and parallel fibers in the Purkinje layer. Golgi cells exhibit widespread axon branching and inhibit numerous granular cells. The axons of these cells exhibit significant overlap, indicating extensive connectivity and potential for synchronized inhibitory influence. Activity of Golgi cells is indispensable as they suppress the activity of granular cells and prevent excessive activity at the parallel fibers (Figure 1.1**a**).

Basket cells, like Purkinje cells, possess a flat dendritic structure, although it is less dense compared to Purkinje cells. In the molecular layer, parallel fibers exert inhibitory effects on basket cells. The axons of basket cells run perpendicular to the parallel fibers and inhibit Purkinje cells. Interestingly, the inhibitory influence of a basket cell does not directly affect the neighboring Purkinje cell, but rather extends to those that are two or three cells away. As a result, parallel fibers that excite a Purkinje cell are unlikely to inhibit it through a basket cell (Figure 1.1**a**).

Stellate cells exhibit a dendritic structure resembling that of basket cells. These cells can be classified into two types based on the pattern of their axon distribution. Stellate type A cells project their axons to neighboring Purkinje cells, while stellate type B cells target Purkinje cells that are not in immediate proximity. Similar to basket cells, stellate cells receive excitatory input from parallel fibers and play a role in regulating the activity of Purkinje cells by exerting inhibitory control over them(Figure 1.1**a**).

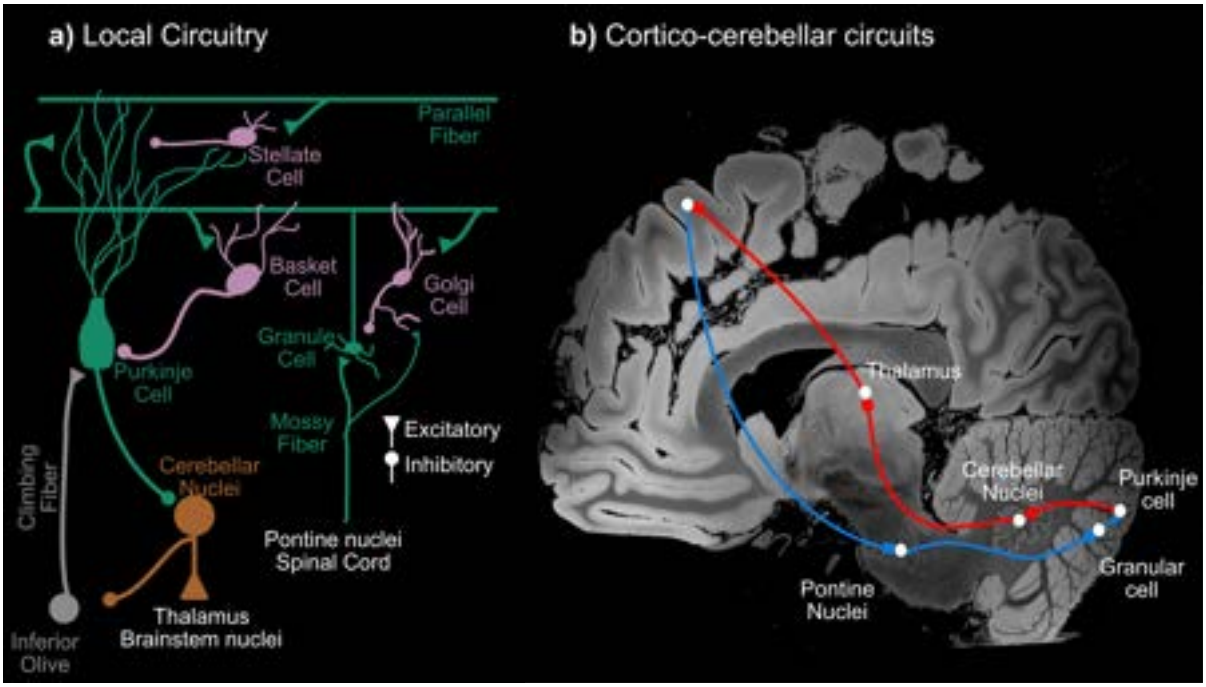

Figure 1.1: **Cerebellar circuitry**. **a)** An overview of cerebellar microcircuit. This circuitry is homogeneous across the cerebellar cortex. **b)** A schematic of cortico-cerebellar connections on top of a high resolution image. There are multiple closed-loop circuits between the cerebellum and neocortex. The intricate folding of the cerebellar cortex alongside the Dentate nucleus is also evident in the image

Marr-Albus-Ito theory of cerebellar function

What is the function of this microcircuit? David Marr (Marr, 1969), James Albus (Albus, 1971), and Masao Ito (Ito, 1989) introduced a model, which still forms - 54 years later - the basis of our understanding of how the cerebellum work, albeit with minor refinements (Diedrichsen et al., 2019).

The model is based on the idea that the cerebellum functions as a powerful pattern recognition and error correction system. According to this model, the incoming information through mossy fibers undergoes significant expansion due to the abundance of granular

cells in the cerebellar cortex. This information expansion makes the cerebellum an effective pattern recognition machine enabling the precise representation of contextual details.

The granular cells then send information to Purkinje cells through activity through parallel fibers. The input from climbing fibers serves as a teaching signal for supervised learning. A complex spike causes long term depression (LTD) in the synapses between parallel fibers and Purkinje cells (Ito, 1989). Through this learning process, an association is formed between a specific pattern of parallel fiber input and a subsequent climbing fiber activity .

As learning progresses, even in the absence of the teaching signal, the corresponding parallel fiber activity elicits a reduction in Purkinje cell activity, thereby disinhibiting the deep cerebellar nuclei. Conceptually, the Marr-Albus-Ito model asserts that a Purkinje cell predicts its climbing fiber input corresponding to the context provided in parallel fiber.

1.1.2 Closed-loop cortico-cerebellar circuits

The cerebellum-neocortical connections have been a subject of interest since the early 1970s, with early investigations by Brodal in cats (Brodal, 1971) and rhesus monkeys (Brodal, 1978). Originally, the prevailing view was that the cerebellum exclusively played a role in motor function leading to the belief that multiple neocortical regions sent projections to the cerebellum, while the cerebellum primarily sent projections back only to the motor areas. However, this perspective underwent a significant shift when Kelly and Strick's work demonstrated that the cerebellum also projects to associative areas of the neocortex, challenging the notion that its connections were solely motor-centric (Kelly and Strick, 2003).

Kelly and Strick (2003) focused on bi-directional projections from the neocortex to the cerebellum and back. They utilized rabies virus, a neurotropic virus capable of tracing synaptic connections across multiple neurons. This innovative method allowed them to map

the anatomical connections spanning multiple synapses in both directions. Using rabies virus, they discovered that the connectivity between the cerebellar cortex and neocortex exhibits a topography characterized by numerous parallel closed-loop circuits, wherein A projects to B and B reciprocates to A (Figure 1.1 b). Importantly, these circuits extended beyond motor areas, encompassing higher-order cognitive regions such as the prefrontal and parietal cortex (Kelly and Strick, 2003).

These findings provided compelling evidence that the cortico-cerebellar communication network possesses an anatomical foundation extending beyond motor control. Additionally, it dispelled the notion of a singular, extensive open-loop circuit, instead highlighting the presence of multiple parallel closed-loop circuits sub-serving cognitive and motor function. Nonetheless, the precise contribution of the cerebellum within these circuits remains elusive. In the following section, we will overview the large body of work that has led scientists to reconsider how they think about, and investigate cerebellar function.

1.2 Cerebellum and cognition

The evolutionary trajectory of the cerebellum across different species provides valuable insights into its role in cognition. In primates, the posterior cerebellum, also known as the neocerebellum, has undergone remarkable expansion at a rate comparable to that of prefrontal cortex. This unusual enlargement has been suggested to contribute to the cognitive abilities that sets primates apart from other vertebrates (Barton and Venditti, 2014).

In humans, computational neuroanatomy has revealed that compared to Neanderthals, early homo sapiens exhibited relatively larger cerebellar hemispheres but comparable parietal lobes, suggesting that it has led to significant differences in cognitive and social abilities between Neanderthals and early homo sapiens (Kochiyama et al., 2018).

Trans-neuronal viral tracing studies have provided compelling evidence supporting

the presence of an anatomical foundation for cortico-cerebellar communication that extends beyond the motor domain (Kelly and Strick, 2003). The existence of these anatomical connections certainly argues for a cerebellar role in cognition. In humans, resting state functional connectivity, as a non-invasive indirect measure of structural connectivity has been used to map the connections between the cerebellum and neocortex. These studies have demonstrated that the larger portions of the neocerebellum exhibit strong connectivity with associative regions of the neocortex (Buckner et al., 2011; Marek et al., 2018).

1.2.1 Insights from neuroimaging and patient studies

Studies of cerebellar patients have contributed substantially to our knowledge of cerebellar function. These patients typically exhibit prominent motor deficits, such as uncoordinated limb and eye movements (Bodranghien et al., 2016; Schmahmann, 2004). However, since the cerebellum is also connected to cognitive regions of the neocortex, it is reasonable to expect cognitive impairments as well. Several reports have documented various cognitive deficits, although they are generally milder compared to motor deficits (Schmahmann, 2004). While studies involving cerebellar patients are valuable in confirming the existence of cognitive deficits, the location of lesions can vary widely among patients, and these lesions can sometimes co-occur with lesions in other parts of the brain. Consequently, attempts to replicate previously reported deficits in different patients are occasionally unsuccessful. This necessitates the use of functional imaging techniques to investigate cerebellar function.

Perhaps the first evidence from neuroimaging indicating the involvement of the cerebellum in cognitive processes was a study conducted by Petersen et al. (1989), which utilized Positron Emission Tomography (PET) to identify activated regions during a language task. Their results revealed that the cerebellum was engaged in the word generation even if motoric aspects of the task were controlled for.

Functional magnetic resonance imaging (fMRI) has brought about a paradigm shift

in understanding the human brain and its operations. fMRI allows for the non-invasive examination of brain activity with remarkable spatial resolution. By using alterations in blood oxygenation level as an indirect measure of brain activity, it has played a crucial role in studies of various brain structures, including the cerebellum.

FMRI studies have demonstrated that the cerebellum is activated by a wide range of tasks (for a comprehensive overview and meta-analytic approaches, see (Strick et al., 2009; Stoodley et al., 2012; Buckner, 2013; Stoodley, 2012). In a pivotal study, King et al. (2019) explored the richness of cerebellar function utilizing a multi-domain task battery (MDTB) and showed that for almost any conceivable task, there is discernible activation within the cerebellum. This led to the identification and mapping of functional territories within the cerebellum. Subsequently, using a cognitive atlas, they assigned distinct cognitive and motor functionalities to specific cerebellar regions, as illustrated in Figure 1.2. This emerging field of research has made significant progress, aided by advancements in imaging technology, analysis methods, and modeling techniques, leading to substantial evidence supporting the notion that the cerebellum is not solely dedicated to motor functions. However, due to the diverse array of tasks that activate the cerebellum, the presence of mild and less persistent cognitive deficits in cerebellar patients, and the involvement of other brain structures in different tasks, pinpointing specific function(s) of the cerebellum in these cognitive domains has proven challenging.

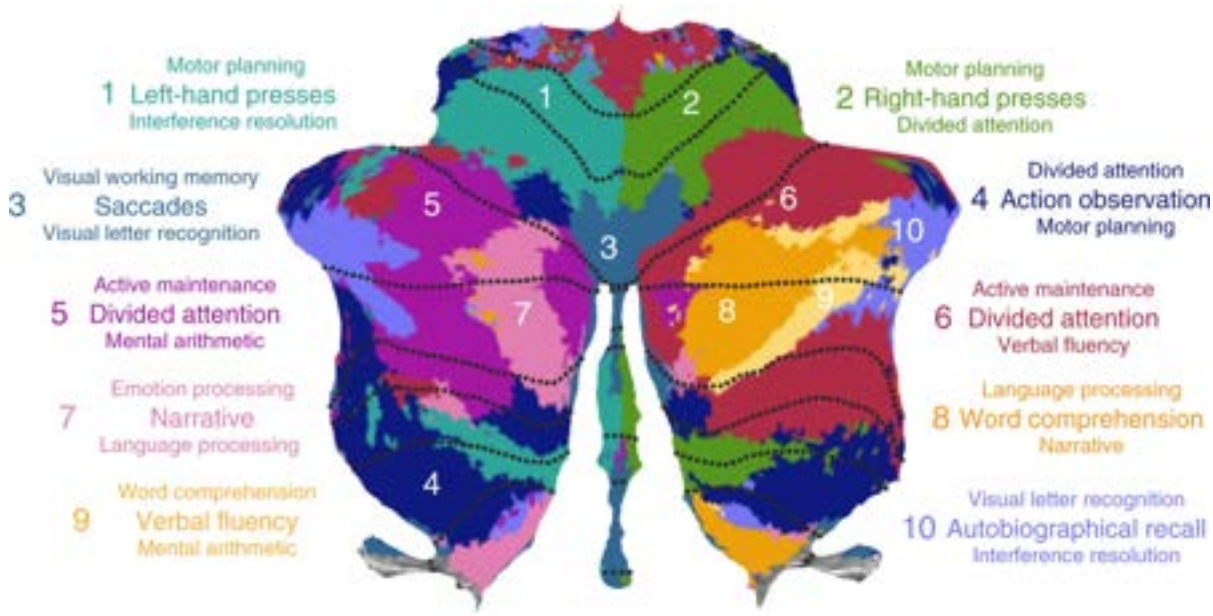

Figure 1.2: **Functional atlas of the cerebellum**. Adapted from (King et al., 2019). Using a multi-domain task battery, the cerebellum was divided into discrete regions. Using an encoding feature model, each region was then assigned with a term from a cognitive atlas. The figure summarizes the cognitive and motor domains that have been shown to activate the cerebellum

In the following section, we describe one of the most popular theories about cerebellar function which was inspired by its uniform architecture. We will then cover the basics of functional magnetic resonance imaging with a special focus on the cerebellum and what has to be taken into account when looking at images of cerebellar task activation. Finally, we will bring together what has been discussed so far to motivate the idea behind the thesis.

Universal cerebellar transform (UCT) vs multiple functionality

Histology of the cerebellar cortex reveals a remarkably uniform cytoarchitecture. Building upon this observation, Leiner et al., suggested that the cerebellum contributes to mental skills in the same way as it contributes to the motor domain, a hypothesis later referred to as

the "Universal cerebellar transform" (Leiner et al., 1986, 1991; Schmahmann, 2004). Within this framework, the variations in cerebellar function across different tasks can be attributed to the diverse connections it forms with the neocortex, brainstem structures, and spinal cord. This stands in contrast to the neocortex, where distinct localized cellular structures give rise to highly specialized regions.

In search for the universal cerebellar transform, scientists have put forth various theories based on the observed motor deficits, among which are prediction (Miall et al., 1993), timing (Ivry and Keele, 1989), and internal models (Ito, 1993; Wolpert et al., 1998). Nevertheless, the primary challenge lies in designing experiments that can effectively test these hypotheses across diverse task domains such as working memory, social cognition, language processing, and more. This has hampered the field in making progress through the generation of falsifiable predictions about the cerebellar function.

This prompted us to question whether it is feasible for the cerebellum to implement a single transformation across various tasks; perhaps we should reassess our approach in finding answers to the question of cerebellar function. But what is the implication of the homogeneous circuitry? To answer this question, we can consider this problem in Marr's 3 levels of analysis: What is the task that this uniform circuitry tries to solve? (computation level), How does it solve the task? (algorithmic level), and how is the computation implemented by neurons within the cerebellum? (implementation level).

From a computational standpoint, diverse tasks undeniably present distinct problems to address. At the implementation level, the uniform cerebellar circuitry of the cerebellum implies that all these different functions are achieved using the same "hardware". Yet, at the algorithmic level, two possibilities emerge. One perspective, as posited by the Uniform Cerebellar Theory (UCT), is that this circuitry primarily serves a singular algorithmic function relevant across all tasks. Alternatively, it is possible that this uniform circuitry executes varied algorithms tailored to the computations specific to each task. As illustrated in Figure 1.3, this suggests the cerebellum might house multiple functionalities at the algorithmic tier.

The "multiple functionality" idea motivates the approach to develop precise hypotheses about cerebellar function in specific cognitive domains and to test these ideas with targeted experiments. It also fits seamlessly with the overarching idea of functional specialization observed throughout the brain: Just as different parts of the cerebral cortex are implementing different functions at the algorithmic level, distinct cerebellar regions may also be adept to implement custom algorithms tailored to unique tasks.

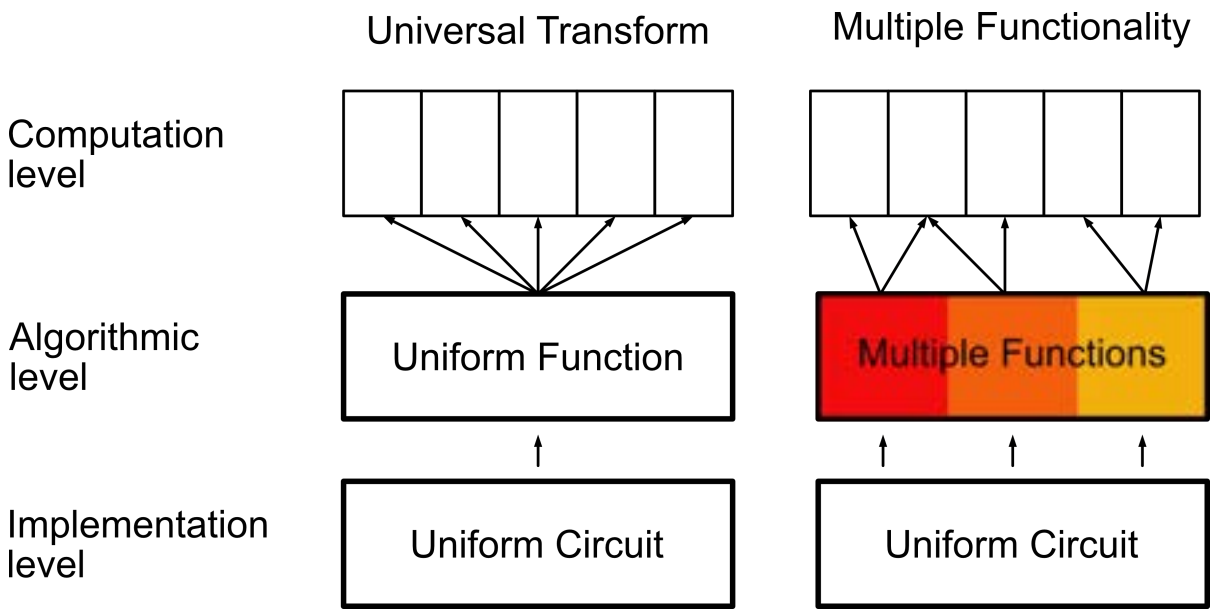

Figure 1.3: **Universal cerebellar transform vs multiple functionality**. Adapted from (Diedrichsen et al., 2019). The schematic figure depicts the Universal Cerebellar Transform (UCT) and the multiple functionality frameworks within Marr's three levels of analysis. These frameworks at the algorithmic level. UCT proposes a unified function at the algorithmic level, while multiple functionality suggests that multiple functions are achieved at this level, leading to the emergence of various tasks at the computation level.

1.3 fMRI of the cerebellum

Compared to other brain structures, the cerebellum has received less attention in fMRI studies for a number of reasons. First, it is compressed into a small volume, resulting in intricate folding (Sereno et al., 2020). This intricate folding, combined with the high functional diversity of the cerebellum, presents technical challenges when attempting to resolve its distinct functional regions at standard resolutions. Second, apart from the long-standing assumption that cerebellar function is purely motor related, the relationship between the BOLD signal and neural activity in the cerebellar cortex differs fundamentally from that observed in the neocortex, thereby complicating its interpretation.

Nevertheless, advancements in imaging techniques and analytical methods have resulted in a shift towards increased investigation of the cerebellum in fMRI studies. In this section, we will provide an overview of these challenges and attempts to overcome them. Importantly, we will first overview the technical challenges facing imaging the cerebellum and the attempts that have been made to conquer them. Next, we will go over the origins of the fMRI signal, the Blood Oxygen Level Dependent (BOLD), with an emphasis on its origin in the cerebellar cortex which has significant implications for interpreting its activations.

1.3.1 Technical challenges in imaging the cerebellum

The cerebellum presents a series of formidable technical challenges when studied with functional imaging techniques. One of the primary challenges lies in its composition; It is densely populated with various types of neurons, all nestled tightly in a limited space. This complex neural landscape results in tight folds that measure approximately 1-2mm in width (Braitenberg and Atwood, 1958). Moreover, despite a seemingly uniform cytoarchitecture, it is now consensus that there is functional diversity across different regions of the cerebellum. This diversity is shaped by heterogeneous connections that exist between the cerebellum

and other brain structures such as basal ganglia and various neocortical regions (Kelly and Strick, 2003, 2004). These characteristics culminate in a compact structure with closely packed functional areas. At conventional spatial resolutions used in fMRI, discerning these distinct functional regions is therefore challenging.

Another layer of complexity is added by the natural anatomical variability that exists between individuals. Just like fingerprints, no two cerebellums are identical, making standardized imaging interpretations a challenge. Furthermore, the cerebellum's anterior regions lie in close vicinity to the inferior parts of the neocortex, making it challenging to isolate it from these parts of the neocortex. The task of accurately summarizing and representing the cerebellum's myriad activations becomes all the more difficult due to these factors. In this section we will overview the attempts made to tackle these challenges.

Cerebellar normalization

In fMRI, given the high individual variability of brain anatomy, the use of an atlas is crucial for integrating and comparing data among participants. As a solution, the MNI152 atlas was developed by averaging anatomical images of 152 healthy subjects, accounting for differences in overall size of the brain (Fonov et al., 2011). However, this atlas was not specifically optimized for the cerebellum and lacks the necessary level of detail required for precise alignment of this brain region (Diedrichsen, 2006). Consequently, a dedicated atlas specifically designed for the cerebellum was created: This is the Spatially Unbiased Infra-tentorial Template or SUIT (Diedrichsen, 2006). Figure 1.4 shows the cerebellum transformed to MNI (Fig. 1.4 **a)**) and SUIT (Fig. 1.4 **b)** standard spaces through non-linear transformation. Evidently, the level of visible details in the SUIT space is higher than in the MNI space.

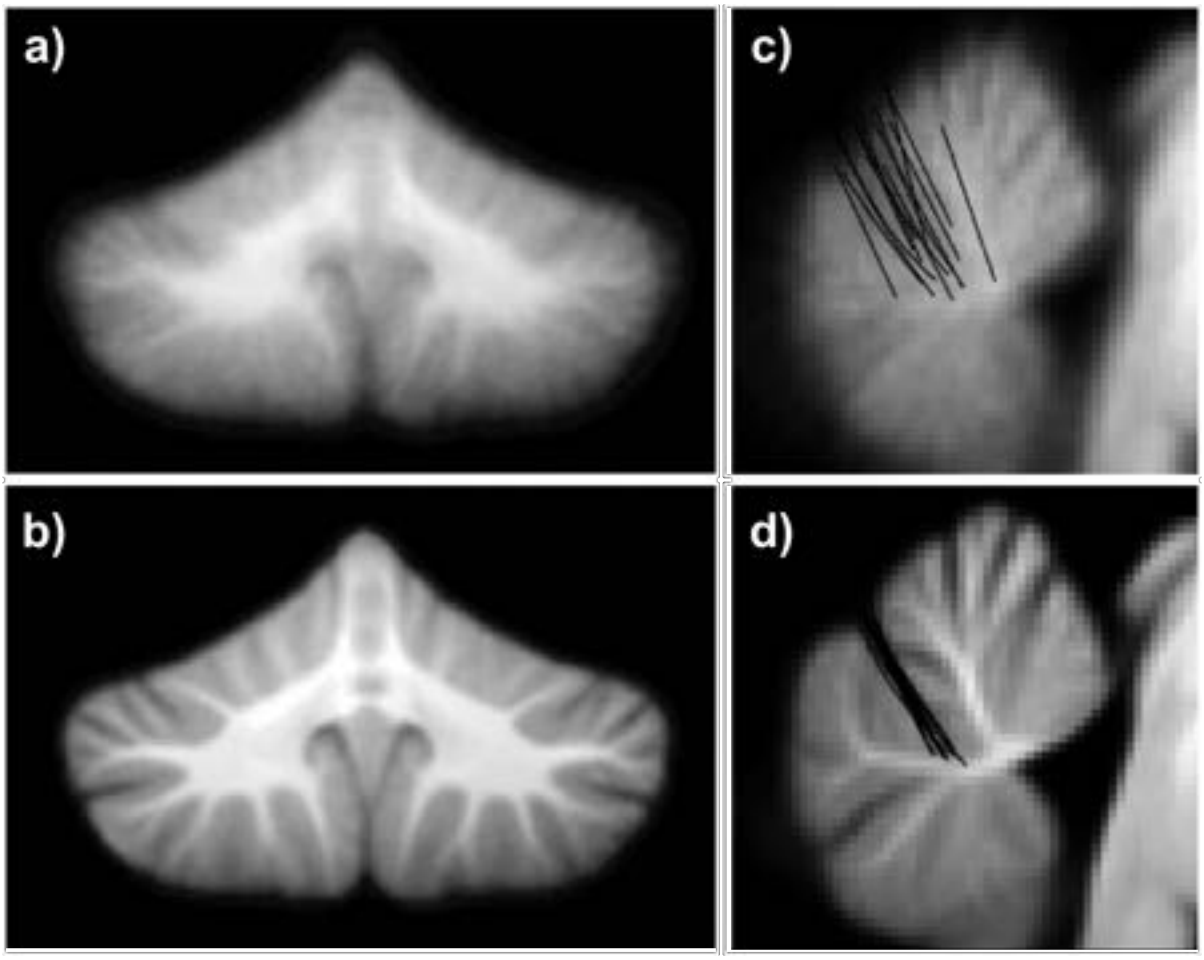

Figure 1.4: **Cerebellar normalization**. Adapted from (Diedrichsen, 2006). **a)** Shows cerebellum normalized to the MNI152 atlas. **b)** Shows cerebellum normalized to the SUIT atlas. A comparison between the two normalized cerebellar images reveals that the MNI normalized version appears blurry and lacks visible detail compared to the SUIT normalized version. **c)** Location of individual primary fissures following normalization to MNI152. **d)** Individual primary fissures after normalization to SUIT atlas. It is evident that the fissures are more aligned in the SUIT-normalized cerebellum, demonstrating its superiority over the MNI152- normalized cerebellum.

A flat representation of the cerebellum

Due to an intricate folding structure, capturing detailed information within single cerebellar folds becomes exceedingly challenging using standard resolutions in human fMRI imaging. To overcome this challenge, various approaches have been explored, including one proposed by (Van Essen, 2002), who employed a single anatomical image at 1mm resolution to reconstruct a cerebellar surface aiming to depict cerebellar folding at a level of accuracy that captures groups of folia. When volumetric data are projected onto this surface, contiguous activation loci become fragmented due to the fact that the high level of anatomical detail cannot be adequately resolved at 1mm resolution (Figure 1.5)**a**).

In another attempt, Diedrichsen and Zotow (2015) tailored a customized flat representation of the cerebellar cortex, enabling a comprehensive visualization of functional activations within a single view. Their goal was to create a flat surface that, instead of unfolding cerebellar folia, depicted each cerebellar lobule with an area proportional to the volumetric space it occupies. They also ensured that clusters of activations observed in the volumetric data were faithfully represented as clusters in the two-dimensional (2D) presentation (Diedrichsen and Zotow, 2015). This presentation will be used throughout the thesis to show cerebellar activations (Figure 1.5)**b**). As a downside, a single spot on the surface averages across a number of folia, obscuring more detailed functional specializations.

a) Flatmap representing folia

b) Flatmap representing lobules

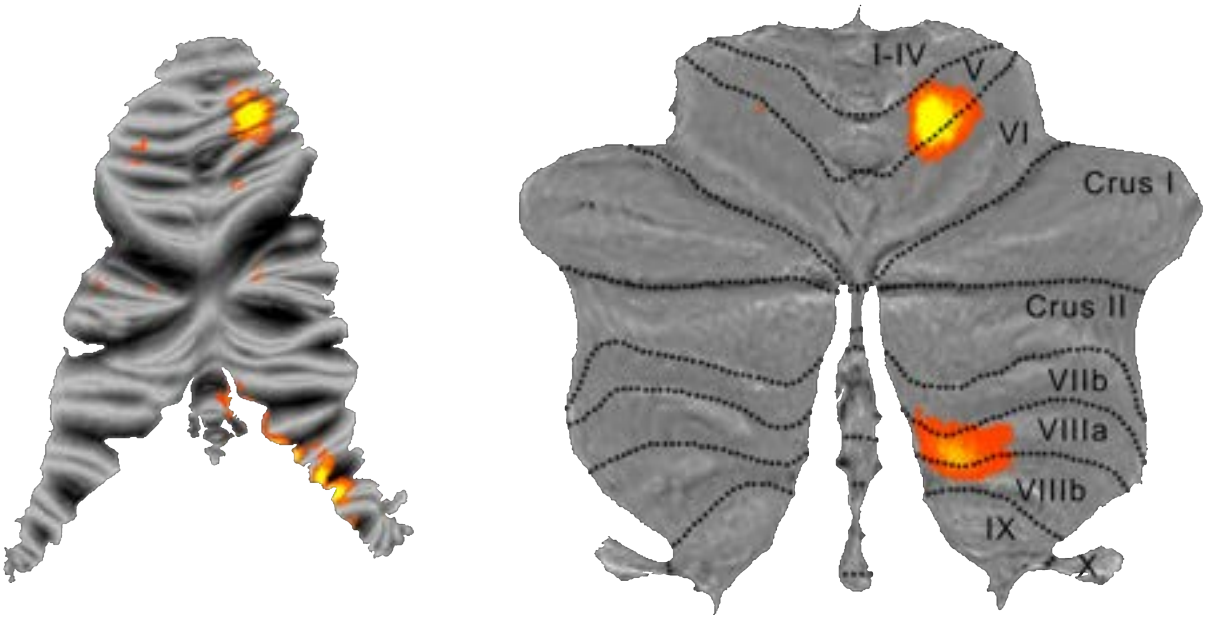

Figure 1.5: **Flat representation of the cerebellum**. Adapted from (Diedrichsen and Zotow, 2015). **a)** Shows a flat representation derived from a single anatomical image. This flatmap aims to depict a 2-D representation of the cerebellum, with resolved folia at an accuracy possible at 1mm resolution. **b)** Shows a flat representation that rather than focusing on resolving folia, aims to show the lobules. This presentation is not a real flattened cerebellum, rather, it is tailored so that each lobular area is proportional to the volume that lobule occupies. In this representation, unlike the flatmap in **a**, the activations appear as contiguous clusters rather than fragmented activations.

Isolating the cerebellum from neocortex

Another important challenge in imaging the cerebellum is isolating it from its surrounding tissue including the abutting inferior neocortical areas. This is especially challenging as the cerebellar cortex and neocortex exhibit the same contrasts on MRI scans. The SUIT approach is tailored for cerebellar normalization rather than for the entire brain. Hence, it becomes imperative to ensure a complete isolation of the cerebellum from its surroundings in

order to achieve optimal performance of the normalization algorithm. Beyond normalization, it is important to to prevent activation spillover from nearby inferior and occipital cortices. Otherwise, there is a risk of misreading cerebellar activation maps, incorrectly attributing activity to the anterior cerebellum when in fact it originates from the inferior temporal or occipital areas. To overcome this, Diedrichsen (2006) developed a dedicated automated isolation algorithm to generate a mask specifically for the cerebellum (see Figure 1.6 for effect of isolation on an activation map on the flatmap).

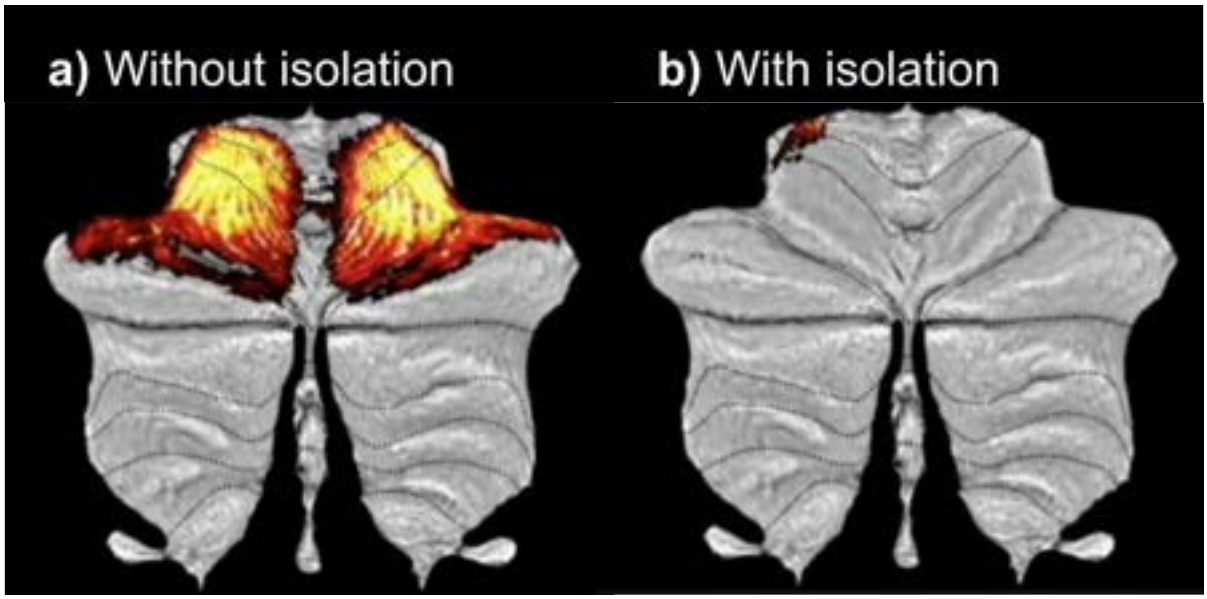

Figure 1.6: **Effect of cerebellar isolation**. Isolation of the cerebellum through masking ensures that there is no spurious activation in the anterior part of the cerebellum. The presence of false activation in the anterior part of the cerebellum is demonstrated in **(a)**, while **(b)** shows that the effect of activity leak is significantly reduced when the cerebellum is properly isolated through masking.

1.3.2 Origins of BOLD signal in cerebellar cortex

The BOLD signal reflects the ratio of oxygenated to non-oxygenated blood, and is therefore only an indirect measure of neural activity. To interpret cerebellar fMRI activation in relation to cognition, it is crucial to have a clear understanding of which neuronal processes are reflected in the BOLD signal. In this section, I will first provide an overview of the fundamental mechanism that underlies changes in the BOLD signal in general. Subsequently, I will concentrate on understanding the origin of this signal change within the cerebellar cortex, as it informs the hypotheses we are investigating.

Neurovascular coupling, the interplay between neuronal activity and the vascular system, forms the foundation of the BOLD signal. When neurons in a specific brain region become active, their energy demand increases, necessitating elevated supply of oxygen and glucose. This leads to an increase in blood flow, a process known as the hemodynamic response. As a result, the proportion of oxygenated hemoglobin in the blood rises. This discrepancy in oxygenation levels induces changes in the magnetic properties of the blood, resulting in changes of the BOLD signal. Thus, the BOLD signal indirectly reflects neural activity and depends on intrinsic vascular properties of the active brain region (Vanlandewijck et al., 2018).

Neurovascular coupling regulates blood flow; a key contributor to the BOLD signal (Ogawa et al., 1990; Logothetis, 2003). The release of vasoactive substances, particularly Nitric Oxide (NO), plays a critical role in vasodilation and the subsequent increase in local blood flow in response to neuronal activity. In the cerebellar cortex, high levels of NO have been detected in the granular and molecular layers and almost none in the Purkinje cell layer (Mapelli et al., 2017; Gagliano et al., 2022).

Notably, research by (Snyder, 1992) and (Southam et al., 1992) has shown that granular cells and mossy fibers manifest the highest levels of NO in the brain, making these

two cell types the primary contributors to variations in the BOLD signal. Conversely, Purkinje cells, the exclusive output of the cerebellar cortex, lack NO. This suggests that their activity probably does not affect blood flow or the subsequent BOLD signal (Mathiesen et al., 2000). These factors lead to a distinct interpretation of the BOLD signal between the neocortex and the cerebellum. In the cerebellum, BOLD activity might predominantly mirror activity from its connected neocortical regions due to fixed anatomical connections, rather than indicating a specific cerebellar processing requirement.

1.4 Problem statement and thesis overview

Over the past decades, the cerebellum has been implicated in various tasks, yet its specific role in each task remains elusive. Inspired by its uniform cytoarchitecture, scientists have put forth the concept of the universal cerebellar transform, aiming to unravel its function. This has led to a recurring question in studies of cerebellar function: What is the specific function of the cerebellum? This question is never raised in relation to the neocortex.

BOLD fMRI has been extensively used to study cerebellar function. Task-based fMRI activations are often interpreted as evidence of the cerebellum's involvement in a given task. However, this reasoning is flawed since these activations primarily reflect the input to the cerebellum, with mossy fibers carrying information from the Pontine nuclei. The primary source of input to the Pontine nuclei is the neocortex. Consequently, when a neocortical region is activated in response to task demands, the resulting activity in the mossy fibers and granular cells could lead to BOLD activation, irrespective of whether cerebellar computations are indeed needed for the task.

Does this mean that fMRI provides no further insights into the function of the cerebellum? The objective of this thesis is to demonstrate that fMRI remains a potent tool for studying the cerebellum, yet for it to provide more useful information, we need to re-evaluate

our investigative lens and how we interpret its results. We introduce the idea of **selective recruitment** as a means to study cerebellar function using fMRI: We focus on a single domain and formulate specific questions about cerebellar involvement in that particular domain. The two core tenets of this approach are:

1. Hypotheses that are not limited by a unitary cerebellar function, and
2. Analyzing cerebellar activation in the context of the input it receives from the neocortex rather than in isolation.

To take into account the concurrent activations in the neocortex, in **chapter 2** we developed a task-invariant cortico-cerebellar connectivity model using a multi-domain task battery. This model can help us identify the neocortical regions that provide input to the cerebellar region of interest and estimate the expected cerebellar input resulting from these neocortical regions. we demonstrated that a significant portion of variation in cerebellar BOLD activity can be accounted for by neocortical activity. However, despite the success of the model, we observed that there are still proportions of variation in cerebellar activity that remained unexplained by this static task-invariant model. For the subsequent chapters, we shifted our focus to explore this part of the cerebellar activity and tested for selective recruitment.

In **chapter 3**, we put the idea of selective recruitment to the test in the motor domain. Here, we have concrete evidence from patient studies that the cerebellum is specifically required during performance of rapid alternating movements, but not during generation of high force levels (Mai et al., 1988). We would therefore expect that input to the cerebellum is up-regulated when fast coordination of finger movements is required. We designed an alternating finger tapping task in which we could test selective recruitment of the cerebellum in this domain.

In **chapter 4**, we shifted our focus to a higher-order cognitive domain and specifically

investigated the selective involvement of the cerebellum in a working memory task, for which studies of cerebellar patients have shown relatively milder and less consistent impairments (Bolceková et al., 2017). We designed a verbal working memory task involving digit recall and manipulated cognitive components that have been studied in patients: load (number of digits to be maintained) and recall direction (the order in which digits are to be retrieved). Our aim was to identify processes in which the cerebellar input exhibits an up-regulation.

Lastly in **chapter 5**, we contextualize the findings of the projects presented in this thesis, connecting them to past research and prevalent ideas about cerebellar function, particularly the concept of the Universal Cerebellar Transform (UCT). We critically evaluate this concept and highlight its shortcomings in explaining some of the results derived from this thesis. Moreover, we review the limitations of the current projects and suggest potential solutions to mitigate them. We conclude by providing a preliminary roadmap for future research, extending the studies conducted in this thesis.

Chapter 2

A task-general connectivity model reveals variation in convergence of cortical inputs to functional regions of the cerebellum

2.1 Abstract

While resting-state fMRI studies have provided a broad picture of the connectivity between human neocortex and cerebellum, the degree of convergence of cortical inputs onto cerebellar circuits remains unknown. Does each cerebellar region receive input from a single cortical area or convergent inputs from multiple cortical areas? Here we use task-based fMRI data to build a range of cortico-cerebellar connectivity models, each allowing for a different degree of convergence. We compared these models by their ability to predict cerebellar activity patterns for novel Task Sets. Models that allow some degree of convergence provided the best predictions, arguing for convergence of multiple cortical inputs onto single

cerebellar voxels. Importantly, the degree of convergence varied across the cerebellum with the highest convergence observed in areas linked to language, working memory, and social cognition. These findings suggest important differences in the way that functional subdivisions of the cerebellum support motor and cognitive function.

2.2 Introduction

The last 30 years has witnessed a paradigm shift with regards to cerebellar function, with broad recognition that this subcortical structure is engaged in many aspects of human cognition. Since the first report of cerebellar activation in a semantic retrieval task (Petersen et al., 1989), thousands of neuroimaging papers have reported cerebellar recruitment during a broad range of tasks that cannot be attributed to the motor demands of these tasks. Functional interpretations include hypotheses concerning how the cerebellum may facilitate attentional shifts (Allen et al., 1997), stimulus-response mapping (Bischoff-Grethe et al., 2002), higher order rule processing (Balsters et al., 2013), verbal working memory (Marvel and Desmond, 2010), language (Fiez, 2016), and social cognition (Van Overwalle et al., 2015). This body of work has produced functional maps of the cerebellum that depict the association of particular cognitive processes with different subregions of the cerebellum (King et al., 2019).

Given the relative uniform cytoarchitecture of the cerebellar cortex, it is assumed that differences in function mainly arise from variation in the input to the cerebellum. Trans-synaptic tracing methods employed in non-human primates studies have revealed extensive reciprocal connections between many frontal and parietal areas and the cerebellum (Dum and Strick, 2003; Kelly and Strick, 2003). These studies have highlighted the closed-loop nature of these connections, with each (neo-)cortical region projecting to a specific cerebellar region, and receiving input from the same area (Strick et al., 2009). In humans, resting state functional connectivity analyses have revealed a set of cerebellar networks,

each one associated with a specific cortical network (Buckner et al., 2011; Ji et al., 2019; Marek et al., 2018).

An important unanswered question is whether each cerebellar region receives input from a restricted cortical region or whether it receives convergent input from multiple cortical regions. Providing an answer to this question has important implications for our understanding of cerebellar function. An architecture marked by a one-to-one relationship between cortical and cerebellar regions would suggest that the function of each cerebellar region is to fine-tune the dynamics in its cortical input. In contrast, a convergent architecture would suggest that subregions within the cerebellum integrate information across disparate cortical regions and may coordinate their interactions. Indeed, recent work in the rodent brain has suggested convergence of mossy fibers from diverse sources onto the same cerebellar region (Henschke and Pakan, 2020; Pisano et al., 2021), or even onto the same granule cells (Huang et al., 2013). Furthermore, the pattern of cortico-cerebellar convergence may vary across the cerebellar cortex, similar to how cortical areas show considerable variation in the degree to which they serve as points of convergence from other cortical regions (Bertolero et al., 2015; Yeo et al., 2014, 2015).

In the current study we introduce a novel approach to study cortico-cerebellar connectivity. Using the data from a large battery of tasks, we derived models that could be used to predict the activity in each cerebellar voxel based on the activity pattern in the neocortex. While this approach allowed us to evaluate the degree of convergence of cortical inputs to the cerebellar cortex, we recognize that the model could also be evaluated in the opposite direction, namely, to predict activity in the neocortex based on cerebellar activity patterns. However, we believe that using the model to make directional predictions from neocortex to cerebellum is most appropriate for fMRI data. The BOLD signal in the cerebellar cortex overwhelmingly reflects cortical input (via the pons) with no measurable contribution from the Purkinje cells, the output neurons of the cerebellar cortex (Mathiesen et al., 2000; Thomsen et al., 2004; Alahmadi et al., 2016, 2015; Mapelli et al., 2017; Gagliano et al.,

2022). In contrast, the neocortical BOLD signal reflects many sources including inputs from other cortical regions, local activity (input and output), as well as ascending input. While the latter will include cerebellar input via the thalamus, this source is likely to make a relatively small contribution to the overall BOLD response in the neocortex. As such, the relationship between neocortical and cerebellar BOLD signals will be most informative in evaluating cortico-cerebellar connectivity.

We trained multiple models of neocortical-cerebellar connectivity on a fMRI data set obtained while human participants completed a large task battery that was designed to engage cognitive processes across a broad range of functional domains (e.g., visual cognition, memory, attention, cognitive control). The models varied in terms of the degree of convergence of cortical inputs onto each cerebellar area. To evaluate the models in a cross-validated fashion, we examined how well each model predicted cerebellar data obtained from different tasks and/or different participants, using only the corresponding neocortical data. These analyses reveal a novel picture of cortico-cerebellar connectivity, one in which the degree of convergence was higher in cerebellar regions associated with more complex cognitive functions.

2.3 Results

2.3.1 Overview

We compared three models of cortico-cerebellar connectivity by using a region-to-region predictive modeling approach (Cole et al., 2016; Mell et al., 2021). For each model, the task-evoked activity in each cerebellar voxel was predicted as a linear combination of task-evoked activity patterns across the entire neocortex (2.1). As a model of sparse connectivity, we used a Winner-Take-All (WTA) model which imposes the strong constraint that only a single cortical region is used to predict the activity in each cerebellar voxel. The other two

models allowed for some degree of convergence. Models estimated with Lasso Regression (L1 regularization) find sparse solutions, minimizing the number of cortical inputs by setting to zero those weights that make a negligible contribution to the predicted activity. Models estimated with Ridge Regression (L2 regularization) allow for a wide distribution of inputs, keeping each weight as small as possible. For model input, we used a set of cortical parcellations that varied in terms of their level of granularity. We trained the models on cortical and cerebellar fMRI data obtained from 24 participants who performed a task battery with 29 task conditions (Task Set A, 2.1 A). These were acquired over two sessions on separate days, with the tasks identical across sessions. These data were used to estimate the connectivity weights $\hat{\mathbf{W}}$ separately for each model and participant (see Methods).

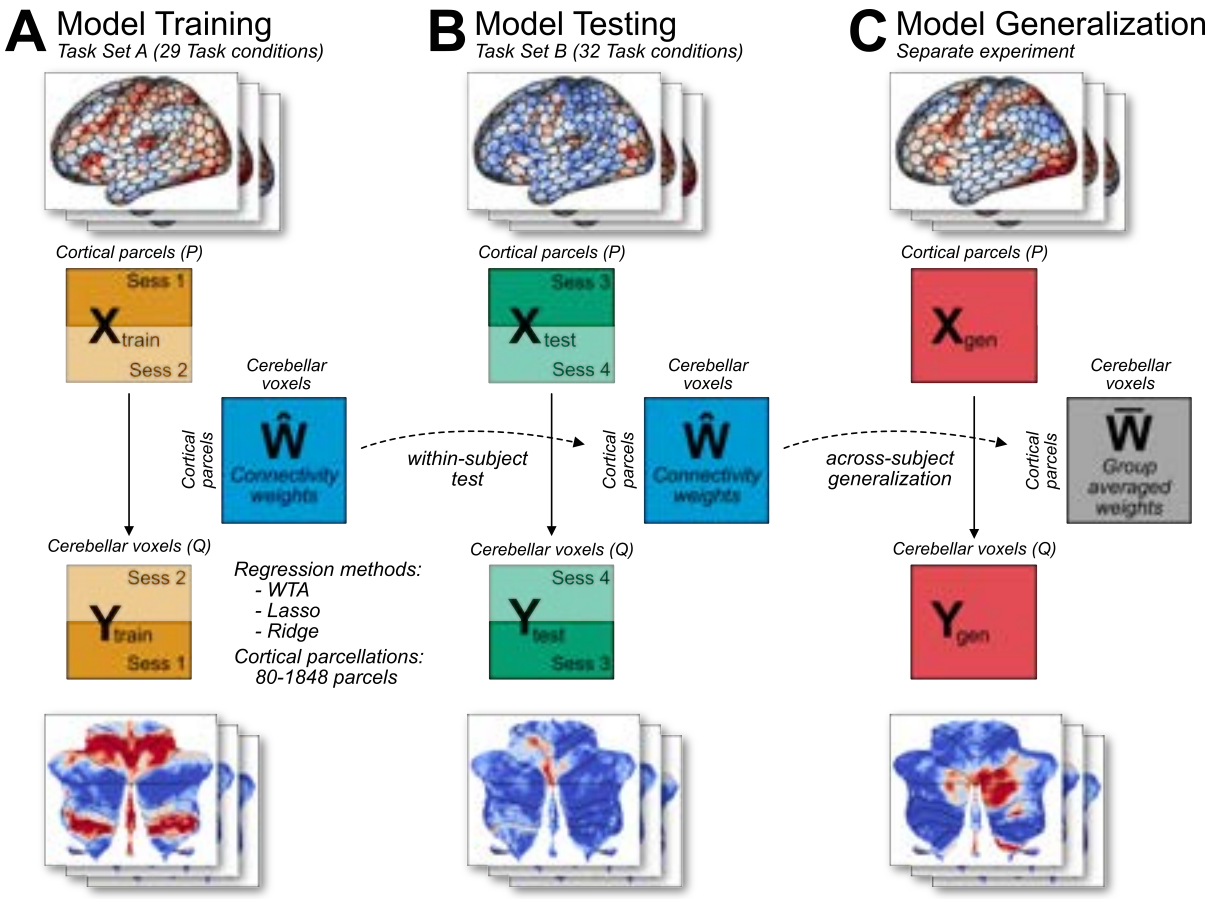

Figure 2.1: **Connectivity model training and evaluation. (A)** Models were trained on Task

Set A (session 1 and 2) of the multi-domain task battery (MDTB; (King et al., 2019)). Model hyperparameters were tuned using 4-fold cross validation. Three types of models were used (WTA, Lasso, Ridge), each with 7 cortical parcellations of different granularity. **(B)** Models were tested on an independent Task Set B (session 3 and 4), which included both novel and common tasks. Models had to predict the cerebellar activity solely from cortical activity patterns. To avoid the influence of shared noise correlations across cortex and cerebellum, the models were trained and tested by using cortical and cerebellar activity patterns from different sessions within each task set (see Methods). **(C)** As a test of generalization, the models were used to predict cerebellar activity from cortical data obtained from a separate experiment (King et al., unpublished data).

To compare the models, we tested their prediction performance on two independent datasets. First, we used data from the same 24 participants when tested in two different sessions (Task Set B) that included 18 novel conditions and 14 conditions repeated from Task Set A (2.1 B). To predict the cerebellar activity patterns, we used the observed cortical activity patterns from Task Set B and the estimated connectivity weights ($\hat{\mathbf{W}}$) from Task Set A for each participant. Note that because the model predictions relied on a single set of connectivity weights across all tasks, the input is based only on the cortical activity patterns without reference to any features of the tasks themselves. Second, we also tested how the models would generalize when tested with data from a new group of participants tested on a set of novel tasks (2.1 C).

The use of separate training and evaluation datasets allowed us to determine the best task-general model of cortico-cerebellar connectivity without overfitting the data. To validate that this approach enabled us to distinguish between different forms of cortico-cerebellar connectivity, we conducted a range of model recovery simulations (see Methods for details). Using the measured cortical activity for each participant, we generated artificial sets of cerebellar data imposing either a one-to-one or a many-to-one mapping. Following the procedure used with the real data, we trained the three models on Task Set A and tested them on Task Set B. The simulations (2.3) showed that the WTA performed best if each cerebellar

voxel was connected to only one cortical parcel, whereas ridge regression performed better if there was substantial convergence, with Lasso performing at an intermediate level. Thus, despite the presence of some degree of collinearity between the cortical parcels, these simulations demonstrate that our modeling approach is able to distinguish between different forms of connectivity.

2.3.2 Cortico-cerebellar connectivity is best captured by models with convergence

We first compared the different models, asking how well they predicted activity patterns obtained when the same participants were tested on Task Set B (2.2 A). Models allowing for some degree of convergence outperformed the WTA model, and this advantage was observed across all levels of cortical granularity. Indeed, the prediction performance for the Ridge, Lasso, and WTA models was relatively independent of granularity. Averaged across all levels of granularity, the Ridge models outperformed the WTA models ($F_{1,23} = 47.122, p < .001$). Post-hoc tests revealed that this advantage for the Ridge model was consistent across all levels of granularity, starting with a parcellation of 80 regions ($t_{23} = 5.172, p < .001$). We also found a significant difference in predictive accuracy between the Ridge and Lasso model ($F_{1,23} = 15.055, p < .001$). Post-hoc tests showed that there was no significant difference in predictive accuracy at the lowest level of granularity ($t_{23} = 1.279, p = 0.213$), whereas the difference was significant for the finer parcellations (all $t_{23} > 10.937, p < .001$).

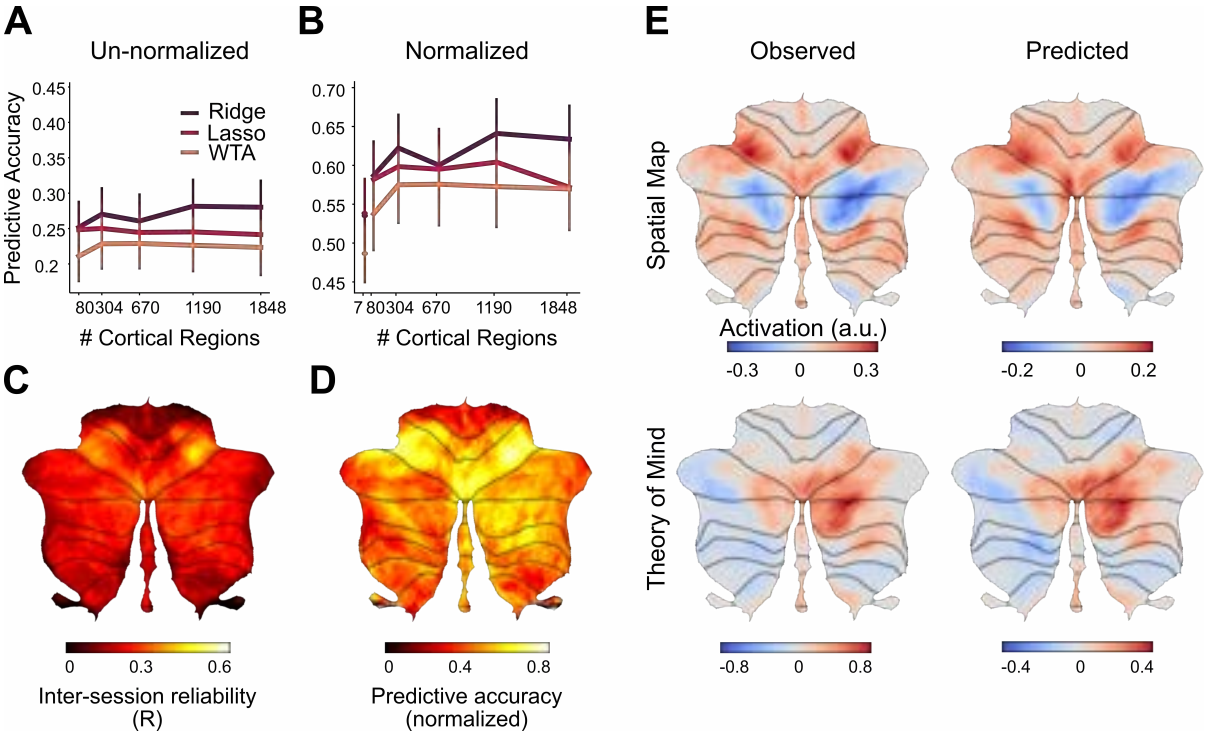

Figure 2.2: **Performance of cortico-cerebellar connectivity models.** **(A)** Predictive accuracy (Pearson correlation) of the Ridge, Lasso, and WTA regression models for the test data of Task Set B. **(B)** Predictive accuracy normalized to the noise ceiling based on reliability of both cerebellar and cortical data (see Methods)**(C)** Voxelwise map of inter-session reliability of the test data. **(D)** Voxelwise map of predictive accuracy of the Ridge model (1848 parcels), normalized to the noise ceiling. **(E)** Observed and predicted activity for a novel task involving spatial working memory (Spatial Map) and a social cognition task (Theory of Mind). The spatial map task was not included in Task Set A.

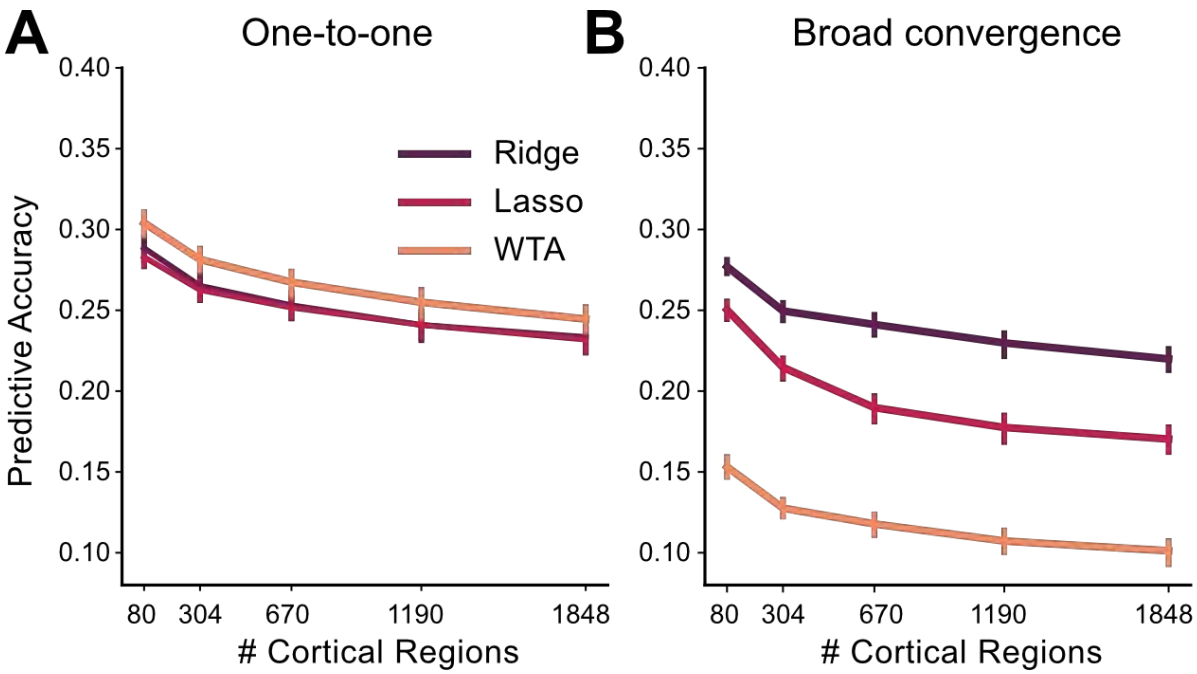

Figure 2.3: **Model recovery simulations** demonstrate the ability to identify different forms of cortico-cerebellar connectivity. Predictive accuracy for Ridge, Lasso, and WTA models trained and tested on simulated data generated using (A) one-to-one connectivity with each cerebellar voxel connected only to one randomly selected cortical region (B) broad convergence with connectivity weights being drawn from a Gaussian distribution. Data were simulated using the observed cortical activity for Task Set A and B for training and test data, respectively (see Methods for details). As expected, the WTA model provided the best prediction for the one-to-one architecture and the Ridge model provided the best prediction for the convergent architecture.

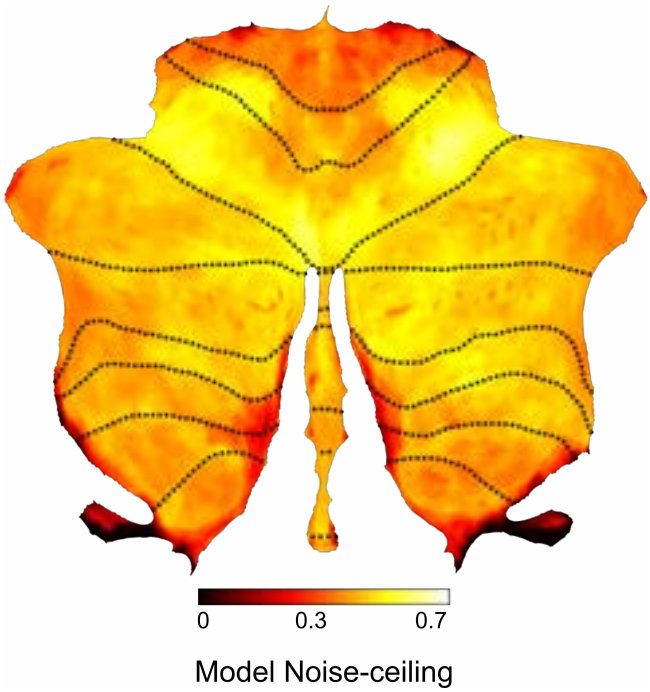

Figure 2.4: **Noise ceiling for Ridge model.** Expected predictive accuracy assuming that the fitted Ridge model (1848 parcels) reflects the true cortico-cerebellar connectivity. The noise ceiling takes into account the reliability of the cerebellar data, as well as the reliability of the prediction based on the measured cortical data.

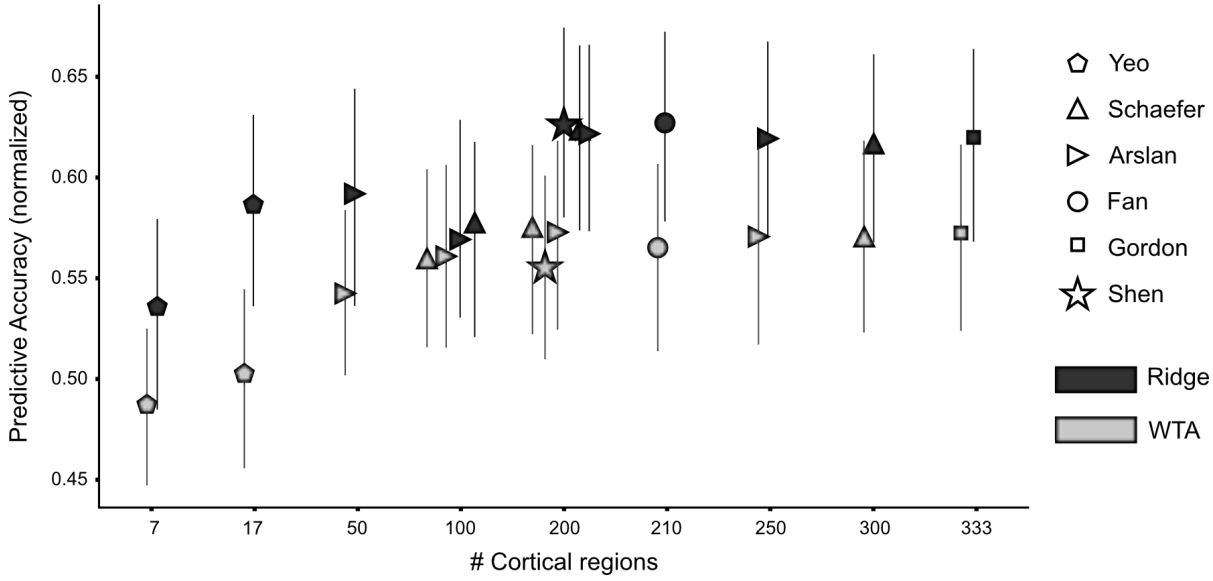

Figure 2.5: **Predictive accuracy for Ridge and WTA models using functional cortical parcellations** ((Yeo et al., 2011; Schaefer et al., 2017; Arslan et al., 2015; Fan et al., 2016; Gordon et al., 2016; Shen et al., 2013), denoted by first author). Predictive performance is normalized to the noise ceiling. The number of cortical parcels varied from 7 to 330 regions. All evaluated parcellations are available at `github.com/DiedrichsenLab/fs_LR_32` (Zhi et al., 2022).

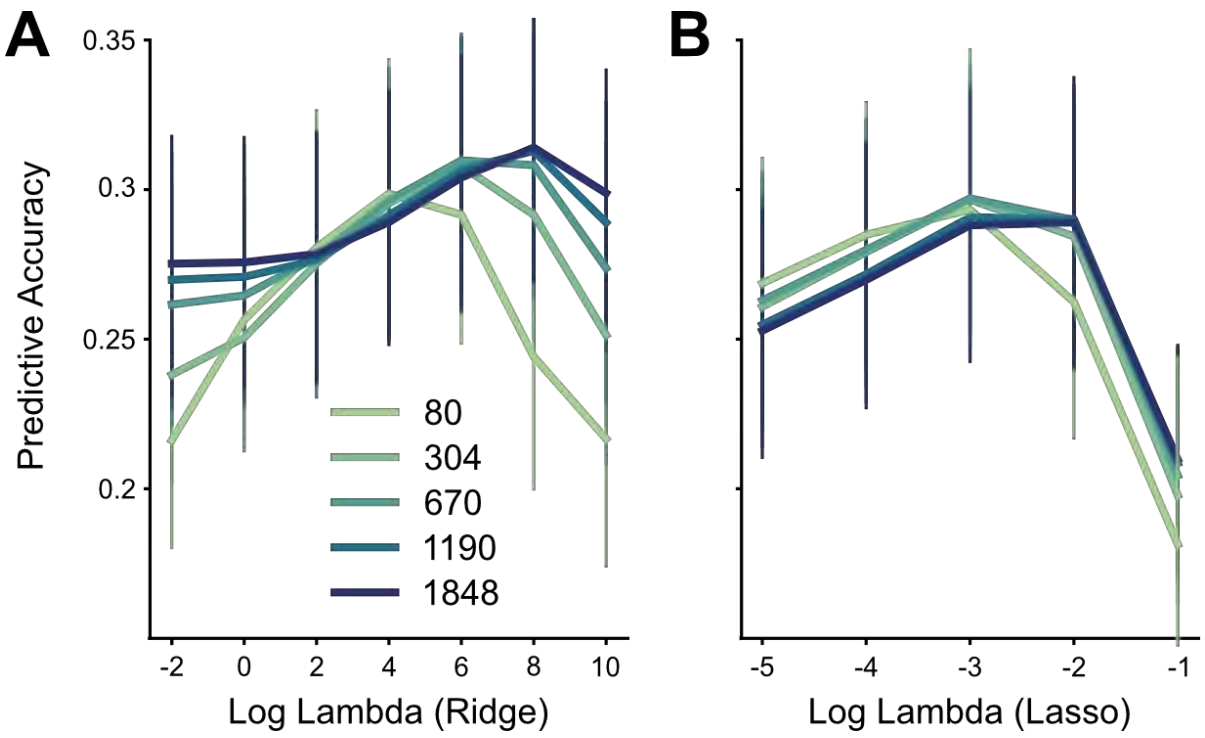

Figure 2.6: **Hyper-parameter tuning for connectivity models.** Predictive accuracy for Ridge **(A)** and Lasso **(B)** models using different regularization coefficients (log-lambda values) across five levels of granularity, and cross-validated over 4 folds of the training data. The WTA model did not use a hyper-parameter.

The mean predictive accuracy of the Lasso and Ridge models was 0.257 (2.2 A). There are two issues of note here. First, the models predicted activity of individual voxels, without any smoothing across cerebellar voxels. Thus, the upper bound for the predictive

accuracy is limited by the reliability of the cerebellar test data. The correlation of the measured cerebellar activity patterns across the two sessions of Task Set B was, on average, r = 0.51 (SD = .102). Reliability was fairly consistent across the cerebellum (2.2 C), with some decreases in lobules I-IV. This dropoff likely reflects the fact that our battery only included hand and eye movements, and did not activate the lower body representation that is prominent in this area. Second, predictive accuracy is also limited by the reliability of the cortical data that was used to make the prediction. This is an especially limiting factor for WTA models that use fine granularity, since the predictions will be based on data obtained from a small cortical region.

Given these issues, we calculated a noise ceiling for each model, taking into account the reliability of the cerebellar data, the reliability of the cortical data, and the effect of granularity (see Methods, 2.4). As an unbiased comparison of the model predictions, 2.2 B re-plots the predictive accuracy of each model normalized by its noise ceiling. As with the original analysis, the Ridge model significantly outperformed the WTA model ($F_{1,23} = 16.49, p < .01$), and in post-hoc tests, the advantage was especially pronounced for finer parcellations (1848 regions; $t_{23} = 5.073, p < .001$). Overall, the noise ceiling calculation showed that the Ridge model was able to predict approximately 45% of the systematic variance of the cerebellar activity patterns across tasks (average R2=0.672). While the predictive accuracy (2.2 D) was best in anterior motor regions, it was reasonably high across the entire cerebellar surface.

The predicted and observed activity patterns for two exemplary tasks (2.2 E) demonstrate the quality of these predictions at the group level. In both of these examples, (spatial working memory and social cognition tasks), the connectivity model predicted the pattern of task activity with a high degree of fidelity. This is especially compelling for the spatial working memory task as the training set did not include a task with similar characteristics.

To ensure that our results were not biased by the use of an essentially arbitrary parcellation of the neocortex, we repeated the analysis using a range of published functional

parcellations. For example, we used a 7-network cortical parcellation based on resting state fMRI data (Yeo et al., 2011) to train and test the three models. Here, too, the WTA model was inferior to the Ridge models ($t_{23} = 2.956, p < .01$), with no performance difference between Ridge and Lasso models ($t_{23} = -1.235, p = 0.229$). The same pattern held when we used other common functional parcellations of the neocortex (2.5). In summary, these results demonstrate that models which entail some degree of convergence from the neocortex to the cerebellum outperform a model in which cerebellar activity is based on input from a single cortical region. This conclusion holds across a broad range of cortical parcellations (Zhi et al., 2022).

2.3.3 Convergence of neocortical inputs varies across the cerebellum

To gain insight into where these cortical inputs came from, we visualized the cortical weights for each of the 10 functional regions of the cerebellum (2.7). As expected given the crossed connectivity between M1 and lobules IV/V (Kelly and Strick, 2003; Krienen and Buckner, 2009; O'Reilly et al., 2010), the input to the hand regions of the cerebellum (regions 1 and 2) was centered around the contralateral primary sensorimotor cortex with some additional input from premotor and parietal cortex. Regions 3 and 4 are the other two cerebellar regions associated with motor function. Activity in region 3, the oculomotor vermis, is predicted by a bilateral set of cortical regions including the frontal eye fields (FEF), regions in the intraparietal sulcus, and extrastriate visual regions. Region 4, an area strongly activated during action observation, is predicted by a bilateral network of regions including premotor cortex, supplementary motor cortex (SMA) and parietal cortex. Cerebellar regions 5-10, the regions associated with more cognitive processes are predicted by a distributed set of cortical regions, with stronger input coming from the contralateral cortical hemisphere. For example, cerebellar region 5, a region restricted to the left cerebellum, receives much stronger input from the right cerebral hemisphere. In summary, these results suggest that most cerebellar regions are best predicted by multiple cortical regions, pointing to some

degree of cortical-cerebellar convergence.

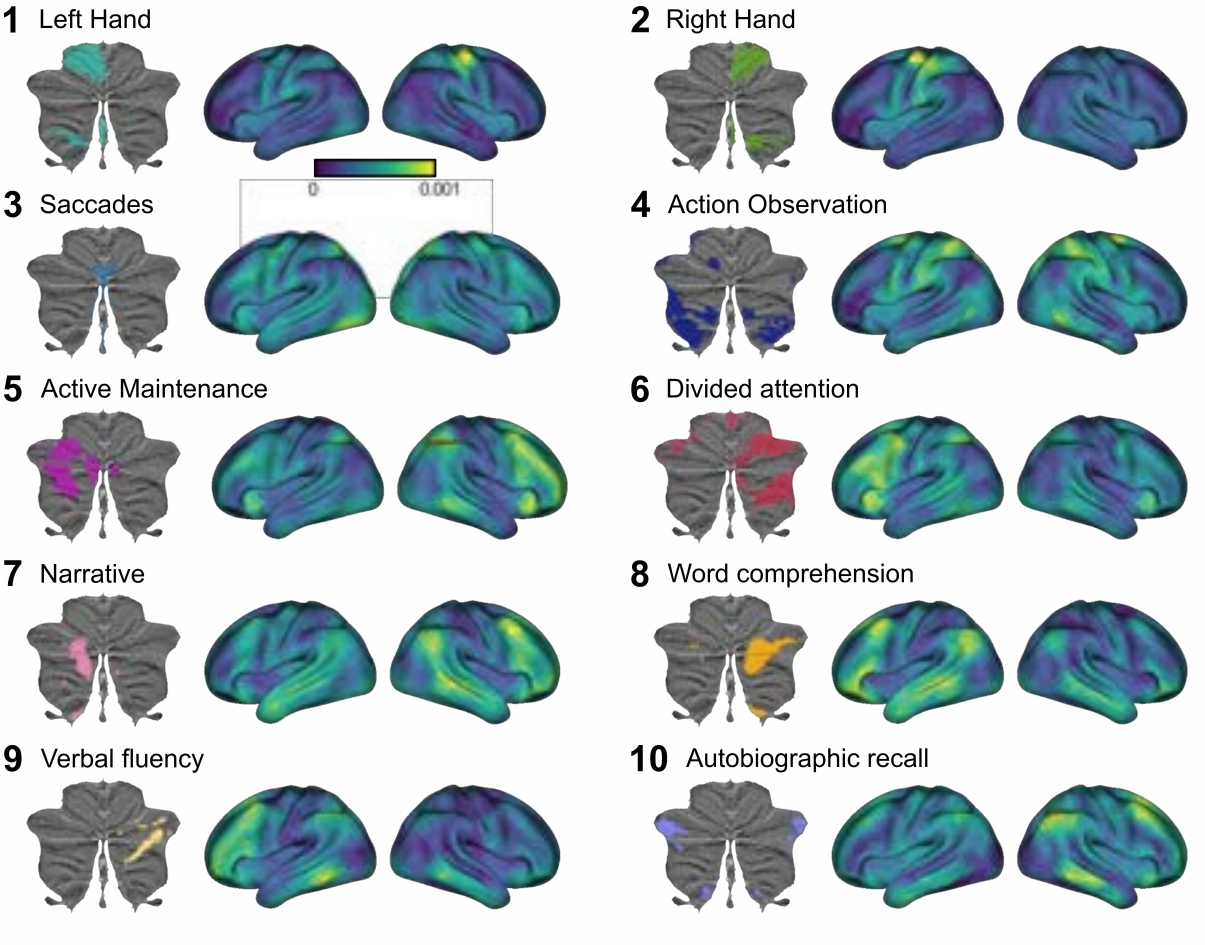

Figure 2.7: **Cortical connectivity weight maps** for the Ridge regression model with 1848 cortical parcels for each of 10 functional cerebellar regions. Each region is denoted by the most important functional term (King et al., 2019). Results are averaged across participants. Regression weights are in arbitrary units. See Figure 3-animation 1 for a gif of the connectivity weight maps, and see 2.8 for the corresponding analysis using Lasso regression. 2.7 has been adapted from Figure 5 from King et al. (2019)

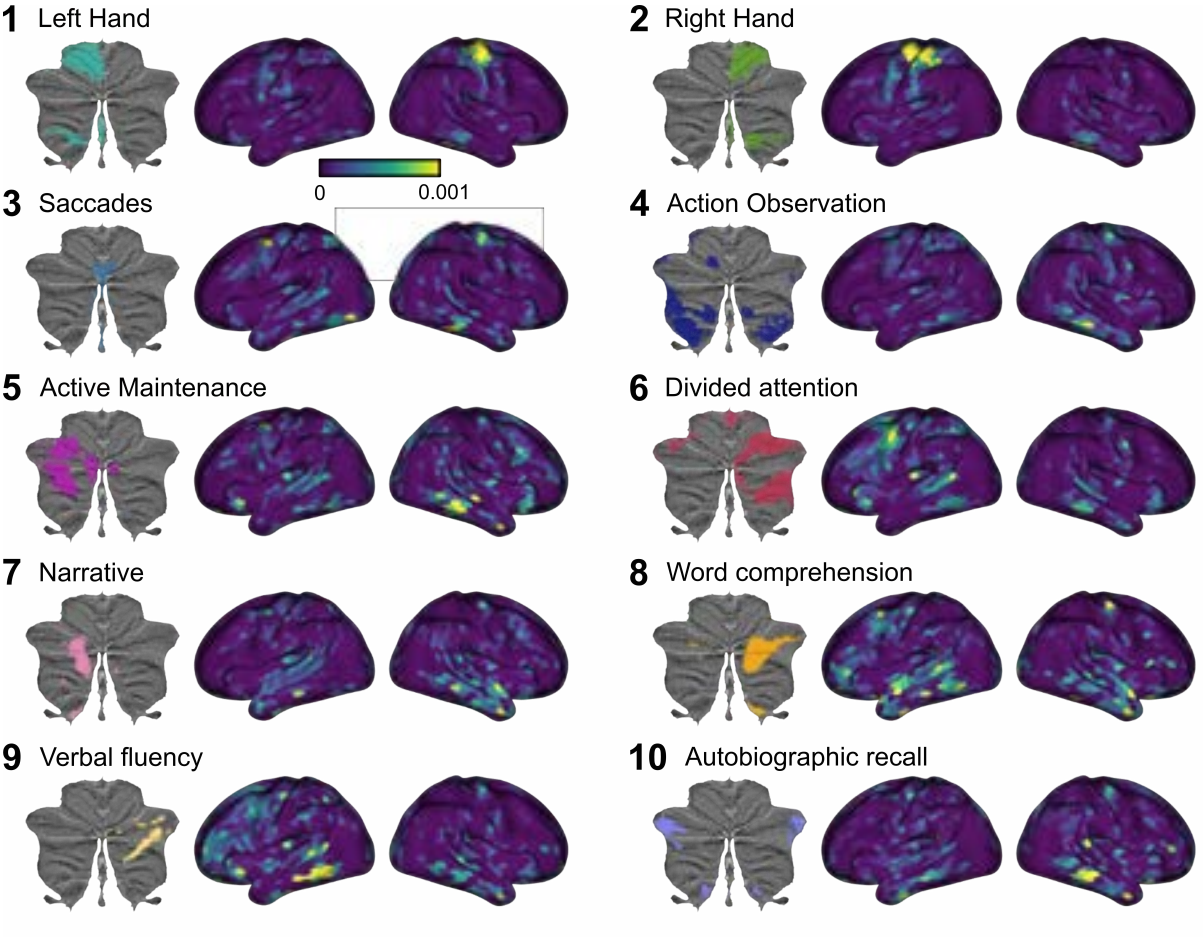

Figure 2.8: **Cortical connectivity weight maps for the Lasso model with 1848 cortical regions.** As in 2.9, the results are averaged across individuals for each of the 10 functional regions defined on the MDTB data set, with each region denoted by the most important functional term. Results are averaged across participants and voxels within each cerebellar region. Regression weights are in arbitrary units.

Visual inspection of the connectivity patterns (2.7) also highlights interregional variation of convergence. For example, inputs to hand motor regions MDTB (regions 1 & 2) arise from a relatively small area of the neocortex, while inputs to regions in lobule VII (regions 3-10) come from a larger area. To quantify this observation, we tallied the number of non-zero regression weights for each cerebellar voxel as a measure of its input surface area. For this calculation, we used the Lasso model (80 cortical parcels) since it uses the

minimal set of cortical areas necessary for predicting each cerebellar voxel. As the Lasso model forces the estimates of the other weights to zero, it allows for a quantification of input area without applying an arbitrary threshold. This calculation revealed a substantial variation in the degree of convergence across the cerebellar cortex (2.9 A). For example, predicting the activity pattern of voxels within Crus I required inclusion of up to 10% of the cortical surface whereas predicting the activity of voxels in the anterior lobe required less than 5% of the neocortex.

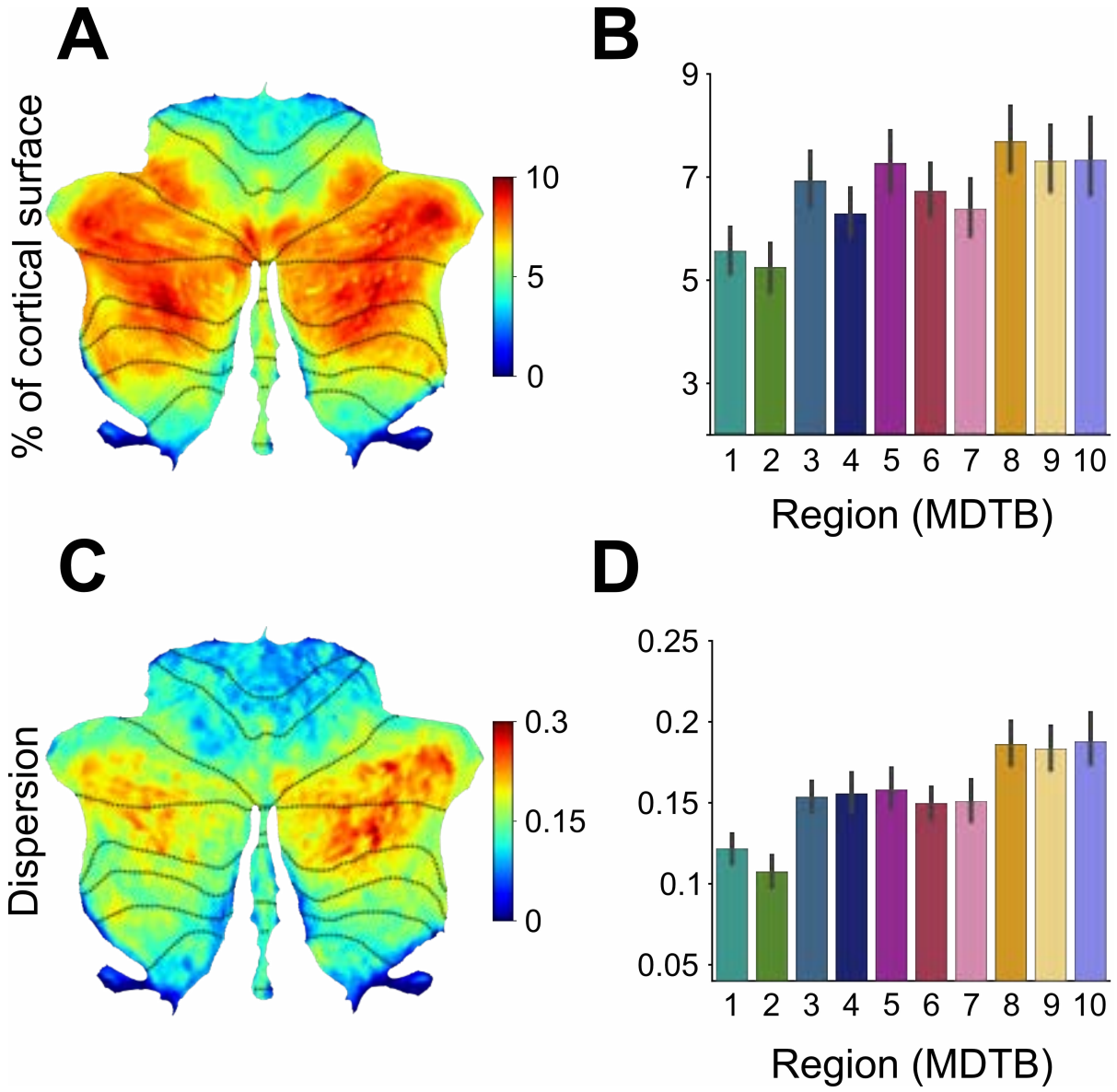

Figure 2.9: **Figure 4. Cortico-cerebellar convergence measures using the Lasso model.** **(A)** Map of the cerebellum showing percentage of cortical parcels with non-zero weights for the Lasso model (n=80 parcels). **(B)** Percentage of parcels with non-zero weights for functional subregions of the cerebellum. **(C)** Spherical dispersion of the connectivity weights on the cortical surface for each cerebellar voxel. **(D)** Average cortical dispersion for each functional subregion of the cerebellum. Error bars indicate standard error of the mean across participants. See 2.10 for the same results using Ridge regression.

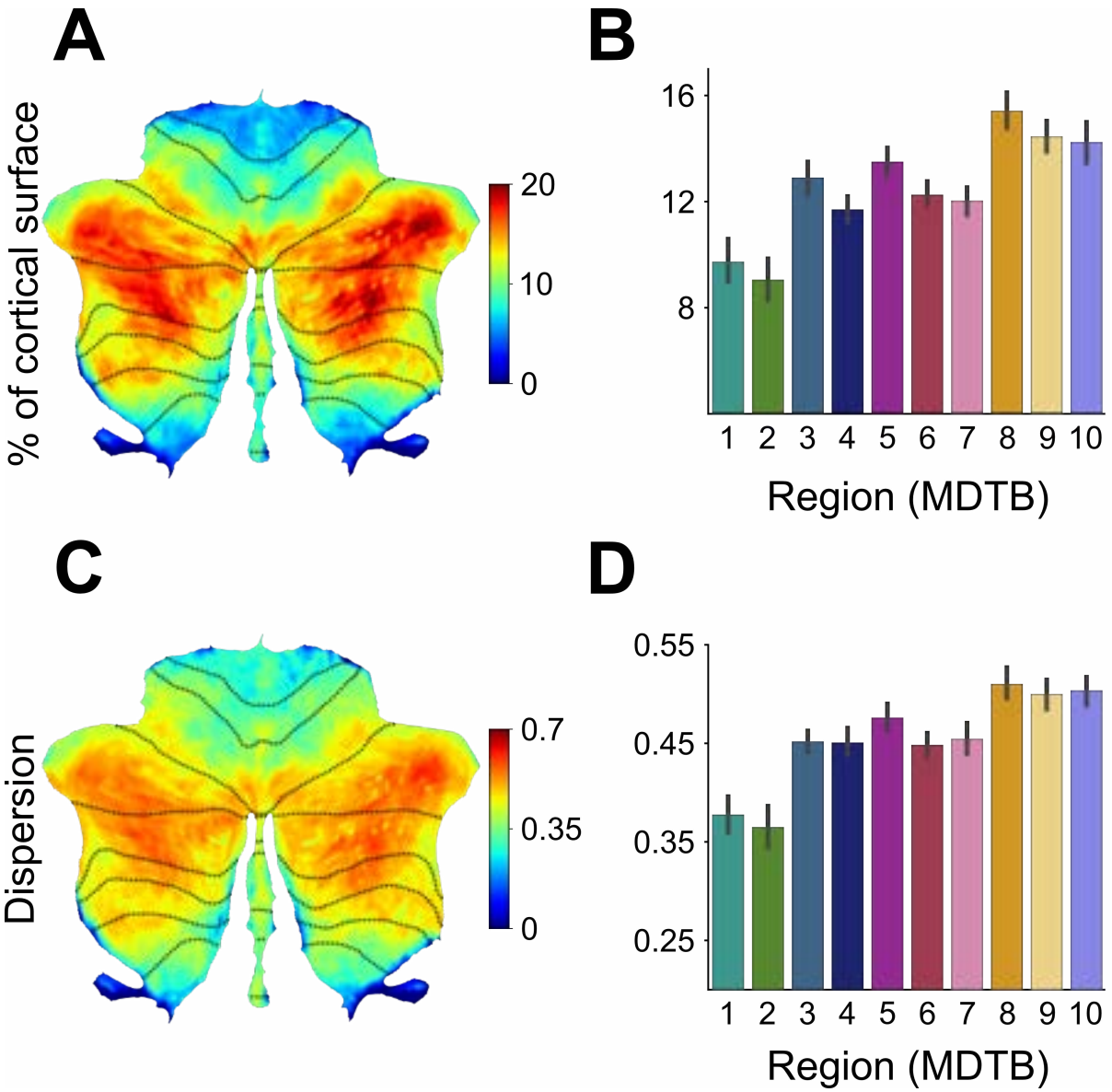

Figure 2.10: **Cortico-cerebellar convergence measures using the Ridge model. A)** Map of the cerebellum showing percentage of cortical parcels with coefficients for the Ridge model (n=80 parcels) above threshold (see Methods). **B)** Percentage of parcels with weights above threshold for functional subregions of the cerebellum. **C)** Spherical dispersion of the connectivity weights on the cortical surface for each cerebellar voxel. **D)** Average cortical dispersion for each functional subregion of the cerebellum. Error bars indicate standard error of the mean across participants.

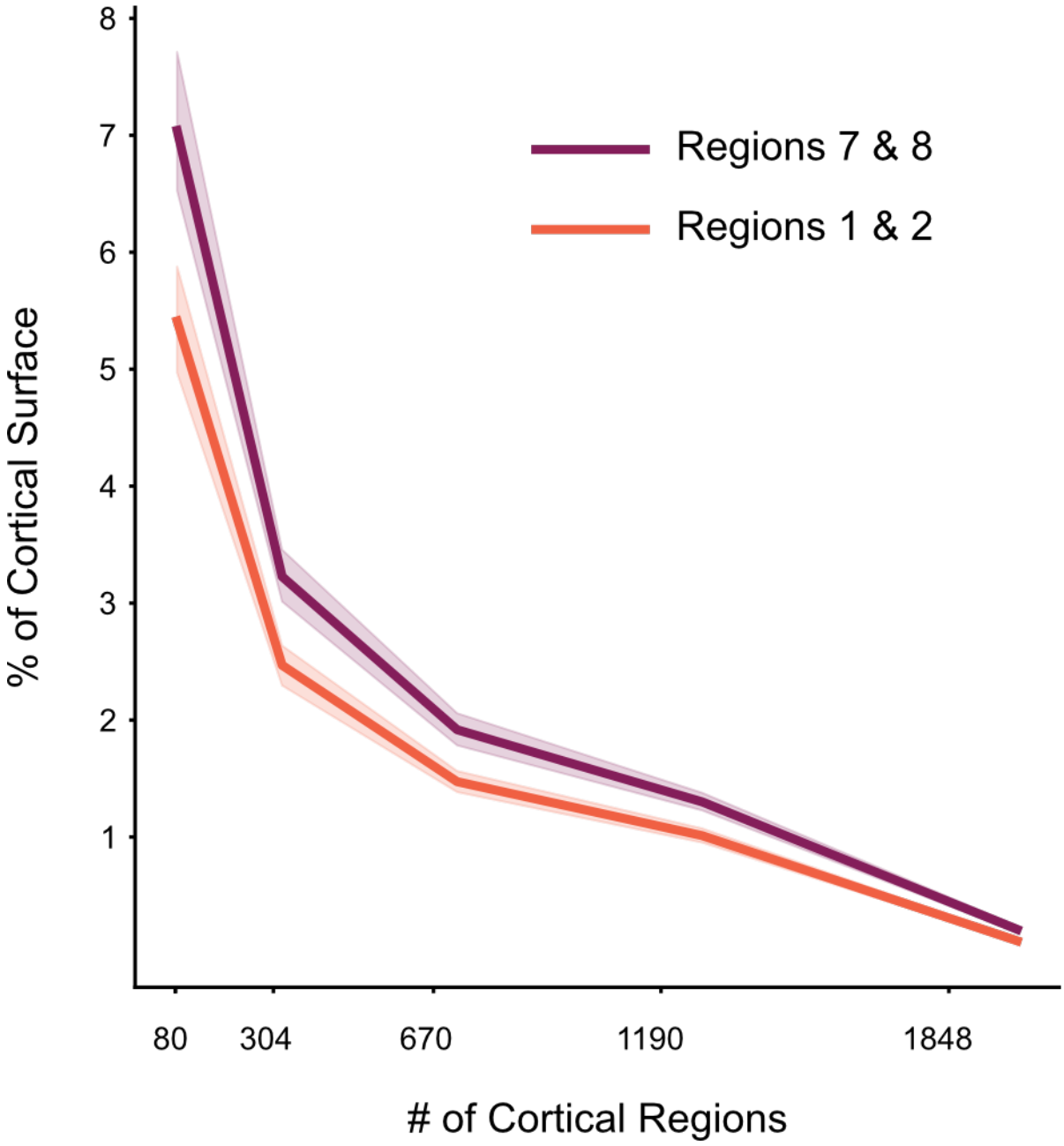

Figure 2.11: **Percentage of cortical surface across levels of granularity for Lasso regression model.** Calculation is performed as in 2.7 B. The results are averaged across the two hand regions of the cerebellum (MDTB functional parcellation, regions 1 and 2), and regions related to narrative and word comprehension (regions 7 and 8).

To statistically analyze these data, we opted to bin the cerebellar data using a

functional 10-region parcellation of the cerebellum (King et al., 2019). This analysis confirmed that the size of the estimated cortical input area differed across functional regions ($F_{9,207} = 7.244, p < .001$, 2.9 B). The lowest level of convergence was observed for regions 1 and 2, the anterior hand regions of the cerebellum. The highest levels of convergence were found in regions of the cerebellum associated with more cognitive functions (e.g., regions 7 and 8, areas engaged during language comprehension). Noteworthy, this pattern holds for cortical parcellations of different levels of granularity (2.11), as well as for the thresholded coefficients from the Ridge regression models (2.10A, B).

To assess whether these differences were driven by the collinearity of the cortical data, rather than by cortical-cerebellar connectivity, we ran a simulation (see Methods, model recovery simulations) in which we replaced the cerebellar data with the activity profile of the most similar cortical parcel. In this simulation, we did not find any differences in the area of estimated input across cerebellar regions ($F_{9,207} = 1.762, p = 0.076$). Thus, the observed variation in convergence cannot be explained by the collinearity between different cortical input regions.

As an independent method to quantify convergence, we determined the spatial spread of the inputs across the cortical surface. For example, MDTB region 4, which is activated by action observation, is explained by a set of cortical regions with a relatively small surface area. Nonetheless these regions are spread widely across the cortex (e.g., fusiform gyrus, parietal and premotor regions).For a measure of dispersion, we calculated the spherical variance of the non-zero connectivity weights on an inflated model for each cerebral hemisphere (see Methods). This analysis revealed a similar pattern as seen in the surface area measure (2.9 C, D, $F_{9,207} = 18.322, p < .001$). For example, the cortical inputs to the hand motor regions of the cerebellum were more concentrated whereas the cortical inputs to lobule VII were more dispersed. Again, this pattern also holds for the Ridge models (2.10 C, D).

In summary, we observed variation in the degree of cortico-cerebellar convergence

across the cerebellar cortex. In particular, cerebellar motor areas such as the hand region in lobule V and VIII received relatively focal cortical input whereas cerebellar areas associated with cognitive processes (e.g., language, working memory) in lobule VII exhibited a higher degree of convergence.

2.3.4 Cortico-cerebellar connectivity model predicts new cerebellar data

A strong test of a model is how well it predicts novel data obtained in contexts distinct from that data used to develop the model. We conducted a generalization test using data from a separate experiment involving novel tasks and new participants. The data came from a study in which participants were trained over multiple sessions on five tasks, selected to span a set of distinct cognitive domains.

All three model types (WTA, Lasso, Ridge) were evaluated, using the connectivity weights estimated from Task Set A of the main study. Because the new study had different participants, we averaged the weights for each model across the individuals in the training set. These group-averaged weights were then used to predict cerebellar activity patterns for the new data.

As shown in 2.12, the connectivity models were generally successful in predicting cerebellar activity patterns for the new dataset. The overall pattern is quite similar to that seen in the initial model tests (in which we had used data from different tasks) but involved training and test data from the same participants). Predictive accuracy was stable across levels of cortical granularity and the Ridge model provided the best overall predictive accuracy (r = .657) and the WTA (r = .352) the worst predictive accuracy. These results provide evidence that our cortico-cerebellar connectivity models capture important aspects of connectivity that are stable both across tasks and participants. Moreover, in accord with the earlier analyses based on predictions at the individual level, this generalization analysis

again suggests that approximately 43% of the variation of cerebellar activity across tasks can be predicted by cortical activity alone.

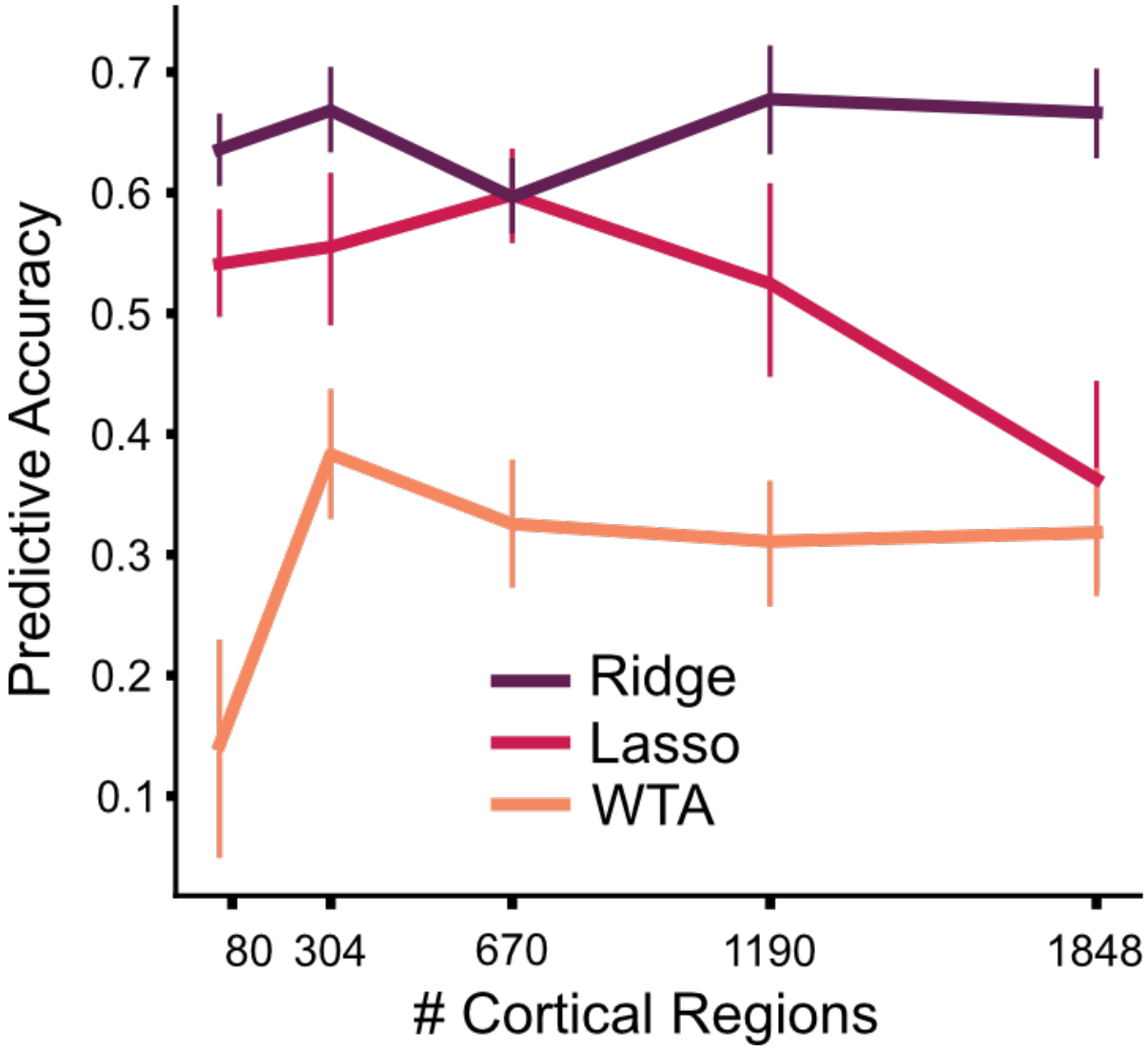

Figure 2.12: **Figure 5. Generalization to new dataset.** Models of cortico-cerebellar connectivity are tested in a new experiment. Each model is tested across different levels of cortical granularity. Predictive accuracy is the Pearson correlation between observed and predicted activity patterns, normalized to the noise ceiling.

2.4 Discussion

To date, models of connectivity between the human neocortex and cerebellum have been based on fMRI resting-state data (Buckner et al., 2011; Ji et al., 2019; Marek et al., 2018). This work demonstrates that each region of the cerebellum receives input from a distinct set of cortical regions. For example, anterior and posterior cerebellar motor regions show correlated activity with contral-lateral sensorimotor cortex and non-motor or "cognitive" cerebellar regions show correlated activity with specific parietal and frontal association areas.

Despite these important insights, previous work has not been designed to examine the patterns of convergence between the neocortex and cerebellum. Resting state connectivity maps are generally produced by assigning each cerebellar voxel to a single cortical network, a de facto winner-take-all model. In the present study, we quantified and compared models of cortico-cerebellar connectivity. The models differed in the degree of convergence of cortical inputs to each cerebellar region, ranging from an architecture constrained to a strict one-to-one mapping to architectures that allowed for distributed inputs. We evaluated these models in terms of how well they could predict cerebellar activity patterns on a novel Task Set. For nearly the entire cerebellum, models that allowed for some convergence predicted cerebellar activity better than the WTA model.

2.4.1 Convergence differs across Cerebellar Circuits

Importantly, the amount of convergence differed across the cerebellar cortex. Specifically, regions in anterior (lobules I-V) and inferior cerebellum (lobules VIII-X) were well predicted by a relatively small and concentrated area of the neocortex. In contrast, regions in lobule VI and especially lobule VII required input from a larger and spatially more dispersed set of cortical regions that were primarily located in association areas of prefrontal, parietal,

and cingulate cortex. This finding underscores the heterogeneity of cortico-cerebellar connectivity with some cerebellar areas functioning in nearly a 1:1 relationship with a single cortical region, whereas other areas integrate input from a more diverse set of cortical regions.

This variation bears some resemblance to a motor/cognitive gradient identified from resting state data (Guell et al., 2018). However, there are a few notable exceptions. First, based on our evaluation metrics, Region 3 (oculomotor vermis) was best explained by a large and relatively dispersed set of cortical regions, including intraparietal sulcus, the frontal eye fields (FEF), and extrastriate visual areas (2.9). Second, sub-regions of lobules IX, functionally associated with non-motor tasks (Buckner et al., 2011), are best explained by a relatively restricted set of cortical regions (2.9 A, C). Thus, rather than following a functional distinction, it appears that regions with strong convergence are anatomically restricted to lobules VI and VII, two areas that have disproportionately increased in size during primate evolution (Balsters et al., 2010).

Variation in cortico-cerebellar connectivity has important implications for theories of cerebellar function (De Zeeuw et al., 2021; Diedrichsen et al., 2019; Henschke and Pakan, 2020). A cerebellar region that forms a closed-loop circuit with a single cortical region can only fine-tune the computational processes that are ongoing in its connected cortical region. In contrast, a cerebellar region that receives convergent input would be able to coordinate the interactions between dispersed cortical regions. Indeed, using a rodent model, Pisano et al. (2021) have identified cerebellar areas that project back to multiple cortical areas, providing a substrate by which the cerebellum can influence neuronal dynamics not only in a focal cortical area but also interactions within networks of cortical areas (Pisano et al., 2021).

2.4.2 Task-based vs. resting-state connectivity analyses

While our modeling approach could be applied to resting-state data, we opted to use the data from the multi-domain task battery for a variety of reasons. First, the breadth of tasks included in the battery assured that there would be reliable variation in activity across most of the neocortex and cerebellum, a necessary precondition for building a complete connectivity model. Second, the dataset allowed us to avoid biases that arise from correlated noise across abutting cortical and cerebellar regions (Buckner et al., 2011). We used the cortical activity patterns from one session to predict cerebellar activity patterns in a different session, relying on the fact that measurement noise is independent across sessions. Third, the MDTB data set allowed us to test the model across a broad set of tasks and mental states. While resting-state correlations are predictive of task-based activation patterns (King et al., 2019; Tavor et al., 2016; Zhi et al., 2022), resting in an fMRI scanner is arguably a relatively restricted situation. Our generalization test shows that the connectivity model can robustly predict activity patterns for new tasks and participants.

2.4.3 Directionality of the model

We opted in the present study to model the correlations between neocortical and cerebellar activity in a directional manner, making inferences from these data about connectivity from the neocortex to the cerebellum. We recognize that the two structures communicate with each other in a closed loop. Our decision to focus on cortico-cerebellar connectivity is based on studies of cerebellar blood flow in rodents. Increases in cerebellar blood flow, a major contributor to the BOLD signal, are the result of increases in mossy fiber activity, the primary input to the cerebellar cortex (Alahmadi et al., 2015, 2016; Gagliano et al., 2022; Mapelli et al., 2017; Mathiesen et al., 2000; Thomsen et al., 2004). In contrast, even a dramatic increase in the (complex or simple spike) firing rate of Purkinje cells does not produce a measurable change in blood flow within the cerebellar cortex (Thomsen et al., 2004, 2009).

Thus, the cerebellar BOLD signal provides a relatively clear image of the cortical inputs to the cerebellum; importantly, this signal does not provide information about the output of the cerebellar cortex (or cerebellum in general). In contrast, the BOLD signal in the neocortex reflects a combination of signals including local inputs/outputs across cortical layers, inputs from other cortical regions, and ascending inputs such as from the thalamus which will include input from the cerebellum. Given this asymmetry, a priori, we should expect that correlations in the fMRI signal between the neocortex and cerebellum will more strongly reflect the flow of information from the cortex to the cerebellum than the reverse.

Nonetheless, it is possible that some of the convergent inputs identified in our modeling work may be due to divergent projections from a single cerebellar region to multiple cortical regions. Indeed, recent viral tracing work has shown that some cerebellar areas project to the reticular nuclei in the thalamus, which in turn projects to a wide array of cortical regions (Kelly and Strick, 2003; Pisano et al., 2021). A complete analysis of the entire cortico-cerebellar circuit will require the methods such as viral tracing techniques (Kelly and Strick, 2003; Pisano et al., 2021) or functional activation measures that target key nodes in the ascending pathway (deep cerebellar nuclei, thalamus).

2.4.4 Methodological limitations

Inter-region correlations of fMRI data can of course only provide indirect evidence of true functional connectivity. As such, it is important to consider methodological limitations that may influence the validity of our conclusions. From a statistical perspective, it was not clear, a priori, that we would have the power to distinguish between models of connectivity given that there can be substantial collinearity between different cortical regions. The model-recovery simulations (2.3 A, B) suggest that the present dataset was suitable to make such inferences, namely, activity patterns in different cortical regions were sufficiently de-correlated, likely reflecting the use of a broad task battery. Thus, we were able to recover

the correct model used to simulate the data, regardless of whether we assumed one-to-one connectivity or different degrees of convergence.

However, the simulations also indicated that the approach (and data) was not sufficient to determine the absolute degree of convergence with high confidence. For example, the size of the cortical input area for each cerebellar region differed substantially between the Ridge and Lasso regression models (2.7 vs. 2.8). Nonetheless, the two models result in similar predictive accuracy when using real data. Therefore, the true extent of the cortical input to a cerebellar region likely lies somewhere between the extremes provided by the Ridge and Lasso models. Importantly, this ambiguity does not impact the core observation that the degree of convergence varies systematically across the cerebellar cortex. Whether using measures based on cortical surface area or dispersion, the general picture of variation in connectivity holds for both the Ridge and Lasso models, as well as when using cortical parcellations of different granularity. Thus, we are confident that the variation in convergence reflects a stable, method-independent characteristic of the cortico-cerebellar system.

2.4.5 Future directions

Our approach was designed to identify the best task-general model of cortico-cerebellar connectivity. The connectivity model was able to take cortical activity patterns to make fairly accurate predictions of cerebellar activity, even when the data were obtained in a completely separate experiment from that used to build the model. This finding suggests that a substantial proportion of the cortico-cerebellar communication can be described by fixed information flow (Cole et al., 2016); that is, each area of the cerebellum simply receives, independent of task, a copy of the neural activity occurring in the corresponding cortical areas.

However, the task-general model did not provide a perfect prediction of cerebellar activity. While these predictions may improve with more training data, we believe that there

will likely be some systematic failures of the model. Such task-dependent deviations from the model prediction may offer important insights into cerebellar function, indicating that the cerebellum is more active than predicted by the cortical activity for some tasks and less for others. This pattern would suggest a "gating" of cortical input to the cerebellum, perhaps within the pontine nuclei, which is the main relay station of cortical inputs to the cerebellum. Rather than just transmitting cortical input to the cerebellar cortex, these nuclei may serve as an adaptive gate (Schwarz and Thier, 1999), amplifying or attenuating information as a function of the relative importance of cerebellar processing for the current task.

The models presented here allow us to detect such deviations by comparing the observed cerebellar activity for any task against the activity that is predicted by a task-invariant connectivity model. As such, the model provides a potent new tool to test hypotheses concerning cerebellar function.

2.5 Methods

2.5.1 Multi-domain task battery

To build models of cortico-cerebellar connectivity, we used the publicly available multi-domain task battery dataset, MDTB; (King et al., 2019). The MDTB includes fMRI data from two independent Task Sets (A & B). Each set consists of 17 tasks, eight of which were common to both sets. The 26 unique tasks were designed to sample activity during a broad range of task domains including motor (e.g., sequence production), working memory (e.g., 2-back task), language (e.g., reading), social (e.g., theory of mind), cognitive control (no-go, Stroop), and emotion (e.g., facial expression) (see Supplemental Table 1 in (King et al., 2019)).

24 participants (16 females, 8 males, mean age = 23.8) were scanned during four

sessions, with Task Set A employed in sessions 1 and 2 and Task Set B in sessions 3 and 4. Within a session, there were eight 10-minute runs, with each run composed of 17 blocks of 35 s each. Each block involved a unique task and included an initial 5 s instruction period. Most tasks contained multiple conditions (i.e., different levels of difficulty), resulting in a total of 47 unique task conditions.

2.5.2 Image acquisition and preprocessing

All fMRI and MRI data were collected on a 3T Siemens Prisma located at the Center for Functional and Metabolic Mapping at Western University, Canada. The protocol used the following parameters: 1 s repetition time; field-of-view measuring 20.8 cm; P-to-A phase encoding direction; 48 slices; 3 mm thickness; in-plane resolution 2.5×2.5 mm2 . In order to localize and normalize the functional data, a high-resolution anatomical scan (T1-weighted MPRAGE, 1 mm isotropic resolution) of the whole brain was acquired during the first session.

Functional data were realigned for head motion artifacts within each session and different head positions across sessions using a six-parameter rigid body transformation. The mean functional image was co-registered to the anatomical image and this rigid-body transformation was applied to all functional images. No smoothing or group normalization was applied. SPM12 (`www.fil.ion.ucl.ac.uk/spm/doc/spm12_manual.pdf`) and custom-written scripts in MATLAB were used to conduct data pre-processing.

2.5.3 General Linear Model (GLM)

To generate estimates of the activity related to each task condition, a general linear model (GLM) was fitted to the time series data of each voxel (ti). This was done separately for each imaging run and Task Set (A & B). The Design matrix for the GLM ($\mathbf{Z_1}$) of the GLM

consisted of the regressors for the different conditions, plus separate regressors for each of the 5-second task-specific instructions period. For each Task Set, the beta weight for each task condition was averaged across the 8 runs within a session, resulting in the average activity estimate for that session ($\bar{\mathbf{b}}_j$) for each voxel. The regressor for Task Set A resulted in 46 activity estimates (17 Instructions + 29 condition regressors) per session and Task Set B resulted in 49 activity estimates (17 instructions + 32 conditions regressors) per session.

2.5.4 Neocortex Surface Reconstruction

For each of the 24 participants, the anatomical surfaces of the cortical hemispheres were reconstructed using the standard recon-all pipeline of the FreeSurfer package (Fischl, 2012) (v. 5.0). The pipeline included brain extraction, generation of white and pial surfaces, inflation, and spherical alignment to the symmetric fsLR-32k template (Van Essen et al., 2011). Individual surfaces were re-sampled to this standard grid, resulting in surfaces with 32,492 vertices per hemisphere.

2.5.5 Spatial Normalization of Cerebellar Data

The cerebellum was isolated and normalized to the high-resolution Spatially Unbiased Infratentorial Template of the cerebellum using the SUIT toolbox (Diedrichsen, 2006). This non-linear transformation was applied to both the anatomical and functional data. Task condition activity estimates (i.e., the beta weights) were resampled to a resolution of 3 mm isotropic and resliced into SUIT space. The cerebellar isolation mask was edited to remove voxels in the superior cerebellum that abutted voxels in the primary visual cortex. Functional images were masked with the cerebellar isolation mask resulting in activation signals that originate only from the cerebellar cortex. The cerebellar data were visualized using a surface-based representation of the cerebellar gray matter included in the SUIT toolbox (Diedrichsen and Zotow, 2015). This flat map is not intended to represent a true unfolding

of the cerebellar cortex, but rather provides a convenient way to visualize volume-averaged cerebellar imaging data in a 2d representation.

2.5.6 Connectivity Models

All of the task-based connectivity models were, in essence, multiple-regression models in which the data for each of cerebellar voxels (yi) was modeled as a linear combination of Q cortical parcels (X, see next section).

$$\mathbf{y}_i = \mathbf{X}\mathbf{w}_i + \mathbf{e}_i \tag{2.1}$$

By combining the data (Y), the connectivity weights (W), and the measurement error (E) for each cerebellar voxels as columns into a single matrix, the entire model could be written as:

$$\mathbf{Y} = \mathbf{X}\mathbf{W} + \mathbf{E} \tag{2.2}$$

The connectivity approach that we used relied only on task-evoked activity: model training and testing were done on the fitted time series rather than the full or residual time series (as done in many other connectivity approaches). We multiplied $\mathbf{Z}_j$ from the first-level GLM with the 46 (for training) or 49 (for testing) activity estimates ($\bar{\mathbf{b}}_j$) from the first-level GLM with the first-level design matrix ($\mathbf{Z}$) to obtain the fitted time series the first-level design matrix for each session ($\mathbf{Z}_j$) from the first-level GLM with $\mathbf{t}_{\mathbf{fitted}_i}$ for each voxel (see General Linear Model). This was done for both the cortical and the cerebellar voxels.

In calculating the variances and covariances between cortical and cerebellar data (which are computed in the multiple regression models), this procedure reweighted the activity estimates to account for the fact that estimates for the instructions were based on 5 s of fMRI data, while estimates for the conditions were based on 10-30 s of data. For example, the covariance between the cortical and cerebellar time series is:

$$\mathbf{Y}^T\mathbf{X} = \bar{b}\mathbf{X}^T\mathbf{Z}^T\mathbf{Z}\bar{b}\mathbf{Y} \tag{2.3}$$

Therefore, if we had used the task-evoked activity estimates ($\bar{b}$) for cerebellar and cortical data, but reweighted the influence of each regressor by the diagonal of $\mathbf{Z}^T\mathbf{Z}$, we would have obtained similar results. Because of the off-diagonal terms, this method also mitigates problems that may arise in event-related designs due to correlations between regressors (Mumford et al., 2012), one example is the estimation covariance between the instruction period and the task-related regressor that follows immediately afterwards. We normalized the fitted time series by dividing them by the standard deviation of the residuals from the first-level GLM. This procedure emphasized voxels with large signal-to-noise ratios over voxels with low signal-to-noise ratios. The normalized time series were then averaged within all Q cortical parcels, resulting in a TxQ matrix (X) of cortical features. For the cerebellum, we modeled each of the P=6937 cerebellar voxels separately (SUIT atlas space with 3 mm resolution), resulting in a TxP data matrix (Y). The cortical data were further z-standardized (as in a partial correlation analysis) before entering them into regression models (see Model Estimation).

When estimating connectivity models, correlated fMRI noise across the cortex and cerebellum (e.g., head movement, physiological artifacts) can lead to the erroneous detection of connectivity between structures. This is especially problematic for the superior cerebellum and the directly abutting regions of the occipital and inferior temporal lobes. To negate the influence of any noise process that was uncorrelated with the tasks, we used a “crossed” approach to train the models. Because there were two sessions (same tasks, different order) in each task set (A & B), we were able to predict the cerebellar fitted time series for the first session by the cortical time series from the second session, and vice-versa (see 2.1).

$$\mathbf{Z}_1\mathbf{b}_1\mathbf{X} \sim \mathbf{Z}_1\mathbf{b}_2\mathbf{Y} \tag{2.4}$$

We did this separately for each task set, and given that the sequence of tasks was randomized across sessions, we could conclude from this approach that this prediction was based on task-related signal changes rather than fluctuations attributable to noise processes given

that noise is not shared across scanning sessions.

2.5.7 Cortical parcels

We created a set of models that used different levels of granularity to subdivide the cortex. Specifically, each hemisphere was divided into a set of regular hexagonal parcels, using icosahedrons with 42, 162, 362, 642, or 1002 parcels per hemisphere (see (Zhi et al., 2022) for details). Parcels that were completely contained within the medial wall were excluded, resulting in 80, 304, 670, 1190, or 1848 parcels combined for the left and right hemisphere. Activity within a parcel was averaged across voxels for each condition, defining the Q regressors for each model.

The regular icosahedron parcellations are arbitrary in the sense that they do not align to functional boundaries in the human neocortex more than expected by chance (Zhi et al., 2022). We therefore also employed functionally-defined parcellations, repeating the main analyses using 12 different parcellations derived from resting state fMRI data (2.5).

2.5.8 Model Estimation

We used three regression methods to estimate the connectivity matrix $\hat{\mathbf{W}}$ at the individual participant level. In the core analyses, each of these methods was combined with the five arbitrary cortical parcellations, resulting in 15 connectivity models. Each method was selected to favor a specific pattern of cortico-cerebellar connectivity. For the winner-take-all models, we assumed that the time series of each cerebellar voxel is explained by one and only one cortical region. To build this model, we simply chose the cortical region with the highest correlation with the cerebellar voxel in question. The connectivity weight corresponding to the rest of the cortical regions were set to 0. The other two methods allowed for some degree of convergence in the cortical input to each cerebellar voxel. Lasso

regression (least absolute shrinkage and selection operator(Tibshirani, 1996)), seeks to explain activity in each cerebellar voxel by a restricted set of cortical features. Specifically, Lasso minimizes the squared-error, plus an additional penalty calculated as the sum of the absolute values (L1-norm) of the regression coefficients:

$$\hat{\mathbf{W}} = \underset{\mathbf{W}}{\operatorname{argmin}} ||\mathbf{Y} - \mathbf{XW}||_2^2 + \lambda ||\mathbf{W}||_1 \tag{2.5}$$

In contrast, Ridge regression penalizes large connectivity weights, attempting to find a broad set of cortical regions to explain each cerebellar voxel. Ridge regression minimizes the following loss function:

$$\hat{\mathbf{W}} = \underset{\mathbf{W}}{\operatorname{argmin}} ||\mathbf{Y} - \mathbf{XW}||_2^2 + \lambda ||\mathbf{W}||_2^2 \tag{2.6}$$

Both Lasso and Ridge models include a hyperparameter λ that must be tuned in model estimation. The value of these regularization parameters was determined using gridsearch with 4-fold cross-validation on the training set. We divided the conditions of the training set into four non-overlapping subsets, reconstructed the time series using tasks from three of the four subsets and evaluated the model using the left-out subset. 2.6 depicts the average predictive accuracy for the training set and the optimal value of λ for the Lasso and Ridge models.

2.5.9 Model Testing

After model training with task set A, task set B was used as the test set. We applied the same procedure to construct the $\mathbf{X}$ and $\mathbf{Y}$ matrices. We then used the estimated weights for each model to generate predicted voxel-wise cerebellar activity patterns from the observed cortical time series. These predictions were generated at each level of granularity for each participant. Model performance was measured by correlating predicted and observed cerebellar time series for each voxel. As with the procedure for model training, the cortical

and cerebellar time series were crossed: Cortical time series from session 3 were used to predict cerebellar time series from session 4 and vice versa. Model predictions were calculated separately for each cerebellar voxel and visualized on voxelwise maps of the cerebellar cortex.

In sum, we evaluated 15 models in which the cortical parcels were based on an arbitrary icosahedron, based on the combination of three regression methods and five levels of granularity. For the 12 functionally-defined parcellations (2.5), we limited the evaluation to the WTA and Ridge models.

2.5.10 Noise Ceiling

For each model evaluated in the current study, the noise ceiling quantifies the expected performance of each model, under the assumption that the estimated weights reflect the true connectivity between the neocortex and cerebellum. When predicting the cerebellar activity patterns, our models are limited by two factors: Measurement noise associated with the cerebellar data and measurement noise associated with the cortical data.

To estimate these sources of noise, we used the fitted cerebellar time-series for the two sessions, assuming that each session's data are composed of the true time series $\mathbf{Y}^*$ plus noise $\boldsymbol{\epsilon}$: $\mathbf{Y}_i = \mathbf{Y}^* + \boldsymbol{\epsilon}$. If $\mathbf{X}_i\mathbf{W}$ signifies the variance of the true time series , and σ^2_ϵ the variance of the noise, then the correlation between the two sessions, i.e. the split-half reliability, is:

$$r(\mathbf{Y}_1, \mathbf{Y}_2) = \frac{\sigma^2_Y}{\sigma^2_Y + \sigma^2_\epsilon} \tag{2.7}$$

Similarly, the reliability of the prediction, even if we knew the true connectivity weights $\mathbf{W}$, is limited by the noise on the cortical data $\mathbf{X}$. The prediction $\mathbf{X}_i\mathbf{W}$ has noise variance σ^2_{XW}, which can be estimated by calculating the split-half reliability across the two sessions:

$$r(\mathbf{X}_1\mathbf{W}, \mathbf{X}_2\mathbf{W}) = \frac{\sigma^2_Y}{\sigma^2_Y + \sigma^2_{XW}} \tag{2.8}$$

Thus, for the true model the expected correlation would be:

$$r_{ceil} = r(\mathbf{X}_i\mathbf{W}, \mathbf{Y}_i) = \frac{\sigma_Y^2}{\sqrt{\sigma_Y^2 + \sigma_{XW}^2}\sqrt{\sigma_Y^2 + \sigma_\epsilon^2}} = \sqrt{r(\mathbf{Y}_1, \mathbf{Y}_2)r(\mathbf{X}_1\mathbf{W}, \mathbf{X}_2\mathbf{W})} \tag{2.9}$$

Because we do not know the true weights, we use the estimated weights from each model to estimate the noise ceiling. Thus, the noise ceiling is model dependent, specifying what the correlation would be if the current model was the true model.

2.5.11 Cortico-Cerebellar Convergence

Two measures were used to assess the amount of convergence of cortical inputs to each cerebellar voxel. For the first measure, we calculated the percentage of the cortical surface contributing to the prediction in each cerebellar voxel. We used the estimated weights from the Lasso regression model with the best unnormalized performance (80 cortical parcels). We opted to focus on the Lasso model since it sets weights that make a negligible contribution to the predictions to zero, thus identifying the sparsest cortical input that explains the cerebellar data. To determine the likely input area, we determined the number of non-zero coefficients for each cerebellar voxel, and expressed this as a percentage of the cortical surface. We also repeated these analyses using Ridge regression (2.8). Because Ridge does not result in zero coefficients, we applied a threshold, counting the number of connectivity weights with a value one standard above the mean of the weight matrix.

For the second measure, we calculated the dispersion (spherical variance) of the input weights. Using the spherical representation of the cerebral hemispheres from FreeSurfer, we defined unit vectors $\mathbf{v}_i$, pointing from the center of the sphere to the center of each of the cortical parcels. Each vector was then weighted by the cortico-cerebellar connectivity weight for that region w_i. All negative connectivity weights were set to zero. The spherical variance for hemisphere h across all Q_h parcels of this hemisphere was defined as:

$$var_h = 1 - \left| \frac{1}{Q_h} \sum_{Q_h} w_i \mathbf{v}_i \right| \tag{2.10}$$

To obtain a composite measure, we averaged the variances for the two hemispheres, with each weighted by the size of the summed (non-negative) connectivity weights. For summary and statistical testing, we then averaged the size of the input area, as well as the dispersion, across cerebellar voxels within each of the 10 functionally defined MDTB regions.

2.5.12 Generalization to new participants

Although the models were trained and tested on distinct datasets with more than half the tasks unique to each set, the data for training and testing were obtained from the same set of participants. As a stronger test of generalization, we evaluated the models with data from a new experiment involving naive participants (n=20, 11 females, 9 males, mean age=21.3). These participants were trained to perform a 5-task battery (cognitive control, social prediction, action prediction, visual search, semantic prediction). For each task, there was an easy and hard condition (e.g., 2-back vs 0-back for cognitive control, high vs low predictability), along with the task's associated instruction. Thus, there were a total of 16 conditions when including rest (fixation). Each participant completed five sessions, with fMRI data obtained in the first, third, and fifth sessions. Within a scanning session, there were six 11-minute runs, and each run included three repetitions of each task (35 s) with a 10 s rest period prior to each 5 s instruction period.

The participants were scanned on a Siemens MAGNETOM TrioTim syngo MR B17 located in the Henry Wheeler Jr. Brain Imaging Center at the University of California, Berkeley. The protocol used the following parameters: 1 s repetition time; field-of-view measuring 20.8 cm; A-to-P phase encoding direction; 48 slices; 3 mm thickness; in-plane resolution 2.5×2.5 mm2. To localize and normalize the functional data, a high-resolution, whole-brain anatomical scan (T1-weighted MPRAGE, 1mm isotropic resolution) was acquired during the first session. fMRIPrep(Esteban et al., 2019, 2020)(https://fmriprep.org/en/stable/) was used to preprocess the anatomical and functional data, following the same analysis procedures

as conducted for the main experiment.

To generate estimates of activity (beta weights), a General Linear Model (GLM) was fitted for each voxel to the time series data. Each of the 16 conditions was modeled as a separate regressor, with this repeated separately for each imaging run. Nipype (https://nipype.readthedocs.io/en/latest/) and custom-written scripts in Python were used to estimate the beta weights from a first-level GLM. To evaluate model generalization to this new dataset, we used the full set of cortico-cerebellar connectivity models estimated with the original data set, limiting the analysis to the regular cortical parcellations. Since the participants were different from the original data set, we averaged the model weights for the original 24 participants (i.e., 3 model types x 5 levels of granularity). Each model was then used to predict cerebellar activity from the cortical activity obtained in the new study, with these predictions compared to actual cerebellar activity at the individual level. Given that the experiment was a training study, we expected that both the true activation patterns, as well as the signal-to-noise ratio would change across sessions. We therefore determined the noise ceiling for each session separately by calculating the reliability across odd and even runs within each session. The normalized predictive accuracy was determined separately for each of the three imaging sessions, with the results across sessions averaged.

Data Availability The multi-domain task battery (MDTB) published in King et al. (2019) was analyzed in the current study. The raw behavioral and whole-brain imaging data generated by this task battery are available on the openneuro data sharing repository (https://openneuro.org/datasets/ds002105/share). The cortical parcellations used in the current study are available to download from https://github.com/DiedrichsenLab/fs_LR_32/tree/master, and the cerebellar parcellations and contrast maps are available to download from https://www.diedrichsenlab.org/imaging/mdtb.htm. The cerebellar maps are also available for interactive visualization in an atlas viewer (https://www.diedrichsenlab.org/imaging/AtlasViewer/). Model training and evaluation summary results are included as additional source data in the manuscript.

Code Availability The experimental code is publicly available at `https://github.com/maedbhk/cerebellum_connectivity`

Chapter 3

Selective recruitment: Evidence for task-dependent gating of inputs to the cerebellum

3.1 Abstract

While fMRI studies have documented cerebellar activity across a wide array of tasks, the functional contribution of the cerebellum within these task domains remains unclear. Here we present a new framework to address this problem, asking if neocortical inputs to the cerebellum are gated in a task-dependent manner. We tested this idea in the context of finger movements, where the integrity of the cerebellum has been shown to be essential for the coordination of rapid alternating movements but not grip force generation. While neocortical and cerebellar activity both increased with increasing speed and force, the changes in cerebellar activity associated with speed were larger than predicted by an optimized cortico-cerebellar connectivity model. This suggests a task-specific recruitment of the cerebellum through gating of information between the cerebellum and neocortex.

More generally, this framework offers a new approach to identify cerebellar contributions to function using fMRI.

3.2 Introduction

More than 30 years of neuroimaging has revealed that the human cerebellum is activated in a broad range of tasks including motor (Spraker et al., 2012), language (Petersen et al., 1989), working memory (Marvel and Desmond, 2010), attention (Allen et al., 1997), social (Van Overwalle et al., 2015), and visual cognition (Diedrichsen et al., 2019; Van Essen et al., 2011). The presence of cerebellar activity has often been taken to indicate that the cerebellum plays a specific functional role in these tasks.

However, there is an important problem with this line of reasoning. The cerebellar BOLD signal is dominated by mossy fiber input with very little contribution from the output of the cerebellar cortex, the activity of Purkinje cells (Alahmadi et al., 2015; Gagliano et al., 2022; Mapelli et al., 2017; Mathiesen et al., 2000; Thomsen et al., 2004). The mossy fiber inputs, in turn, arise from a wide array of neocortical areas, including prefrontal and parietal association cortices. This has been demonstrated directly through viral tracing studies in non-human primates (Kelly and Strick, 2003), and indirectly through resting-state functional connectivity (rs-FC) analysis in humans (Buckner et al., 2011; Ji et al., 2019; Marek et al., 2018; O'Reilly et al., 2010). The existence of these anatomical connections certainly argues for a prominent role of the human cerebellum in cognition in general (Leiner et al., 1986; Strick et al., 2009). However, an increase in the cerebellar BOLD signal need not indicate that the cerebellum is making a functional contribution to that specific task: Cerebellar activity could simply reflect the automatic transmission of neocortical activity through fixed anatomical connections. Indeed, if all cerebellar BOLD activity can be perfectly explained by its fixed connectivity with the neocortex, then it would be hard to learn anything specific about cerebellar function from fMRI studies.

But, what if the neocortical input to the cerebellum was amplified when a specific contribution from the cerebellum was required? We refer to this idea as the selective recruitment hypothesis. Such task-dependent gating would make evolutionary sense, given the substantial metabolic cost of granule cell activity (Attwell and Iadecola, 2002; Howarth et al., 2010). In the current study we test the selective recruitment hypothesis in the motor domain, where clinical studies provide a strong a priori hypothesis: Patients with cerebellar damage consistently show impairments in performing rapid alternating movements, a symptom called dysdiadochokinesia (Hallett et al., 1991; Mai et al., 1988). In contrast, these patients are generally able to exert grip forces comparable to healthy controls (Mai et al., 1988). This clinical dissociation suggests that the computations required to produce fast alternating finger movement depend more on the cerebellum than those required to modulate grip force.

To test whether this differential dependency leads to selective recruitment of the cerebellum during rapid alternating movements, we employed a task involving alternating finger presses (Figure 1a). Starting at a baseline level of 1Hz and 2.5N, we either increased the force of the required finger movements, or their speed (Figure 1b). We expected that increases in speed and force would both result in an increased BOLD signal in the neocortex and cerebellum (Spraker et al., 2012). The selective recruitment hypothesis predicts that increases in cerebellar BOLD will be greater for increases in tapping speed compared to increases in finger force output, even when the neocortical activity is matched between conditions (Fig 1c).

This comparative approach requires the definition of a neocortical region that can serve as a control for each cerebellar region of interest. While rs-FC studies (Buckner et al., 2011; Ji et al., 2019; Marek et al., 2018) have identified a system of paired neocortical and cerebellar networks, the 1:1 mapping featured in these networks glosses over the possibility that cerebellar regions may receive input from more than one neocortical region. To test for cortico-cerebellar convergence, we recently developed a series of connectivity models (King

et al., 2023) optimized to predict cerebellar activity patterns from neocortical activity patterns across a wide array of tasks. Models that allowed graded input from multiple neocortical regions predicted cerebellar data better than models that allowed input from only a single region. Thus, we used these models here to obtain predictions of cerebellar activation, assuming that functional connections are fixed (i.e., task-invariant). These predictions serve as a baseline against which we test the idea of selective cerebellar recruitment.

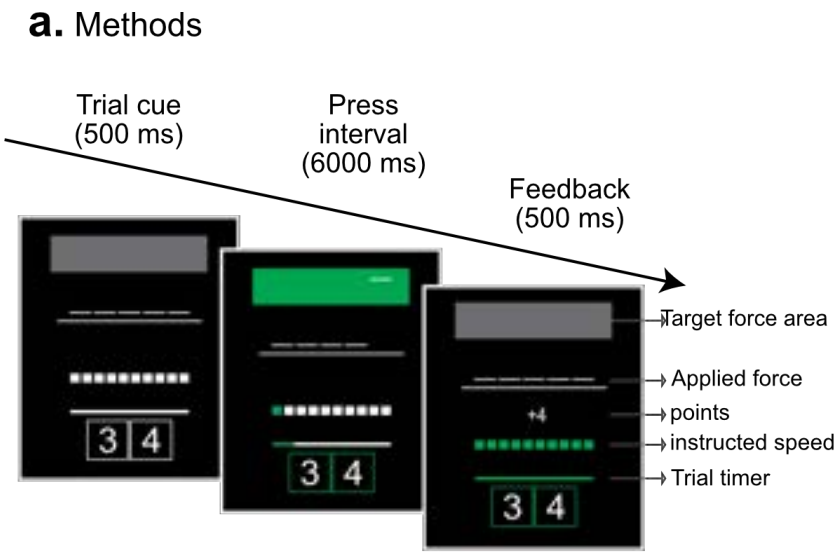

b. Conditions

	Force (N)	Speed (# press)	
High Speed	2.5	18	Speed Level
Medium Speed	2.5	10	
Baseline	2.5	6	
Medium Force	6	6	Force Level
High Force	10	6	

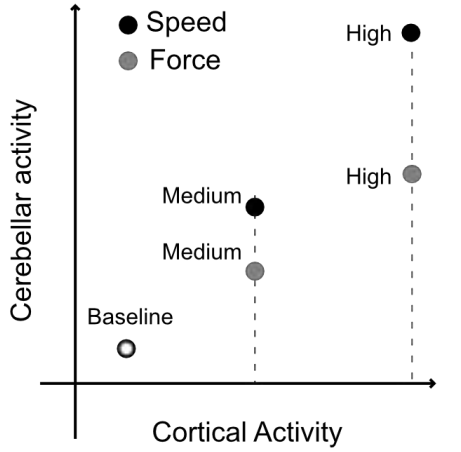

Figure 3.1: **Alternating finger tapping task and expected results from selective recruitment**a) Timeline of events in a single trial. Cues specified the target speed and force level.

During the press interval, participant alternatively tapped the middle and ring finger. Reward feedback (e.g., +4) was based on their performance. b) The 5 force-speed combinations. The baseline condition was performed at the lowest levels of force and speed. For the other conditions, either the target force or speed increased. Speed indicates the number of presses to be produced within a 6 s interval. c) Expected results for the selective recruitment hypothesis: For approximately matched neocortical activity levels (x-axis) in the medium and high conditions (dashed lines), cerebellar activity (y-axis) is expected to be greater for increases in speed compared to increases in force.

3.3 Results

3.3.1 behavioral performance in the scanner

The group-averaged peak forces and number of taps over the 6s interval are presented in Table 3.1. Overall, participants performed as instructed. For all individuals the mean force for each condition was within 80-120% of the target force and the mean number of taps was ±2 of the target number. Trials in which the participant did not perform at the instructed speed (TOO FAST), produce the instructed number of presses (±2) in time, or tapped with the wrong finger were considered errors. The high error rate for the baseline condition reflects the fact that some of the participants had difficulty maintaining the relatively slow rate, completing the 6 taps in less than the minimum interval of 3s. Error trials were excluded from the mean performance data and from the imaging analysis.

Condition	Average Force (N)	Number of taps in 6s	Error rate (%)
High Speed	2.93 ± 0.48	17.72 ± 0.84	5 ± 0.21
Medium Speed	2.84 ± 0.45	10.12 ± 0.44	1 ± 0.12
Baseline	2.80 ± 0.41	6.32 ± 0.80	15 ± 0.36
Medium Force	6.10 ± 0.49	6.04 ± 0.20	4 ± 0.18
High Force	9.73 ± 0.66	6.04 ± 0.20	2 ± 0.13

Table 3.1: Mean and standard deviation of executed force, speed, and error rate for each condition across subjects

3.3.2 Increased activation in neocortical and cerebellar motor network

Given that our task involved right-hand movements, we expected to observe prominent activation in the hand areas of left (contralateral) M1 and S1. This was indeed the case (Figure 2). Compared to baseline, the combined M1/S1 ROI showed a significant increase in activation averaged over medium and high force levels (Figure 2a, t15 = 8.45, p = 4.34×10-7), as well as for the medium and high-speed conditions (Figure 2c, t15 = 5.44, p = 6.87×10-5). Similarly, activity in the right anterior and posterior motor areas of the cerebellum increased with increasing force (Figure 2d, t15 = 9.87, p = 5.93×10-8) and speed (Figure 2f; t15 = 4.98, p = 1.62×10-5). These results replicate the findings from previous studies, showing that activity in the cerebellar hand motor areas are sensitive to parametric variation of force (Spraker et al., 2012)and speed (Jäncke et al., 1999).

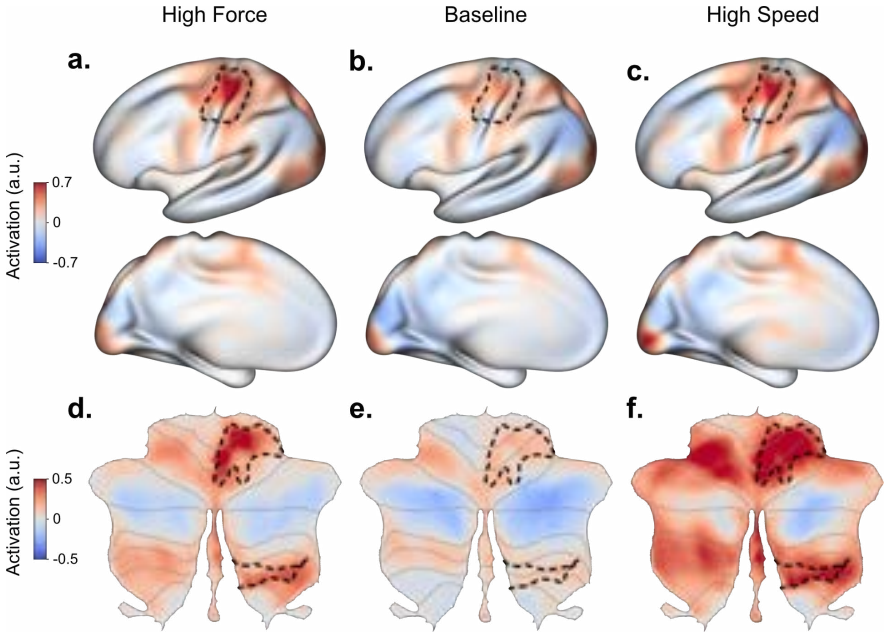

Figure 3.2: **Activation in the cortico-cerebellar motor network compared to rest**. Activity maps are shown for high force (left), baseline (middle), and high speed (right) conditions. High levels of force and speed were chosen to visualize the overall trend in activity increase with increasing force and speed. (a-c) Lateral and medial surface of the left hemisphere with the hand area of M1 and S1 indicated by a black outline. (d-f) Flat map of the cerebellum with anterior and posterior motor areas outlined by black dotted lines. The motor hand area of the cerebellum was selected from the functional parcellation introduced in (King et al., 2019)

Visual inspection of Figure 2 suggests that the cerebellar signal is more strongly modulated by variation in speed than force. However, we cannot use this to infer any preferential functional role for the cerebellum: It is possible that the BOLD activity in the associated neocortical areas is also more sensitive to variation in speed, and that the cerebellar changes simply reflect these neocortical changes.

3.3.3 ROI-based comparison of neocortical and cerebellar hand regions

The preceding discussion makes clear that we need to evaluate the change in cerebellar activity within the context of the activity in neocortical regions that provide input to that cerebellar region. To do so, we focused on the right-hand area of the human cerebellum, as defined by a recent functional parcellation (King et al., 2019). To select the corresponding neocortical area, we assumed in this initial analysis that the contralateral sensorimotor areas of the neocortex are the only regions that provide input to the cerebellar hand area. To define the contralateral M1 / S1 hand ROI, we used a cyto-architectonic atlas (see Methods, Figure 2). The observed activation for each condition was averaged in the neocortical/cerebellar ROIs. As expected, activation in both cerebellar and neocortical motor areas increased with force and speed (Figure 3a). However, the pattern across these two variables was different for the neocortex and cerebellum. For example, in the neocortex, activity in the high-speed condition lay between the medium and high force conditions whereas in the cerebellum, activity in the high-speed condition was larger than in either force condition. Thus, the cerebellar activity was not simply a monotonic function of the neocortical activity.

A different way of showing this is to correct the cerebellar activity for differences in neocortical activity. We fit a linear model between these two variables for each participant (average R2 = 0.58, SE= 0.01). We then computed the residuals of this linear model for each condition. These residuals indicated whether the cerebellum was more or less activated than expected given a fixed connectivity model. The signed residuals averaged for the speed conditions were significantly higher than those for the force conditions ($t15 = 3.01$, $p = 8\times10\text{-}3$). Thus, this initial analysis indicates that, in response to an increase in movement speed, the cerebellar activity increased to a greater degree than expected from the increases in neocortical activation.

3.3.4 Model-based comparison of predicted and observed cerebellar activity

One limitation with our initial analysis is that we assumed that only M1/S1 provides input to the hand area of the cerebellum. Is it possible that the higher activity in the cerebellum was caused by fixed inputs from the additional neocortical areas?

The activation patterns for speed and force conditions were not completely matched: Increases in speed tended to lead to more widespread activations in secondary motor areas than increases in force. Given this difference, the observed differences in cerebellar activity may be a result of additional fixed inputs from premotor and supplementary motor areas, rather than evidence in support of selective recruitment.

To evaluate this hypothesis, we utilized a model of cortico-cerebellar connectivity derived from a large task battery (King et al., 2019). The best-fitting model indicated that cerebellar voxels receive convergent inputs from multiple neocortical areas. The connectivity weights of this model averaged across all voxels in the right cerebellar hand ROI are shown in Figure 3b (Ridge regression, see Methods). As can be seen, input weights are not limited to contralateral M1 and S1, but also include premotor and supplementary motor regions. To determine whether these additional inputs account for the observed differences in cerebellar activity between conditions, we used the connectivity weights from the model to predict the cerebellar activity patterns for each participant and condition from the individual's neocortical activity patterns.

Using the connectivity model, the predicted and observed cerebellar activations levels averaged for the selected cerebellar ROI (Figure 3c), were more closely matched (average R2 = 0.83, SE = 0.07). Nonetheless, the predicted task-specific deviations from the predictions remained. After accounting for the small differences in predicted activity, the average signed residual for the two speed conditions was significantly higher than for the

force conditions (t15 = 3.21, p = 5×10-3). In summary, the increases in cerebellar activity for speed outstripped the activity increases for force, even if we accounted for the activity in the likely neocortical input regions.

3.3.5 Alternative connectivity models

We recognize that our results are dependent on the connectivity model used to predict cerebellar activity. To explore the robustness of our results, we considered two other cortico-cerebellar-connectivity models, one based on a winner-take-all algorithm in which the cerebellar input is restricted to neocortical area with the highest correlation, and a lasso regression model that allows for some convergence of neocortical input (King et al., 2023). We note that, while these models did not perform as well as the Ridge model in predicting cerebellar activity patterns, each provided reasonable predictive accuracy. When these connectivity models were applied to the current data set, we obtained a similar pattern of predictive deviations: The signed residuals were significantly higher for conditions with higher speeds (winner-take-all: t15 = 2.5, p = 2×10-2, lasso regression: t15 = 3.29, p = 5×10-3, averaged over medium and high levels).

3.3.6 Voxel-wise analysis across the cerebellum

The previous analyses focused on a specific region of the cerebellum, the right-hand motor areas. These analyses do not address whether there are other cerebellar regions that also show higher-than-predicted activity for increasing speed, or whether there are cerebellar regions that show the opposite pattern with higher-than-predicted activity for increasing force. To address this, we tested for violations of the prediction of the Ridge connectivity model in each cerebellar voxel. Figure 3c shows the difference between the observed and predicted activity, displayed as a statistical map of the speed vs. force comparison. Voxels that showed higher speed sensitivity (relative to neocortical activity) were found in anterior

and posterior cerebellar motor regions. Additionally, we found higher than predicted activity in default-mode regions of left crus I + crus II, as well as in language-related areas of the right crus I and crus II.

Importantly, we found no cerebellar regions in which the residuals for the high force conditions were greater than those for the high-speed conditions. Thus, the results show that deviations from our task-invariant connectivity model selectively arise when the rate of alternating finger movements increases and that this effect is primarily observed in task-specific areas of the cerebellum.

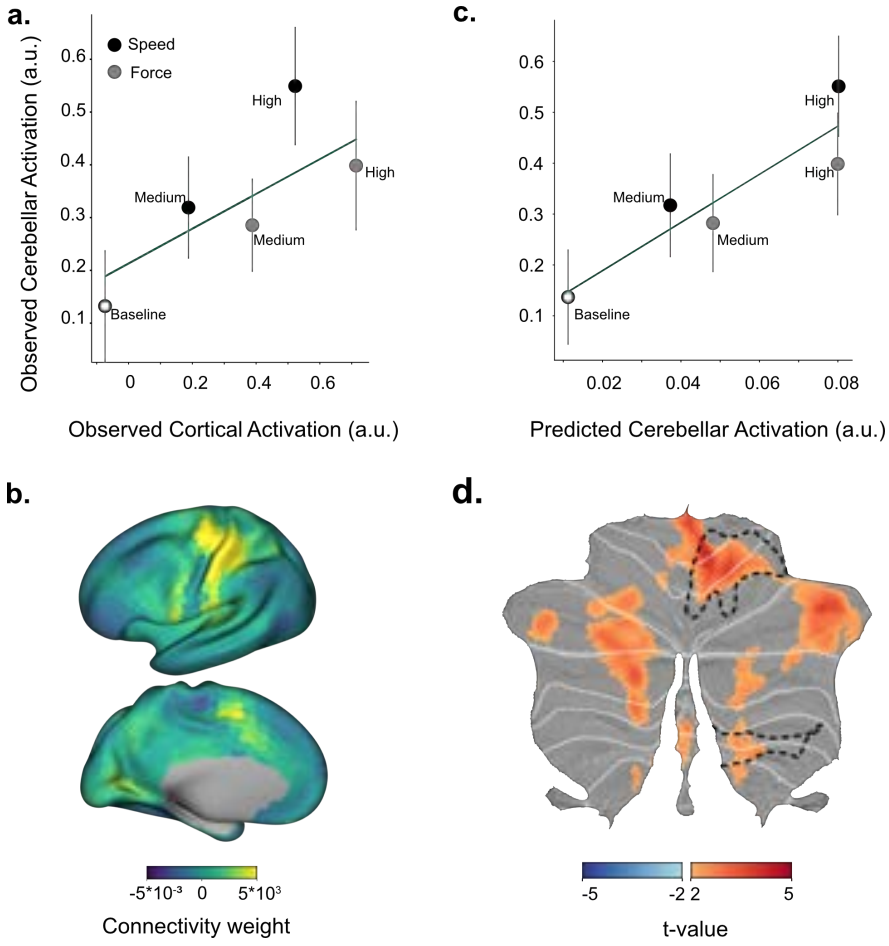

Figure 3.3: **Selective recruitment of cerebellum for fast alternating finger movements**a) Average BOLD activity in the right-hand cerebellar ROI (y-axis) plotted against activity in the contralateral M1/S1 regions (x-axis). Error bars indicate standard error of the signed

residuals from the linear regression model within each participant (see Methods). b) Connectivity weights from a group-level connectivity model (Ridge regression) for the cerebellar motor ROI 25. c) Average observed cerebellar activation (y-axis) plotted against average prediction from the connectivity model (x-axis). The signed residuals were significantly higher for the speed compared to the force conditions. Note that the predicted activations for high levels of force and speed are closely matched using the connectivity model. d) Thresholded map of t-values testing where the residuals for the speed conditions were greater than the force conditions. No cerebellar voxels showed more positive residuals for the force compared to the speed conditions (blue, note that the t-tests were two-tailed).

3.3.7 Discussion

Functional neuroimaging studies have shown that the human cerebellum is activated across a broad range of task domains. However, drawing functional inferences from these activations is limited by the fact that the BOLD signal in the cerebellar cortex is largely dominated by mossy-fiber input (Alahmadi et al., 2015, 2016; Gagliano et al., 2022; Mapelli et al., 2017; Mathiesen et al., 2000; Thomsen et al., 2004, 2009), which mainly carries incoming information from neocortex. Thus, it is difficult to draw inferences about the engagement of the cerebellum by considering cerebellar BOLD activity in isolation; this signal may simply reflect information transmission through fixed anatomical connections.

Our current experiment clearly illustrates this problem. We found highly significant increases in the cerebellar BOLD signal for increases in force. This observation could be interpreted as evidence that the cerebellum is involved in the processes required to generate higher forces. However clinical studies have shown that cerebellar pathology results in the impaired ability to produce fast alternating movements, but does not impact maximal force generation (Mai et al., 1988). Thus, consideration of the changes in the cerebellar BOLD in response to force would not align with this clinical dissociation.

In the present study, we introduce a more stringent criterion to infer functional

involvement of the cerebellum: Rather than focusing on activation per se for a given task, the emphasis should be on whether the cerebellar area exhibits a signature of what we refer to as selectively recruitment. To establish selective recruitment, we need to interpret cerebellar activity in the context of the simultaneously occurring neocortical activity. Specifically, the observed cerebellar activity should be compared to the activity that would be expected if neocortical activity was transmitted over fixed, task-invariant connections.

To enable this comparison, we drew on a cortico-cerebellar connectivity model (King et al., 2023) that was optimized to predict cerebellar activity based only on neocortical activity patterns across a wide array of tasks. This connectivity model provides a carefully constructed null hypothesis of the expected cerebellar activity given a pattern of neocortical activity. Note that this prediction takes into account that some functional networks, such as the fronto-parietal and salience networks, occupy a relatively larger area of the cerebellum than of the neocortex (Buckner et al., 2011; Marek et al., 2018), and that there will be variation in convergence across the cerebellar cortex. As shown in our previous study (King et al., 2023), this model provides a good prediction of cerebellar activity across a broad range of tasks, including those not used in developing the model, confirming that a large proportion of the observed variation of cerebellar activity across tasks can be accounted for by fixed functional connections between neocortical and cerebellar regions.

Here we ask if there are systematic deviations from these predictions. Specifically, the selective recruitment hypothesis proposes that neocortical input is upregulated when the cerebellum is required for a task (and/or downregulated when it is not). If this was true, we should be able to detect specific violations of the task-invariant connectivity model. The current results showed selective recruitment of the cerebellum during rapid alternating finger movements: Activity in the cerebellar hand area increased more when increasing speed as compared to force. Importantly, this dissociation was observed even when the activity in the neocortical hand areas was approximately matched across these conditions. These results provide clear evidence for task-dependent gating (Cole et al., 2021), a signature we take to

indicate tasks that are dependent on cerebellar computations.

There are a number of possible neural mechanisms that could underlie such task-dependent regulation. First, gating may occur in the pontine nuclei, which integrates descending signals from different areas of the neocortex with feedback signals from the cerebellum (Schwarz and Thier, 1999). The cellular properties of pontine neurons makes them ideally suited to gate input signals in a state-dependent manner (Schwarz et al., 1997). Second, gating could be achieved via modulation within the granule cell layer itself, perhaps by recurrent loops involving inhibitory Golgi cells (Maex and Schutter, 1998). Finally, gating may already occur in the neocortex: A recent study (Park et al., 2022) showed more recruitment of neocortical neurons that project to the pons when controlling the spatial aspects of joystick manipulation, and more recruitment of neurons that project intra-cortically or to the striatum when controlling movement amplitude. Because the neocortical BOLD signal reflects the activity of both neuronal populations, pontine-projecting neurons may be more engaged during fast alternating movements, even though the fMRI activity is the same as during the production of high forces. Whichever combination of mechanisms is responsible for our observed effect, task-dependent gating of inputs to the cerebellum would be highly adaptive from a metabolic standpoint (Attwell and Iadecola, 2002), such that the costly mossy-fiber system is most activated when cerebellar computation is required.

One drawback of our new approach is that it heavily depends on the connectivity model that is used to make predictions about the expected cerebellar activity. Here we considered a range of models, starting from a simple one-to-one connectivity model that only uses the most likely neocortical input area (in the present study, M1/S1) to full connectivity models that were optimized to predict cerebellar activity across a large array of tasks. The latter models allow for the convergence of inputs from multiple neocortical areas and provide significantly better predictions than a simple one-to-one pairing of cerebellar and neocortical areas (King et al., 2023). Similar to our earlier work, the full connectivity model provided better predictions of the current data than the simple ROI approach. These findings

emphasize the importance of using a model that approximates the true cortico-cerebellar connectivity as closely as possible. This will be especially important for cognitive regions in lobules VII, which appear to receive input from an even wider array of regions (King et al., 2023).

A second limitation of our approach is that the connectivity model as currently constructed does not predict the absolute level of cerebellar activity, but rather activity for one condition relative to other conditions. This limitation arises from the fact that the absolute magnitude of the BOLD signal in the cerebellum depends on many measurement-related factors, which may differ between the study used to estimate the connectivity model and a subsequent experiment that draws on this model. To address this uncertainty, we fit the average numerical relationship between neocortical and cerebellar activity for each participant separately. Thus, our approach relies on the comparison to a control condition (here force generation) that activates similar neocortical regions but does not (or to a lesser degree) rely on the cerebellum. From this we can conclude that the input gain in the speed condition was higher than in the force condition. Whether this was achieved by a specific upregulation in the speed condition, or a downregulation in the force condition is unclear.

This leads to question of why cerebellar activity, if it was functionally not important for pressing harder, increased in the force condition at all. One explanation is that the cerebellum is, alongside neocortex, functionally involved in the force conditions, perhaps for accurately maintaining the target force levels (Mai et al., 1988), or for avoiding finger-to-finger enslaving effects that emerge at high force levels (Brandauer et al., 2012). We designed our force task to have minimal force accuracy (accepted forces range from 80% to 120% of the target force) and individuation requirements, with the idea that satisfactory task performance could be achieved with minimal cerebellar involvement during force processing given the clinical literature.

A more likely explanation is that the force-related increases in cerebellar activity occur because neural gating is not complete: Neocortical inputs to the cerebellum are

attenuated when cerebellar function is not required but are not entirely shut down. Given the diversity of neocortical functions combined with the uncertainty about which function will rely on cerebellar computation, a partial task-invariant information transmission to the cerebellar cortex certainly seems functional. If gating is indeed incomplete, then we should expect to observe increases in cerebellar activity (as here in the force condition) even when the cerebellum makes minimal contributions to task performance.

In summary, we outline here a new approach for using fMRI data to evaluate hypotheses about cerebellar function. Rather than just showing that the cerebellum is activated for a specific task, we apply a more stringent criterion, asking if the cerebellum is more activated than predicted by a task-invariant connectivity model. Tasks that meet this criterion, especially when compared to control conditions in which cerebellar activity is well predicted by the connectivity model, will provide strong evidence that cerebellar computations are important for those tasks. Our results provide an important first validation of this approach showing that fMRI activity, and therefore likely cortico-pontine-cerebellar input, is modulated in a task-dependent manner. As expected from clinical observations, we showed that the cerebellar hand area is selectively more activated for increases in speed relative to increases in force. The framework developed here in the motor domain where we had strong a priori expectations of selective recruitment offer a new approach to test for selective recruitment in cognitive domains where the functional contribution of the cerebellum remains elusive. More generally, by systematically applying the approach across task domains, we are positioned to test domain-general hypotheses of cerebellar computation (Diedrichsen et al., 2019).

3.3.8 STAR Methods

Participants

All participants gave informed consent under an experimental protocol approved by the institutional review board at Western University. None of the participants reported a history of neurological or psychiatric disorders or current use of psychoactive medications. A total of 21 participants started the experiment. Of these, 4 participants were not scanned because of their poor performance during the behavioral training session. The remaining 17 participants performed the tasks inside the scanner and data for one participant was excluded due to an incidental finding. Therefore, the analyses were based on the data from 16 participants (8 female, 8 male, mean age = 25, std age = 2)

Apparatus and Stimuli

Participants used a custom-made 5-key finger keyboard to make alternating presses with the middle and ring finger. A force transducer, located under each key (FSG15N1A, Honeywell Sensing and Control; dynamic range, 0 –25 N), continuously recorded the isometric force exerted by each finger at a rate of 500 Hz. We recalibrated each sensor (no force applied) at the beginning of each run to correct for drift. The applied force was continuously displayed to the participants in form of 5 short horizontal lines that moved vertically proportional to force exerted by each finger (Figure 1a: applied forces)

Procedure

Each trial was randomly selected from one of five conditions (Figure 1b). In all conditions, the response interval lasted for 6 s and participants were instructed to adopt a rate to distribute their responses evenly across this interval. For the Baseline condition, the target

force was 2.5 N, and the instructed number of presses was 6 (e.g., optimal performance is 1 response/s). For the increased force conditions, the target force was either 6 N or 10 N, with the target number of presses fixed at 6. For the increased speed conditions, the target number of presses was 10 or 18, with the target force fixed at 2.5 N.

A trial started with a short cueing phase (500ms) during which two numeric characters (3 and 4) were presented on the screen, instructing the participant to tap with the right middle and ring finger. The required force level was indicated by a gray box that extended from 80% to 120% of the trial's target force (Figure 1a, target force area), and the required number of presses by either 6, 10, or 18 small gray squares (Figure 1a, instructed speed).

After the cueing face the two rectangles framing the digits turned from white to green, signaling to the participants to perform alternating finger presses. A horizontal green line (Figure 1a, timer) started growing from left to right, indicating the passing of time. A press was registered when the force exceeded 80% of the target force (lower bound of the target force area). At this point, the force area changed color from gray to green and the color of the corresponding press square changed. When the force level returned to <1N, the force area color changed back to gray.

The response interval lasted for 6 s, with participants instructed to adopt a rate such that their responses were evenly distributed across the response interval. At the end of a trial, participants received performance feedback. If the participant made the required number of alternating movements and completed the set of responses within 3 to 6 seconds, they received visual feedback indicating they had earned 4 points. We acknowledge that our choice of response time window was liberal, but our main focus was not to match speeds exactly, but to get sufficient variation across conditions. All other outcomes were considered errors and were not rewarded (0 points). If the average exerted force for the trial exceeded 120% of the target force, the experimenter provided verbal feedback, asking the participant to press less hard. To ensure that the trial was performed at the instructed speed, the message "TOO FAST" was displayed if total movement time was shorter than 3

s or if the number of produced presses exceeded the instructed number by more than two which means that the alternating movement exceeded the instructed rate of finger taps. The message “TOO SLOW” was displayed if the number of produced presses by the end of the 6 s interval was less than the instructed number of presses. Visual feedback (points or error message) remained on the screen for 500 ms. After a delay of 500 ms (inter-trial-interval), the next trial began with the appearance of the cue.

Experimental design

During a training session, participants completed two types of blocks outside the scanner: 5 blocks of the alternating finger tapping task interleaved with 5 blocks of a working memory task (results not reported in this paper). Each block of the alternating finger tapping task consisted of 5 repetitions of each of the 5 conditions with the order randomized (total of 25 trials, approx. 5 min/block). Each practice block of the working memory task took approximately 7 min.

During the scanning session, the participant performed 5 imaging blocks of the finger tapping task, alternating with 5 blocks of the working memory task. Each block of the alternating finger tapping task lasted for just over 5 minutes, during which 260 volumes were collected. Conditions were fully randomized, each repeating 5 times within a block. Four 12-second periods of rest were interleaved randomly between trials.

Image acquisition

MRI data was acquired on a 3T Siemens Prisma at the Center for Functional and Metabolic Mapping (CFMM) at Western University. A high-resolution whole brain anatomical MPRAGE image was acquired at the beginning of the scanning session (voxel size = 1 mm3, Field-of-view = 25.6×25.6×25.6 cm3. Whole-brain functional images were acquired using an echo-planar imaging sequence with TR = 1000 ms, TE = 30 ms, voxel size =2.5×2.5×3 mm3,

Field-of-view = 20.8×20.8×20.8 cm3, 48 slices, P to A phase encoding direction, with multi-band acceleration factor = 3 (interleaved) and in-plane acceleration factor = 2. Gradient echo field maps were acquired to correct for distortions due to B0 inhomogeneities (acquisition parameters: voxel size = 3×3×3 mm3, Field-of-view = 24×24×24 cm3). Physiological signals of heartbeat and respiration were recorded online during each functional run.

fMRI data processing and first level analysis

We used tools from SPM12 (Friston et al., 1994) and custom written code in MATLAB 2018b to process the functional and anatomical data. We defined an individual coordinate system for each subject by setting the origin of the anatomical image to the approximate location of the anterior commissure. Anatomical images were segmented into gray matter, white matter, csf, and skull. Functional images were corrected for head motion using the six-parameter rigid body transformation and were then co-registered to the individual anatomical image. The mean functional image and the results of anatomical segmentation were used to generate a gray matter mask for functional images. Slice timing correction, smoothing, and group normalization were not applied at this stage.

A GLM was fit to the time series of each run separately using SPM12. Each condition was modeled as a separate regressor using a 6-sec boxcar covering the response interval, convolved with a canonical hemodynamic response function (HRF). Error trials (approx. 5% of all trials) were modeled as one single regressor in the GLM and this regressor was discarded from further analysis. Rest was not modeled as a separate condition but served as the implicit baseline, captured by the intercept term. Beta weights estimated by the first level GLM were divided by residual-root-mean-square image resulting in normalized activity estimates for each voxel, condition, and run.

Cerebellar normalization

The cerebellum was isolated from the rest of the brain and segmented into white and gray matter using the Spatially Unbiased Infratentorial Template (SUIT) toolbox (Diedrichsen, 2006), followed in some cases by hand correction. Cerebellar white matter and gray matter probabilistic maps were deformed simultaneously into SUIT atlas space using a non-linear deformation algorithm (Ashburner, 2007). The deformation was applied to both anatomical images, and the normalized beta weights from the first level GLM. Before normalization, the isolation mask was applied to discard the influence of adjacent inferior and occipital neocortical areas. For visualizations, the functional maps were projected onto a flat representation of the cerebellum (Diedrichsen and Zotow, 2015) using the SUIT toolbox.

Neocortical normalization

For each participant, the anatomical image was used to reconstruct neocortical white matter and pial surface using Freesurfer (Fischl, 2012). Reconstructed surfaces were inflated to a sphere and registered to the fsLR 32k node template (Van Essen et al., 2011) using a sulcal-depth map and local curvature. Neocortical activity patterns were projected onto these surfaces by averaging the activation values of voxels touching the line between corresponding vertices of the individual white matter and pial surface.

Region of interest (ROI) approach

For the main analyses, we focused on the hand motor area of the cerebellum derived from a multi-domain functional parcellation of the cerebellum (King et al., 2019). This ROI consisted of a superior (lobules V/VI) and an inferior (lobule VIII) component. For the neocortex, we used a cytoarchitectonically defined primary sensorimotor area (motor: BA4; sensory: BA

3a,3b,1,2) based on a surface-based probabilistic atlas (Fischl et al., 2008). To limit the ROI to the hand area, we selected the area 1.5 cm above and below the hand knob in the central sulcus (Yousry et al., 1997). For the initial comparison of cerebellar and neocortical activation, we averaged the activations within each selected region of interest.

Connectivity model

To take into account the possible convergence of neocortical inputs onto cerebellar circuits, we used a task-invariant model of cortico-cerebellar connectivity (King et al., 2023) that models activity in each cerebellar voxel as a linear combination of neocortical inputs. The model was estimated on an openly available dataset that consisted of two sets of tasks spanning a large range of motor and cognitive domains (King et al., 2019). Each task set was performed in two sessions. For each participant, the neocortical surface was subdivided using an icosahedron parcellation, with the parcellation varying from 80-1848 parcels. The functional data within these parcels was averaged and then a matrix of neocortical predictors was constructed to serve as the input to the model. Three models (Winner-takes-all, Lasso, and Ridge regression) were trained to predict the activity of each cerebellar voxel in SUIT atlas space based on these inputs.

The first task set was used to estimate the connectivity weights for each model (King et al., 2023). The second task (independent data containing multiple novel tasks) was used to evaluate the trained models. Predictive accuracy of the model was defined as the Pearson correlation between the observed and predicted response profile of each voxel across the tasks. For this paper, we selected the model that had the highest predictive accuracy across subjects, a ridge-regression model with 1848 neocortical parcels/predictors. The group level matrix of connectivity weights was constructed by averaging weights from the best model across the 24 participants of that study.

The group connectivity weights were used to predict cerebellar activity in SUIT space

(resampled to the same 3mm isotropic resolution used when estimating the connectivity weights). Neocortical activations estimates were averaged within each neocortical parcel. The matrix of neocortical activations was multiplied using the group-averaged connectivity weights to arrive at the prediction for each cerebellar voxel.

As in (King et al., 2023) we adopted a crossed approach. We split the data set into two odd and even runs and predicted cerebellar activity patterns in one half of the data from the neocortical activity in the other half. This procedure ensures that successful predictions are not caused by correlated noise-processes across spatially adjacent regions of the neocortex and cerebellum (Buckner et al., 2011).

Given that weights were derived from a different dataset with different subjects and different signal to noise ratios (SNR), we fitted a linear regression line (without intercept) for each participant between the observed cerebellar activation and the model predictions. The slope of the line accounts for differences in SNR between the two datasets. The residuals from this regression analysis were then used for statistical testing across participants.

Chapter 4

Working memory in the cerebellum

4.1 Introduction

Historically thought to be a motor structure, the cerebellum is now under the spotlight for its possible involvement in cognitive processes, including working memory. Its functional involvement in working memory tasks is supported by transneuronal viral tracing studies which have shown reciprocal connections between the cerebellum and the prefrontal and parietal cortices (Kelly and Strick, 2003). Further support comes from studies of cerebellar patients showing working memory deficits, albeit mild compared to motor deficits (Peterburs et al., 2010; Kirschen et al., 2008; Leggio et al., 2000; Stoodley, 2012).

Working memory deficits in cerebellar patients have been shown to be modality-specific with verbal span tasks demonstrating most pronounced deficits (Ravizza et al., 2006). In addition, the nature of the reported deficits appears to be related to the location of the lesion. For instance, disruptions in rehearsal mechanisms have been linked to lesions in the right cerebellum (Starowicz-Filip et al., 2021; Pleger and Timmann, 2018). Additionally, the impairments are more pronounced in backward span tasks where participants are presented with a sequence of items, such as digits or letters, and are required to recall them

in the opposite order to which they were presented (Ravizza et al., 2006).

The reported deficits, nevertheless, have not been replicated as they are largely dependent on the location, size, and onset of the lesion (Hokkanen et al., 2006). In addition, lesions like degeneration often co-occur with lesions in other brain structures such as neocortex. To complicate it even more, cognitive deficits in cerebellar patients are, in general, more subtle and sometimes temporary. These factors make it difficult to draw conclusions about cerebellar function solely based on patient studies.

Task-based fMRI offers a promising avenue to investigating cerebellar function. Working memory tasks have shown robust fMRI activation in hemispheric regions of lobules VI, VII, and VIII (Desmond et al., 1997; Chen and Desmond, 2005). These regions, associated with the fronto-parietal resting state network (Buckner et al., 2011) are known to respond to a broad spectrum of cognitively demanding tasks, serving as integral parts of the multi-demand network (Assem et al., 2022).

Interpreting the functional significance of these BOLD activation, however, is more difficult, because activation in itself does not mean that a region plays causal role in a behavior. In the cerebellar cortex, BOLD signal predominantly reflects activity in the incoming mossy fibers, while the output activity is largely absent (Mathiesen et al., 2000; Alahmadi et al., 2016; Gagliano et al., 2022). This implies that the cerebellar BOLD signal is primarily driven by input originating from the neocortex. Therefore, when a neocortical area is activated, we may observe BOLD activation at the cerebellum's input, irrespective of its specific relevance to the processing demands of the task.

To overcome this challenge, we introduced the idea of **selective recruitment**. It posits that the input to the cerebellum is *gated* in a *task-dependent* manner such that it is only up-regulated when specific cerebellar processing is needed (Shahshahani et al., 2023). In the context of task-based fMRI BOLD activation this implies that when cerebellum is not explicitly required, the level of activation at its input can be predicted by the activity levels in

the neocortex. However, when cerebellar processing is necessary, its activation elevates. In Chapter 3, we tested this idea in the context of the well-established causal function of the cerebellum in motor control, showing up-regulation of inputs during the rapid coordination of finger movements relative to the production of larger finger forces.

In this chapter, we will use the same approach to ask which working memory process(es), if any, selectively recruits the cerebellum. Based on reported deficits in cerebellar patients, we chose to manipulate both the load (how many digits have to be remembered) and recall direction (forward vs. backward) in a digit span task. Additionally, we designed the experiment so that we could dissociate the stage of encoding and retrieval.

Before testing which of these processes would lead to a selective recruitment of the cerebellum, the experiment also provided us an opportunity to reassess past hypotheses about the cerebellum's role in working memory. In this context, we specifically aimed to test three hypotheses about the functional specialization of the multi-demand network within the cerebellum: First, we tested for laterality of cerebellar responses, as been shown in previous studies of language-related processes (Desmond et al., 1997; Mariën and Borgatti, 2018; Murdoch, 2010). We then explored whether there are any differences between the processes that engage the superior cerebellum and those that engage the inferior as suggested by previous studies (Desmond et al., 1997; Chen and Desmond, 2005). Lastly, we asked whether the sub-regions within the hierarchy of the multi-demand network show any variations in their responses to our digit span task.

4.2 Results

4.2.1 Behavioral task in the scanner

To study the processes of working memory, we implemented a digit span task requiring participants to memorize and subsequently recall a sequence of visually displayed digits. The task's design was a 2-by-2-by-3 structure, involving three factors (Figure 4.1 a). Each trial sequence began with a brief 500-ms cue phase that signaled the recall direction (forward or backward) and the memory load (2, 4, 6) for the upcoming trial. The cue phase was immediately followed by the encoding phase.

During the encoding phase, digits were sequentially displayed from left to right. Each digit stayed on the screen for one second, after which it either transformed into a hashtag symbol (#), indicating it was a digit to be remembered (memory digit), or it stayed visible (non-memory digit). Participants were tasked with memorizing the digits designated as memory digits.

Following the encoding phase, there was a one-second delay during which participants are supposed to maintain the digits in their memory. The task included both Go and No-go trials. In the Go trials, this brief delay preceded the retrieval phase, where participants were given time to retrieve and reproduce the mixed sequence of memory and non-memory digits. Participants were instructed to reverse the order during retrieval. In No-go trials, there was no retrieval phase; instead, the next began immediately after the one-second delay (Figure 4.1 b).

In this task, digits are presented visually; Some digits remain on the screen and some are masked. The initial information is presented visually. Participants are then reading and rehearsing the digits sub-vocally meaning that verbal processes are at work in encoding and retrieval. Therefore, while the task involves visual elements, it predominantly engages

verbal working memory processes, thus can be classified as a verbal working memory task.

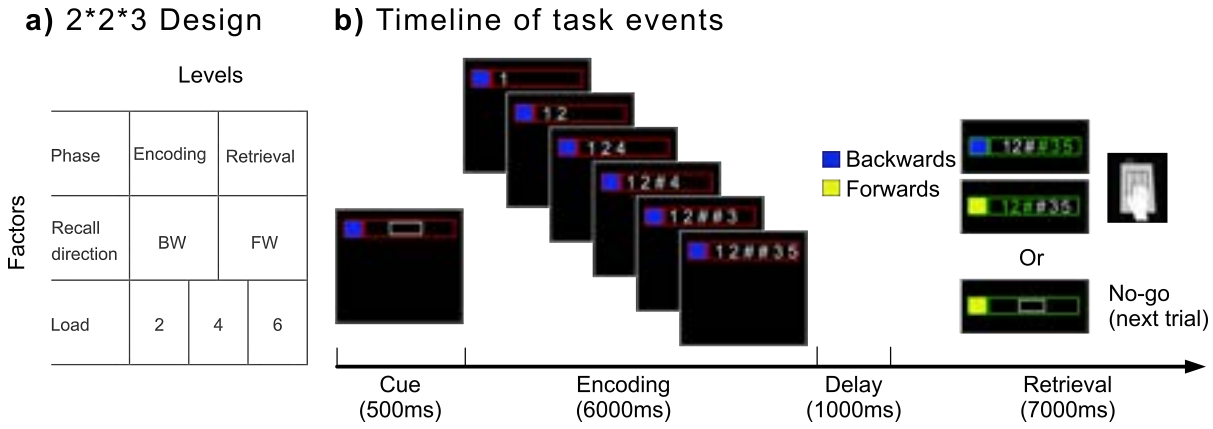

Figure 4.1: **The digit span task**. **a)** Factors included in the task and their respective levels. **b)** Timeline of events happening within the task. Cue phase signals the recall direction and memory load of the upcoming trial (blue for backward condition and yellow for forward). Encoding phase starts after the cue phase. A sequence of 6 digits start appearing on the screen, with memory digits being masked after 1 second and non-memory digits remaining on the screen. After a one-second pause, the task either progresses to the retrieval phase (Go trial) or skips to the beginning of the next trial (No-go trials).

Accuracy was calculated as the percentage of trials where participants made no errors in retrieving the memory digits. Overall performance of the participants is represented in Figure4.2. As expected, accuracy was lower for conditions with backward recall compared to forwards recall. Moreover, as the memory load increases, the accuracy goes down. A two-way repeated measures ANOVA with load (2, 4, 6) and recall direction (forward, backward) as factors showed main effects of load ($F_{2,30} = 15.36, p = 0.00$) and recall direction ($F_{1,15} = 5.44, p = 0.03$)

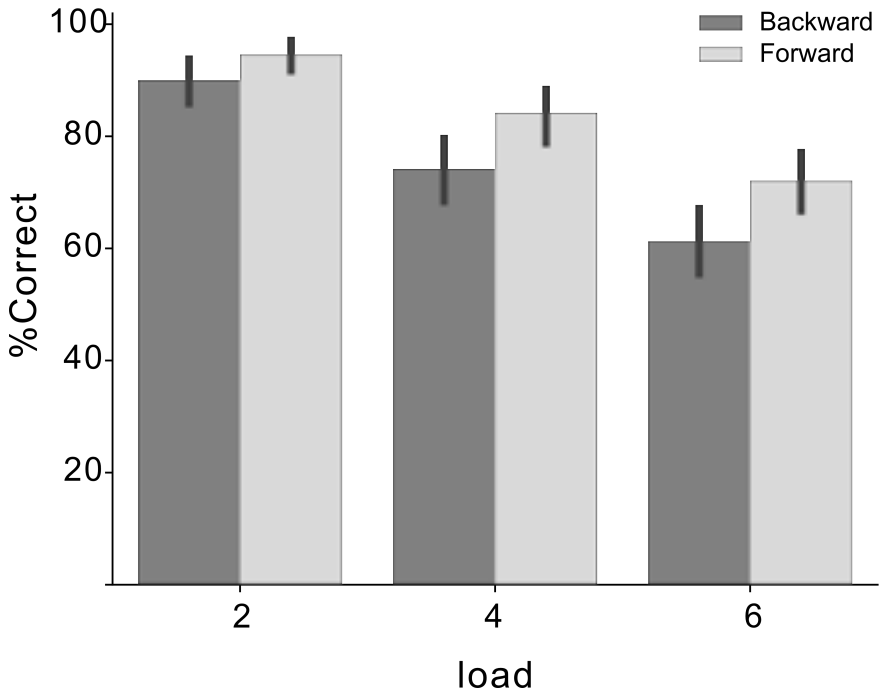

Figure 4.2: **Behavioural performance inside the scanner**. Figure shows percentage of correct trials. As expected, % of correct trials dropped with increasing load. Additionally, participants tend to make more errors during backwards recall

4.2.2 Overview of activation in the working memory network

Our digit span task required participants to memorize visually presented sequences of digits, maintaining them, and retrieving them while performing them as a sequence of finger presses. This makes it an example of a verbal working memory task. As expected, we observed high activity in the fronto-parietal network in neocortex during encoding, which has been previously associated with verbal working memory (Owen et al., 2005). Additionally, since the retrieval phase involved finger presses, we not only observed activations in the fronto-parietal network, but also in the motor cortices (Figure 4.3 - upper panel).

Within the cerebellum, encoding of memory digits led to high activation in both superior and inferior cerebellum. Specifically, we saw activation in areas that have been

shown to be parts of a multi-demand system (Nettekoven et al., *In prep*). Visually, in line with previous studies of verbal working memory, we observed higher activation in the right cerebellar hemisphere compared to left hemisphere (Desmond and Fiez, 1998). Similar to the neocortex, retrieval phase elicited activation in the right hand area of the cerebellum as well (Figure 4.3 - lower panel).

Overall, retrieval phase elicited higher activation compared to encoding both in the cerebellum and neocortex. In the cerebellum, in line with previous studies, activity is observed in lateral parts of lobule VI, extending to Crus I. In the inferior cerebellum, inline with previous studies, activity mainly covers lobules VIIb and VIIIa (Chen and Desmond, 2005) and further extends to VIIIb, particularly during retrieval (Figure 4.3)

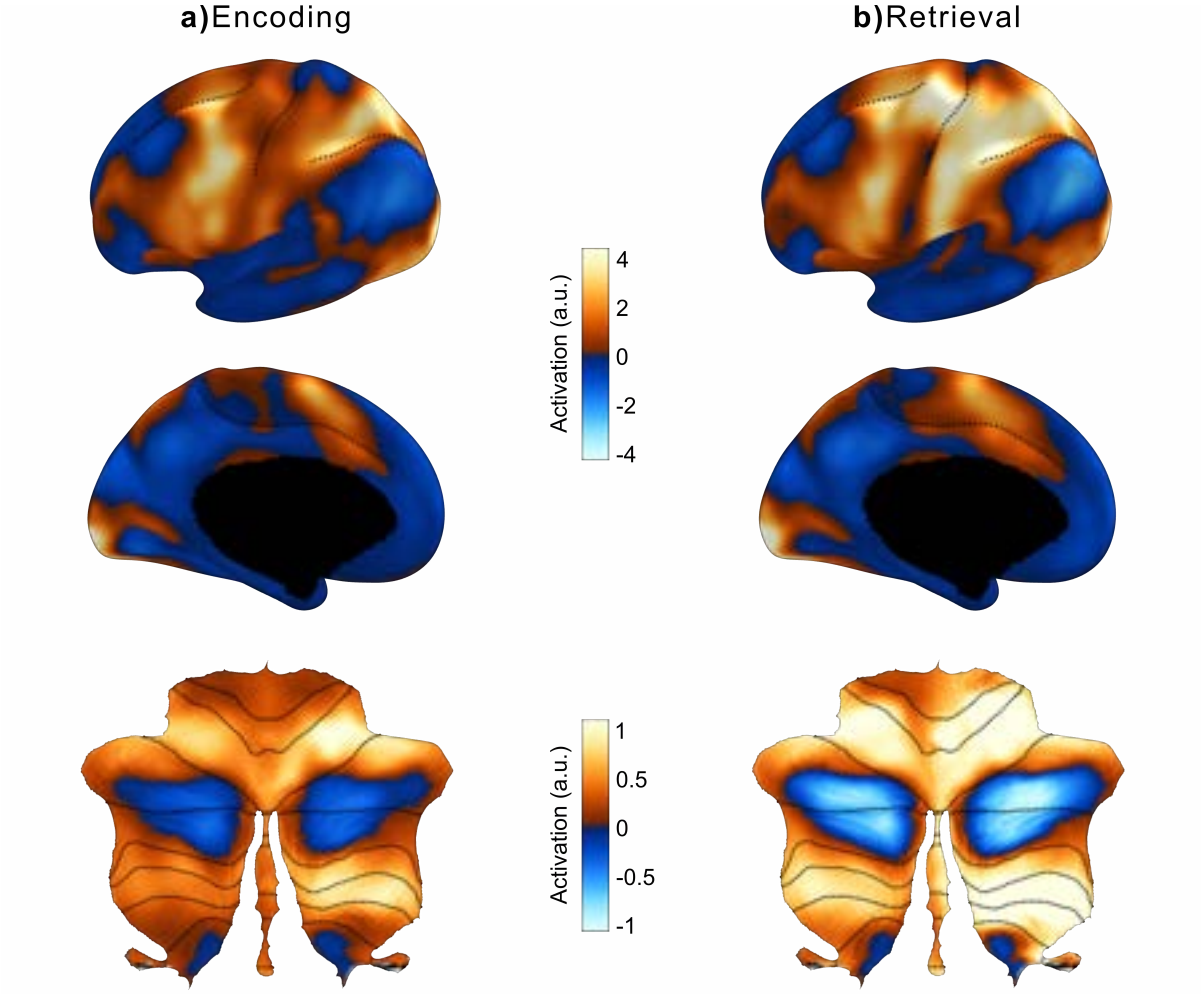

Figure 4.3: **Average activation in the cortico-cerebellar network for working memory. a)** group-averaged activation during the phase when the participants are encoding the digits. Upper two panels show lateral and medial surface of the left hemisphere. Lower panel shows cerebellum as a flatmap. As expected, the regions within frontal and parietal cortices show high activations. In the cerebellum, high activity is observed in lobule VI extending into Crus I. Additionally, in the inferior part, Lobules VIIb, VIIIa, and VIIIb show high activity. **b)** shows activation during the retrieval phase when participants are retrieving memory digits and performing the sequence of finger presses. In addition to the areas activated during encoding, high activation is observed in M1 and right hand area of the cerebellum attributed to finger presses.

As shown earlier in Figure 4.1 a, we tested participants on encoding different number

of items in their memory (Load factor). To identify regions that exhibited increased activation in response to increasing load, we created a load contrast by comparing conditions with high load (6 digits) to those with low load (2 digits) during forward recall. By specifically focusing on forward conditions, we aimed to eliminate potential effects in working memory processes resulting from reversing the serial order. Additionally, our task included backward recall conditions, wherein participants were instructed to reverse the order of the digits during retrieval. To find cerebellar and neocortical regions that show heightened activation in response to this order reversal, we calculated a recall direction contrast. The contrast was calculated by subtracting forward conditions from backward conditions.

In summary, we found activity in all multi-demand regions of the neocortex and cerebellum, with all regions showing some sensitivity to load and to the recall direction. Notably, load effect appears more pronounced during encoding, whereas the recall direction effect is more evident during retrieval. This suggests that the order reversal likely occurred during the retrieval process (4.4).

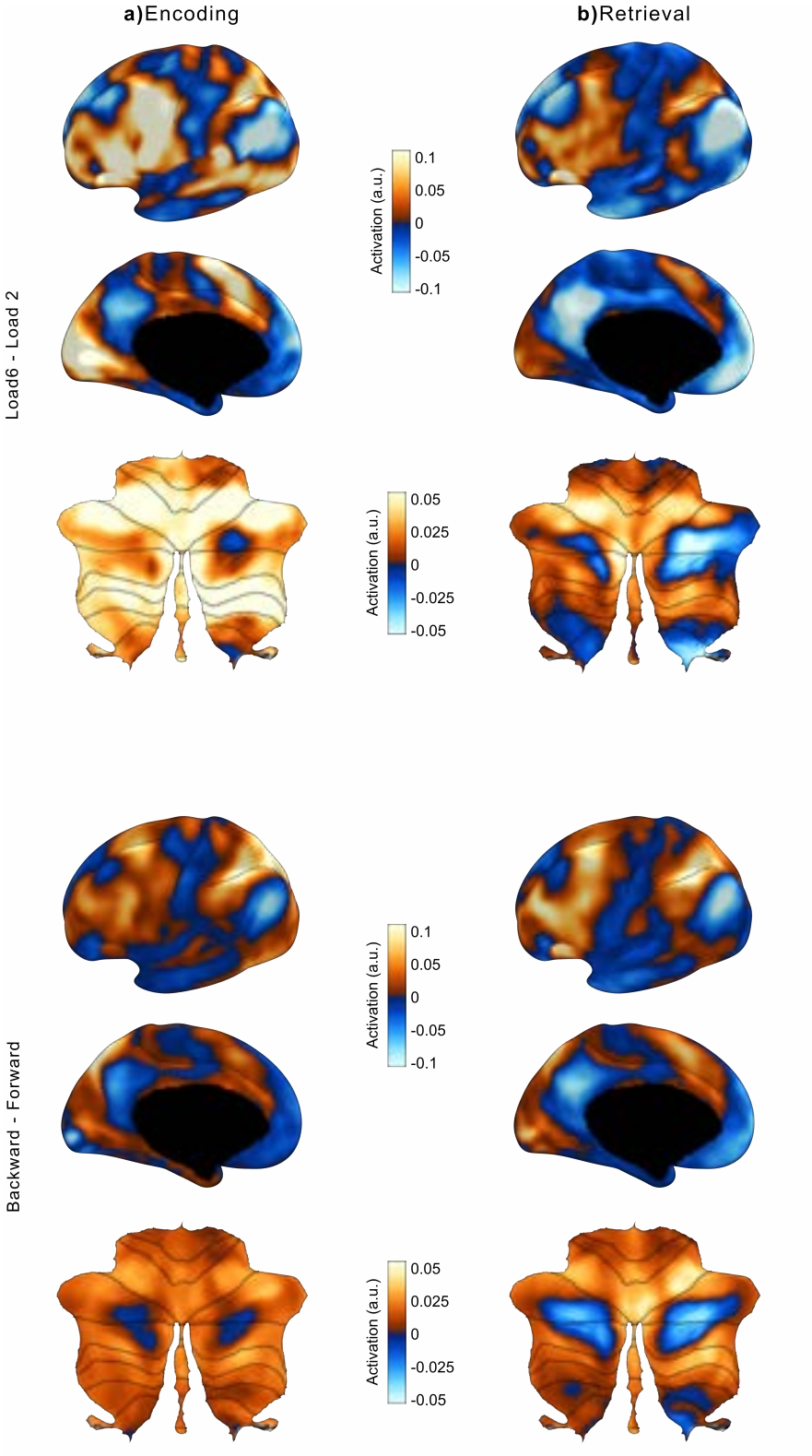

Figure 4.4: **Load and recall direction contrasts a)** During encoding and **b)** during retrieval. Regions of multi-demand network show high activations in both load and recall direction

contrasts. Load effect appears to be more pronounced during encoding compared to retrieval. While the recall direction effect is smaller compared to load effect during both encoding and retrieval. However, it can be seen that the recall direction effect is more pronounced during retrieval compared to encoding.

4.2.3 Functional topography of regions sub-serving working memory

The multi-demand network as a whole exhibits increased activation throughout the task (Figure 4.3). We looked for functional specialization within this broad network by examining the variations in responses among its subdivisions. We investigated three different axes along which we could subdivide this network: Left and right, superior (VI+Crus I) and inferior (VIIb and VIIIa), and finally sub-regions D1-D4 defined in a data-driven hierarchical parcellation.

Laterality of the multi-demand network in the digits span task

Given that we used a verbal working memory task, based on previous studies, we expected to see more right-lateralized activity in the cerebellum, compared to a visual or spatial task (Gatti et al., 2021; Thürling et al., 2012). Consistent with these findings, we found that the right hemispheric part of the multi-demand network displayed significantly greater activation than its left counterpart (Paired t-test: $t_{15} = 5.99, p = 2.46e-5$, Figure 4.5). Therefore, for the rest of the analysis, we will only focus on the right hemisphere of the cerebellar multi-demand network.

Differential engagement of cerebellar lobules during encoding and retrieval

We evaluated a series of hypotheses positing functional specialization of cerebellar regions along the superior/inferior axis in the context of working memory. Firstly, previous studies

involving cerebellar patients have revealed a modality-specific dissociation within the inferior cerebellum, with the right inferior cerebellum being involved in verbal working memory tasks when stimuli is presented visually, and the left inferior cerebellum being implicated in tasks with auditory stimuli (Marvel and Desmond, 2010). Inline with this notion, given that stimuli is presented visually in our task, we observed significant increases in encoding and retrieval activation within the right inferior cerebellum ($t_15 \geq 5.56, p \leq 5.43e-5$),

Second, Marvel and Desmond (2010) found a functional dissociation between the superior (VI + Crus I) and inferior (VIIb + VIIIa) cerebellum. They suggested that the superior cerebellum is involved in speech planning happening during covert reading of letters. In line with their hypothesis, we found significant activation in the superior part of the right multi-demand network during encoding and retrieval phases, since both involve covert reading of digits from the screen.

Furthermore, they suggested that the inferior cerebellum plays a role in maintaining phonological information over time. Given this hypothesis, and considering that our encoding condition involves both subvocal rehearsal and maintaining information through a one-second delay, we expected to see greater encoding activation in the inferior cerebellum compared to retrieval activation. To test this hypothesis, we performed a 2-way repeated measures ANOVA with task phase (encoding, retrieval) and quadrant (superior, inferior) as factors, and average activation as the dependent variable. We found a significant interaction between quadrant and task phase ($F_{1,15} = 23.52, p = 2e-4$). Surprisingly, contrary to the prediction, post-hoc tests revealed that activation in the right inferior cerebellum was instead more activated during retrieval compared to encoding (Figure 4.5a). Given the assumption that maintaining phonological information is particularly relevant during the 1-second delay, this result challenges the notion that the inferior right quadrant of the multi-demand network plays a crucial role in phonological storage.

Lobular specificity of the multi-demand network in load and recall direction effects

Another prediction of the idea that the inferior right quadrant is especially engaged in the phonological storage, is that we should find an especially high load effect in this area. However, when we summarized the load effect (see above) within the quadrants on the right hemisphere, the two-way repeated measures ANOVA showed no significant phase by superior/inferior effect ($F_{1,15} = 0.8, p = 0.38$), leading to no evidence for a differentially high load effect in the right inferior quadrant.

Recall direction effect (see above) on the other hand, would require more sub-vocal rehearsal and hence, this idea predicts that this effect is especially high in the right superior quadrant. However, we found no evidence for regional specialization of this contrast along the superior/inferior axis ($F_{1,15} = 0.3, p = 0.056$, Figure 4.5b).

Thus, our data did not support the predicted functional differentiation of the multi-demand network along the superior and inferior axis with subvocal control processes (superior) and phonological storage (inferior). Only the special engagement of the inferior right quadrant during the retrieval phase suggests some functional differentiation (see discussion).

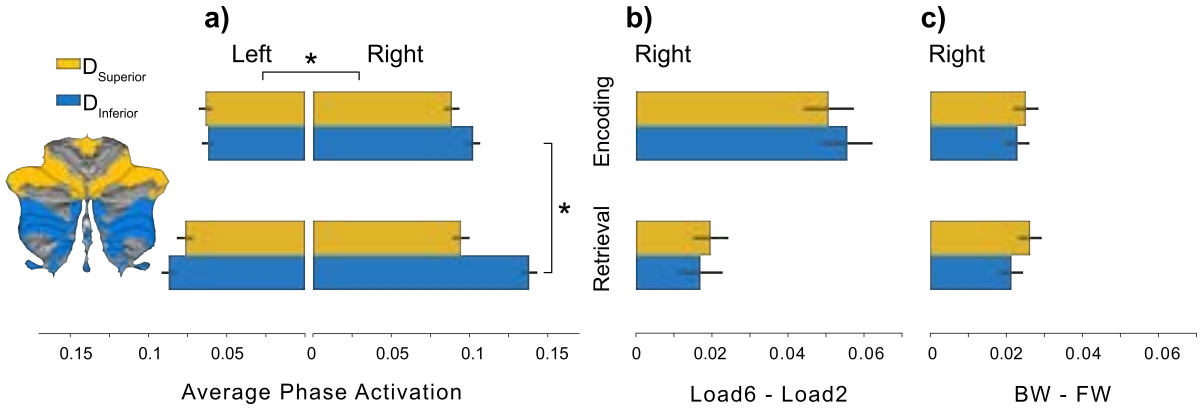

Figure 4.5: **Average activation during encoding and retrieval within the multi-demand**

network. **a)** Left panel shows the superior (yellow) and inferior (blue) parts of the multi-demand network. On average we see that activation within the right half is significantly higher than the left half. This is true for both anterior and posterior parts. Contrary to our predictions, within the right inferior quadrant, we found significantly higher activation in retrieval, compared to encoding. **b)** load and **c)** recall direction effects summarized within the right half of multi-demand network. Neither of these effects showed any evidence for differentiation between right superior and inferior quadrants. It can be seen that the size of these effects are closely matching within encoding and retrieval

Sub-regional specificity of multi-demand network in load and recall direction effect

An alternative approach to subdivide the multi-demand network was recently suggested by a data-driven approach utilizing a range of task-based fMRI studies (Nettekoven et al., *in prep*), wherein this broad network is further sub-divided into smaller sub-regions (D1 - D4). The sub-regions are identified based on the similarity of their activity profiles across a wide range of tasks. Even though these sub-regions have comparable activity profiles, we asked whether there are systematic differences in their responses to two factors manipulated in our task: increasing load (load effect) and reversing the serial order of digits (recall direction effect).

To test for this, we summarized load and recall direction effects in D1-D4. Sub-regions' responses to increasing load appeared to be similar: they show high load effect size during encoding, diminishing during retrieval (Figure 4.6 a). We tested for this statistically with a two-way repeated measures ANOVA with sub-region and task phase as factors and effect size as the dependent variable. Results revealed a main effect of task phase ($F_{1,15} = 4.90, p = 0.042$) and a significant interaction effect ($F_{3,45} = 3.47, p = 0.023$). Conversely, recall direction effect was comparable across D1 to D4 during encoding. However, their responses diverged during retrieval: The effect size in D1 and D3 increased compared to encoding while in D2 and D4 it went down (Figure 4.6 b). This observation was further

supported by the two-way repeated measures ANOVA (this time with recall direction effect as response variable) that showed significant interaction between phase and sub-region ($F_{3,45} = 5.36, p = 0.003$).

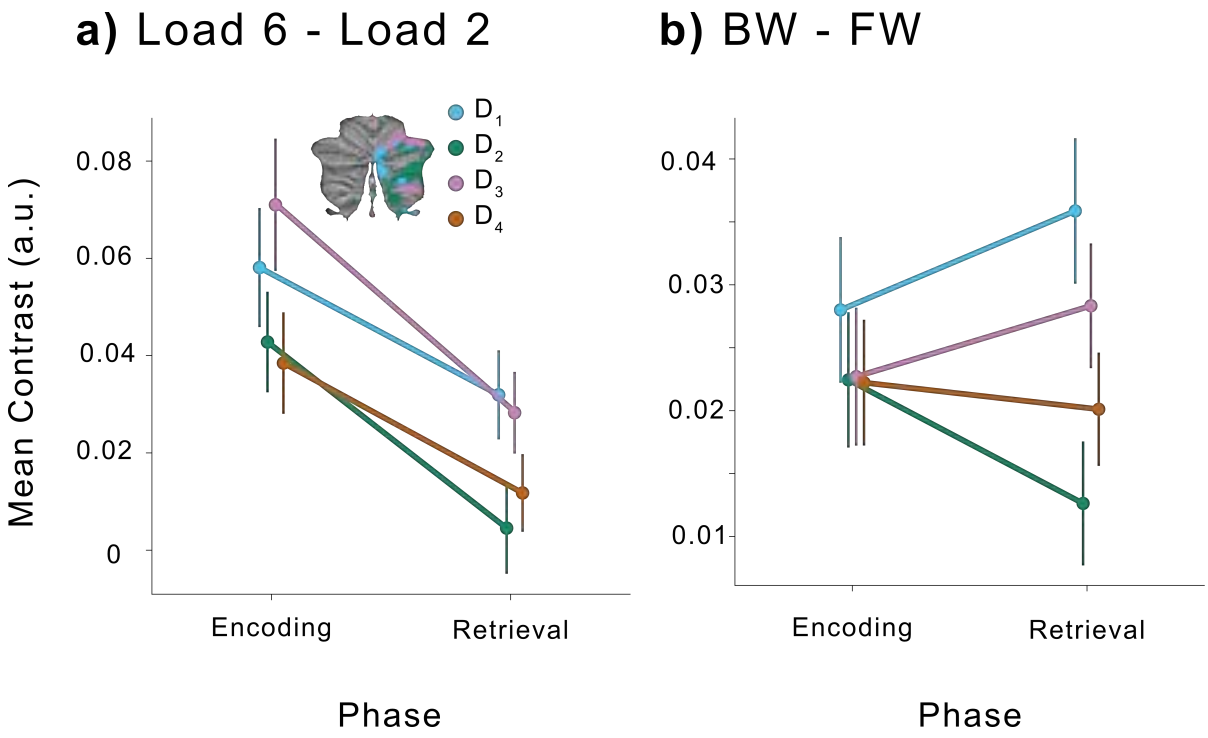

Figure 4.6: **Average activation within sub-regions of the cerebellar multi-demand network**. Multi demand network is hierarchically divided into sub-regions D1-D4. Load and recall direction effects are summarized within these sub-regions. **a)** Shows average load effect during encoding and retrieval. The contrast shows a significant main effect of phase and sub-region by phase interaction. The pattern of change within all sub-regions are similar: Starting at a higher magnitude during encoding and decreasing to a lower value during retrieval. **b)** Recall direction effect only shows a significant sub-region by phase interaction. The magnitudes of the effect within sub-regions start at comparable values during encoding and diverges during retrieval. D1 and D3 show increase in activation, while D2 and D4 show decreases.

Based on these findings, we infer that the different sub-regions contribute to our task

in different ways. This is especially clear when considering the effect of recall direction: During encoding and maintenance of phonological information all regions show approximately the same activation. During retrieval, however, D1 and D3 become more involved for order reversals, whereas D2 and D4's involvement decreases. In sum, these results suggest that the functional difference between the newly identified sub-regions of the cerebellum (each with a superior and inferior component) are bigger than the difference between the superior and inferior aspect of the multi-demand network (Marvel and Desmond, 2010).

Functional specificity of cortico-cerebellar multi-demand sub-networks

While this analysis shows nuanced involvement of multi-demand sub-regions in the digit span task, it does not take into account the fact that neocortical activations are also evident as highlighted in Figure 4.3. This leads to the question - Do the functional dissociations observed in the cerebellar multi-demand sub-regions mirror are the same dissociations in their neocortical counterparts? This warrants further investigation to gain a comprehensive understanding of the intricate interplay between the cerebellar and neocortical sub-regions in the context of the task.

We incorporated neocortical regions into our analysis by assuming a one-to-one correspondence between these cerebellar regions and their neocortical counterparts. We utilized a Winner-Take-All (WTA) approach to model the cortico-cerebellar connectivity using the Glasser et al. (2016) parcellation. Ridge-regression was employed to estimate cerebellar activity in a multi-domain task battery ((King et al., 2019)). Similar to the approach used in Buckner et al. (2011); Marek et al. (2018), we then assigned a single neocortical region to each cerebellar sub-region by choosing the region that corresponded to the maximum regression coefficient. As expected, the identified neocortical regions are sub-regions within the multi-demand network that show activation in working memory (2back vs 0back) and language (math vs story) contrasts (Glasser et al., 2016). Pairs of cortico-cerebellar sub-network identified through this method are depicted in Figure 4.7 a) each with a unique color.

The naming conventions for the neocortical regions are adopted from Glasser parcellation (Glasser et al., 2016).

We investigated the variations in involvement of cerebellar and neocortical compartments of the multi-demand network by normalizing the activations within each region over the group of subjects by subtracting the mean. Overall, activity profiles of cerebellar multi-demand sub-regions follow those of their cortical counterparts closely (Figure 4.7 b) albeit with subtle differences. To determine if these differences were statistically significant, we performed a two-way repeated measures ANOVA for each sub-network. We used structure (cerebellum vs. neocortex) and condition (with a total of 12 conditions) as factors. Significant interactions between condition and structure were found in all instances ($F_{11,165} \geq 2.56, p \leq 6e-3$) but pair 4, comprising of D4 and region 6ma ($F_{11,165} = 1.01, p = 4.4e-1$). For instance, in pair 2, during the retrieval phase, activity in D2 showed minimal variation with changes in load and recall direction. Conversely, in its best matching neocortical counterpart, Glasser's 6r, activity scaled up with load during both forwards and backwards recall.

We delved deeper into these dissociations by employing Multidimensional scaling (MDS) to project the activity profiles of sub-regions onto lower dimensions. As vectors, we plotted contrast vectors that indicated the magnitude and direction of task factors: retrieve (retrieval - encoding), load+ (load 6 - load 2) and backward (backward - forward). This means, movements in the direction of the vector indicate that the corresponding effect was more pronounced in that region. As illustrated in the figure, in pair 1, both D1 and IFJp exhibited a positive effect when comparing backward vs. forward. D2 and 6r both manifested a positive effect of load. Yet, only 6r displayed a positive retrieval effect. D3 indicated positive effects for both load and retrieval, whereas its neocortical counterpart, SCEF, showed only the positive effect of load. Similarly, both D4 and 6ma demonstrated positive retrieval effects (as seen in Figure 4.7 c).

In summary, both visually and statistically, we demonstrated that if we base our

assumptions on the input to each cerebellar region being explained by a single neocortical region, there exists a functional differentiation between cerebellar and neocortical sub-networks. This differentiation implies that the contributions of the cerebellum differ from those of the neocortex - and that there does not exist a simple 1:1 correspondence between cortical and cerebellar sub-networks.

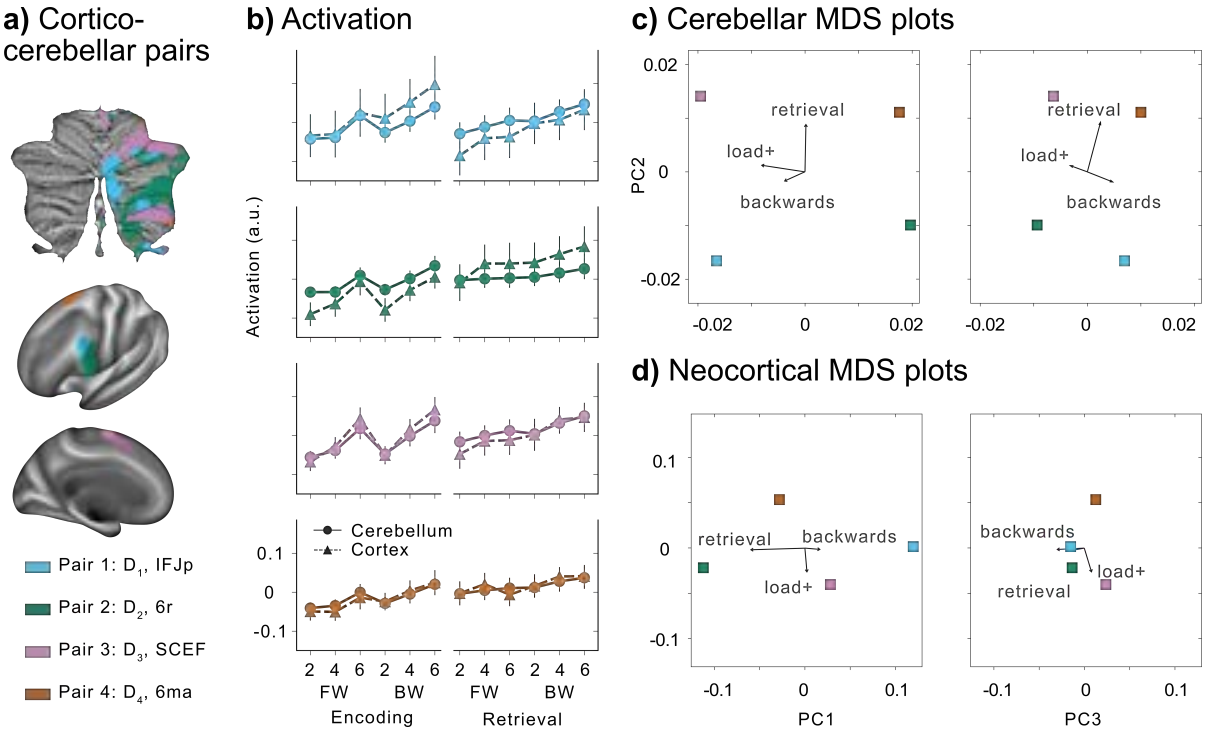

Figure 4.7: **Average activation during encoding and retrieval within the multi-demand cortico-cerebellar network**. **a)** Shows the network pairs identified through a winner-take-all approach. **b)** Activity profiles within cerebellar and neocortical parts of the network pairs. Within each region, activations are normalized by subtracting the mean. **c)** Multi-dimensional scaling applied to the similarity of activity profiles within the cerebellar and **d)** neocortical sub-regions within the network pairs

4.2.4 Cerebellar input is up-regulated during encoding of high load in the digit span task

We now turn the the main question of this chapter - namely to identify conditions under which the input to the cerebellum from the cortical regions maybe selectively up-regulated. In the previous sections, we analyzed the activity across various regions in the neocortex and cerebellum in isolation, making it hard to draw conclusions about any specific functional role for the cerebellum. This is because the BOLD activity in the cerebellar cortex primarily reflects the input it receives from the neocortex. In this section we explore specific functions of the cerebellum in the digit span task by testing for selective recruitment, our novel approach that we established in Chapter 3.

To estimate the input activity in the cerebellar cortex, we again utilized a task-invariant model of cortico-cerebellar connectivity, which was derived from a task battery encompassing multiple domains (King et al., 2023). We first focused on the connectivity weights from the best-fitting model (Ridge regression), specifically on D3 region in the right hemisphere which showed the highest overall activity throughout the cerebellum. As shown in Figure 4.8 a, average connectivity weights from the model suggest converging input from area 55b (located at the inferior end of the middle frontal gyrus), PEF (premotor eye field), area 6r (anterior to the primary motor cortex), and SCEF (dorsomedial frontal cortex from Glasser's parcellation). This connectivity model, although not perfect, provides a baseline against which we can test for up- or down-regulation of the input to the cerebellum.

Using the connectivity model, we predicted the level of cerebellar activation per condition, per subject for the selected region of interest. It is important to note that the incorporated model was L2-regularized and estimated on a different dataset with different subjects. As a result, the predicted values are on a different scale compared to the observed values (Figure 4.8 b). Nonetheless, when we fit a linear regression to account for these differences, we observe that the predicted values are, in general, closely matching the

observed values ($R^2 = 0.71, SE = 0.01$).

Although the model is able to predict a 71% of the variance in the observed cerebellar data, there is one clear deviation from the line: the high load conditions (both forward and backwards) in the encoding phase appear to lie systematically above the prediction line. To quantify whether these deviation are significant, we performed a repeated measures ANOVA on the residuals from the regression, testing if there are conditions that are systematically more or less activated than predicted ($F_{11,165} = 1.96, p = 0.035$). Contrary to what we predicted based on patient studies, the ANOVA reveals a significant 2-way interaction between load and phase ($F_{2,30} = 4.86, p = 1.4e-2$) with no significant effect of recall direction.

Voxel-wise analysis across the cerebellum

In our prior analysis, we closely examined a particular sub-region of the cerebellum within the multi-demand network that consistently exhibited high activation throughout the digit span task. However, it does not explore if other cerebellar regions also demonstrated elevated activations under high load conditions during the encoding phase, exceeding the predictions. To investigate this, we applied the same method to every cerebellar voxel, assessing any deviations from the predictions. the linear regression to bring predicted and observed activations to the same scale is estimated with a single slope parameter across the whole cerebellum. The interaction effect between the phase and load is illustrated in Figure 4.8 c as a statistical map. Notably, we identified voxels in the lateral portions of Crus I and Crus II - both part of the multi-demand network - that displayed increased sensitivity to this interaction. Unexpectedly, there was also a significant effect in the upper section of the cerebellum's right-hand area, potentially indicating the early planning of the sequence during the encoding phase. In essence, our findings suggest that the discrepancies from our consistent connectivity model prominently emerge when there's a high encoding load, with the primary effect centered within the multi-demand network.

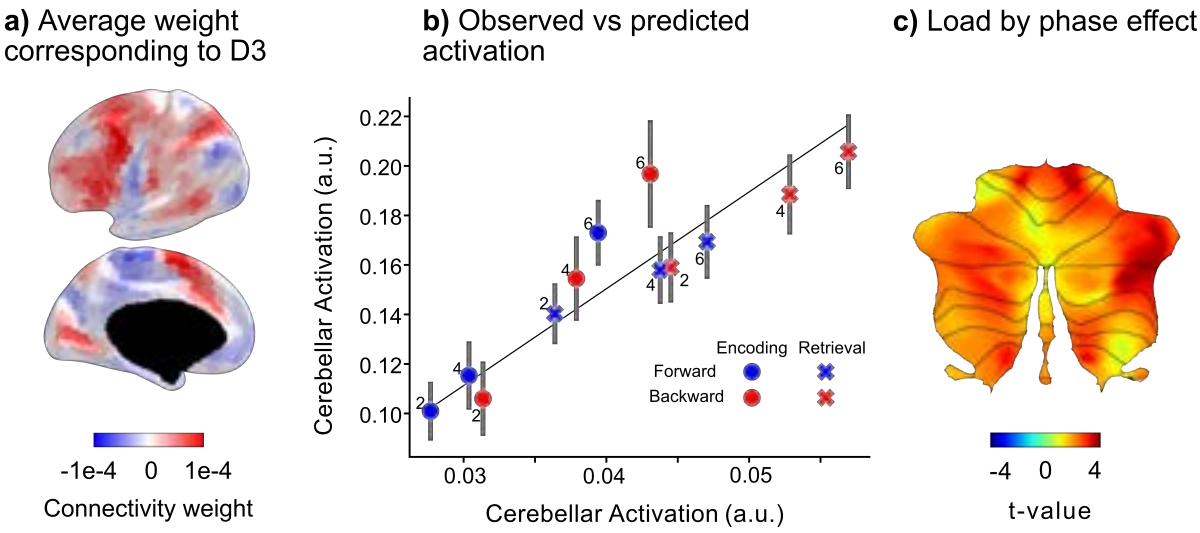

Figure 4.8: **Selective recruitment of the multi-demand sub-region D3R**. **a)** Group connectivity weights are used to select the corresponding neocortical regions to region D3 from the multi-demand network. Connectivity weights are estimated using regularized regression (Ridge regression), therefore, they are shrunken, but not zero. Neocortical regions of the multi-demand network show highest connectivity weights compared to the rest of the neocortex. **b)** Observed activation is averaged across voxels within sub-region D3R of the multi-demand network and plotted against the predicted activation within this region. Predicted activations are estimated using a regularized regression and hence are not on the same scale as the observed activations. A linear regression is therefore fit to the data to account for difference in scale. Systematic deviations are tested for by looking for conditions for which this linear regression residuals are different from 0. Conditions with load 6 during encoding show significantly high positive residuals. **c)** Same method as in **b** is applied on a voxel level and consequently voxel-wise residuals are tested against 0. The t-map depicts results for the test for interaction between load and phase.

4.3 Discussion

Evidence from patient studies and functional imaging supports the involvement of the cerebellum in working memory (Stoodley, 2012). Though cerebellar BOLD activity is

frequently elicited during working memory tasks, it is important not to over-interpret activation in the cerebellum in these tasks. This is because the BOLD signal within the cerebellar cortex largely mirrors its input, which in turn mainly arises from the neocortex (Mathiesen et al., 2000; Kelly and Strick, 2003). Cerebellar activations, therefore, might result from the information flow via the anatomical pathways connecting the cerebellum and the neocortex. Hence, simply detecting activation in cerebellar areas does not directly indicate their involvement in working memory.

In this study, we employed a digit span task to target the multi-demand network - a broad set of regions known for their involvement in executive functions (Assem et al., 2020). The task required participants to encode different number of digits presented sequentially, and then reproduce them either in normal or reversed serial order. Including Go and No-go trials enabled us to study encoding and retrieval processes separately. We first examined the functional topography of the multi-demand network in the digit span task. Subsequently, using a method we introduced in a prior study (Shahshahani et al., 2023), we assessed whether this network exhibited selective recruitment during our task.

In line with prior research on verbal working memory, we found pronounced activation in the right hemisphere of the cerebellar multi-demand network. Notably, the right superior segment (VI + Crus I) exhibited increased activation during both encoding and retrieval. This region is suggested to be involved in the articulatory control of speech, be it overt or covert (Marvel and Desmond, 2010). It is plausible that participants consistently used covert speech during the task, both for encoding and rehearsing items, as well as for their retrieval. Thus, our findings further support the proposed function of this region.

We observed particularly heightened activation in the right inferior cerebellum (VIIb + VIIIa) during item retrieval as opposed to encoding. This contrasts with the hypothesis that the inferior cerebellum primarily functions to maintain items within memory over a period of time (Marvel and Desmond, 2010). According to this hypothesis, there should be a more elevated activation during encoding, given that the short delay between encoding

and retrieval is indeed modeled as part of the encoding phase. To identify the engaging process, we must distinguish between shared and unique processes between encoding and retrieval phases: Both entail reading digits from the screen, prompting inner speech. Additionally, sub-vocal rehearsal, a manifestation of inner speech, likely happens during both stages, but with a more pronounced presence during encoding. The encoding phase also involves maintaining digits in phonological storage. In contrast, retrieval seemingly scans this storage and brings the identified digit to conscious awareness for subsequent action of finger presses. Hence, this specific cerebellar region seems more poised to access and navigate the phonological storage than merely to engage in maintaining items within it.

From another perspective, this region has been linked to concrete control, a type of control that directs attention to stimuli and oversees current actions (D'Mello et al., 2020). Along with navigating the phonological storage and covert speech, the retrieval phase probably demands control over action selection based on context (like Forward or Backward serial recall). Additionally, actions (like pressing keys) are chosen based on the item retrieved. Thus, the retrieval phase indeed encompasses concrete control, and our findings corroborate the suggested function for the VIIb/VIIIa region.

The multi-demand network was further broken down into smaller regions using a data-driven method (Nettekoven et al., *In prep*). At the outset, we assumed uniformity within these sub-regions due to their definition based on comparable activity patterns. Yet, our analysis brought subtle distinctions to light. Every sub-region displayed a decline in the load effect size when transitioning from the encoding to the retrieval phase. However, in evaluating the recall direction effect, contrasting trends appeared: D1 and D3 exhibited a rise in effect size, whereas D2 and D4 saw a decrease. Viewing this from a cognitive control lens, reversing the serial order seems to require managing the context (recall direction) and determining the action at the retrieval stage. The varied roles of these regions can be linked to their distinct participation in control mechanisms. As per (D'Mello et al., 2020), the control over evolving contexts to guide actions likely occurs during encoding and transitions

to a more specific control during retrieval. Thus, it's plausible that D1 and D4 partake in contextual control, while D1 and D3 play a role in concrete control.

Assuming input from a singular functional region in the neocortex, we observed closely aligned activity profiles between sub-regions of the multi-demand and their corresponding neocortical regions, particularly during encoding. Yet, during retrieval, minor discrepancies were apparent. While these observations might suggest a distinct role for the cerebellum during retrieval, this difference might be due to the cerebellar region receiving inputs from multiple neocortical areas. The notion of a direct one-to-one mapping between the two is likely an oversimplified representation of how cerebellar activity is influenced by neocortical activation.

The main research question of this chapter, however, was to ask whether there would be specific conditions on the working memory task that would engage the cerebellum specifically. For this, instead of using a single neocortical region, we employed a connectivity model to predict the input directed to a cerebellar region, subsequently assessing the distinct contributions of the cerebellum. We had previously validated this methodology within the motor domain in **chapter 3**. This marked our first effort to apply it within a cognitive context. Our findings indicated that the cerebellum becomes specifically active when encoding six items in memory. Interestingly, this contrasts with patient study outcomes which suggest that the cerebellum is especially required when reversing the sequence of digits. Hence, while the cerebellum demonstrates pronounced activations across different conditions of the task, these activations do not necessarily provide a clear indication of its specific role within the task. It might merely be mirroring the activities of its corresponding cortical regions. Nonetheless, when encoding six digits, our data offers compelling evidence of the cerebellum's selective engagement.

Several cognitive mechanisms in memory could be responsible for the observed results. Notably, the chunking strategy serves as a tool for participants to enhance memory retention and consequently boost their performance (Thalmann et al., 2019). This technique

taps into the brain's natural tendency to process information more efficiently when it's categorized into meaningful groups rather than as separate, unrelated elements. This benefit of chunking is especially pronounced under high memory loads, like 6. Importantly, chunking functions in a similar manner during both forward and backward recall. Chunking hypothesis proposes that cerebellum is central in the chunking process. However, chunking is also present in load 4, although it is less important in improving performance compared to its utility in load 6.

Moreover, the cerebellum might be specifically requisitioned as task difficulty increases. A measure of task difficulty could be the differentiation in accuracy levels: challenging conditions typically result in more mistakes, reflecting reduced accuracy. Nevertheless, we lack a direct measure to evaluate performance during encoding. Retrieval errors can originate from various factors, such as motor inaccuracies, encoding the wrong digit, or weak maintenance of the digit within the phonological storage. If we take retrieval errors as indicative of encoding mistakes, the heightened errors we observe at load 6 (Figure 4.2) could lend weight to the difficulty hypothesis. Yet, this hypothesis also predicts increased activation under more difficult conditions. The parity in activation during both encoding and retrieval at load 6 casts doubt on the suitability of the difficulty hypothesis to describe our findings, given the selective recruitment is observed exclusively during encoding.

Our task aimed to investigate potential processes dependent on the cerebellum. We designed it based on patient studies that highlighted modality-specific deficits, where verbal working memory demonstrated impairments, but spatial working memory produced similar outcomes between patients and healthy individuals. Notably, in verbal working memory, the deficits in a span task become more evident when reversing the serial order is necessary. We included backwards recall conditions adding an extra layer of cognitive complexity beyond forward recall. Unlike forward recall, which primarily tests short-term storage, backward recall demands both maintenance and manipulation, thereby offering a stringent test of working memory and cognitive control. While our the task offered an opportunity

to test working memory and cognitive control processes, it is essential to acknowledge its limitations that could influence the interpretation of our findings.

Notably, in the task execution, challenges were predominantly observed at load 6. Preliminary piloting revealed that cuing the recall direction at the end of the delay phase rendered the backward recall task exceptionally challenging for certain participants; They gave up and started randomly pressing fingers. To mitigate this and ensure that the memory processes are indeed engaged, we decided to cue the recall direction at the task's onset, ensuring participants were adequately prepared. We explicitly instructed the participants to reverse the serial order during the retrieval phase. Intriguingly, post-task interview revealed that a subset of participants opted to encode items in reverse. Analysis of fMRI data, however, indicated that the majority engaged in reversal during retrieval and only a minority exhibited patterns consistent with encoding-stage reversal. This disparity in approach might account for the observed lack of significant differentiation between forward and backward recall.

Furthermore, we did not account for processes related to language. The cerebellum's role in the verbal working memory task may be due to its association with language functions (Desmond and Fiez, 1998; Chen and Desmond, 2005; Marvel and Desmond, 2010), such as reading or inner speech. A potential method to neutralize the effects of language-related processes is to introduce conditions where participants merely read the digits displayed without memorizing or recalling them. This might involve reading without making any finger movements or reading the digits and then enacting them in a sequence through finger presses. While we lacked such conditions, it is noteworthy that in loads 2 and 4, non-memory digits were displayed on the screen. Hence, language processes tied to reading the digits are present and consistent across both encoding and retrieval phases.

To sum up, in this study we conducted a thorough examination of the cerebellar working memory network. We tested an innovative method using fMRI data to analyze hypotheses about specific cerebellar functions in this domain. Our findings confirm that the

cerebellum is differentially engaged throughout the task. We evaluated prevalent theories on its potential functions in working memory and cognitive control. However, the results did not pinpoint a distinct cerebellar function. Using our newly developed **selective recruitment** approach, we sought to identify any specific conditions in our working memory task that might trigger a cerebellar response beyond what's predicted by a task-invariant connectivity model. This chapter presents the first application of our method in the cognitive domain, revealing that fMRI activity, and by extension, the likely cortico-pontine-cerebellar input, changes based on the conditions at hand. Despite clinical reports of working memory deficits in cerebellar patients, our findings suggest that the cerebellar multi-demand network is specifically engaged when there's an increased load during encoding processes.

4.4 Methods

Participants

21 participants (11 female, 10 male) began the experiment and consented under a protocol approved by Western University's review board. None mentioned any neurological or psychiatric history or current use of psychoactive drugs. Four were not scanned because of their poor performance in during behavioral training. Among those scanned, one was excluded because of an incidental finding. Thus, we ended up with 16 participants (8 women, 8 men, average age = 25, age standard deviation = 2).

Apparatus and stimuli

Participants used a custom-made 5-key finger keyboard with a force transducer located under each key(FSG15N1A, Honeywell Sensing and Control; dynamic range, 0 –25 N) to make finger presses corresponding to memory and non-memory digits (6 presses in total).

Presses were only allowed during retrieval. A press was recorded when the force level exceeded 2N. The key was considered "released" when the force level dropped below 1 N. Sensors were re-calibrated at the beginning of the run by asking the participant to remove their hands from the keyboard.

Procedure

Each trial started with a short cuing phase (500 ms). During this phase, place of the memory digits alongside with the recall direction square would appear on the screen. After the cue phase, the encoding phase started with the first digit (out of 6 digits) appearing on the left inside a red box. Each digit corresponded to a finger (1:thumb, 2:index, 3:middle, 4:ring, 5:pinky). Digits appeared sequentially, with non-memory digits remaining on the screen and memory digits changing to # after 1 second. The encoding phase lasted for 6 seconds (1 second/digit). Participants were instructed to only memorize the memory digits. If a press was made during the encoding phase, the box around the digits turned red and the participant received a penalty of -1 points.

The encoding trial was followed by a 1-second delay, followed by the retrieval phase (go trial) or another encoding trial (no-go trial). Retrieval trial started with the box surrounding the sequence turning green, signaling the participants they can start pressing. In Backwards trial (blue square), participants needed to reverse the sequential order of digits and start pressing the right-most digit (last in sequence cue during encoding). In forward trials, the order of finger presses was the same as the sequential order during the encoding phase. For all the conditions, the retrieval phase lasted for 7 seconds in total, giving participants enough time to rehearse and retrieve digits even for load 6 and backward recall direction. To make sure that the motor output was matched across conditions, they were instructed to evenly spaced their responses throughout the 7 second and received verbal feedback from the experimenter if they did not follow this instruction.

Participants received immediate visual feedback for each press made: green if the press was correct and red if it was wrong. After a retrieval trial, they received an overall feedback (500 ms) based on the number of correct presses: +4 points for all correct, +3 for 1 wrong press, +2 for 2 wrong press and 0 otherwise. This pointing system was selected to encourage participants to employ their working memory even if they have made a wrong press.

4.4.1 Experiment design

During a training session, participants completed two types of blocks outside the scanner: 5 blocks of the alternating finger tapping task (results reported in chapter 3) interleaved with 5 blocks of the working memory task. Each block of the working memory task consisted of 3 repetitions of each unique plus 1 no-go trial per condition with the order randomized (total of 42 trials, approx. 8 min/block).

During the scanning session, the participant performed 5 imaging blocks of the finger tapping task, alternating with 5 blocks of the working memory task. Each block of the working memory task lasted for just over 8 minutes, during which 512 volumes were collected. A total of 42 trials were presented, each of the 3 load and 2 recall directions were repeated 3 times within a block, with one of these three being a no-go trial. Four 12-second periods of rest were interleaved randomly between trials.

Image acquisition

We collected MRI data using a 3T Siemens Prisma located at the Center for Functional and Metabolic Mapping (CFMM) of Western University. At the start of the scan, we obtained a high-resolution whole-brain MPRAGE image with the following parameters: voxel size of 1 mm^3 and a Field-of-view of 25.6×25.6×25.6 cm^3. Subsequently, we captured whole-brain

functional images using an echo-planar imaging sequence, which had settings of TR = 1000 ms, TE = 30 ms, voxel size = 2.5×2.5×3 mm^3, Field-of-view = 20.8×20.8×20.8 cm^3, 48 slices, a P to A phase encoding direction, a multi-band acceleration factor of 3 (interleaved), and an in-plane acceleration factor of 2. To rectify distortions stemming from B0 irregularities, we also recorded gradient echo field maps with parameters: voxel size = 3×3×3 mm^3 and Field-of-view = 24×24×24 cm^3. Additionally, during each functional session, we continuously monitored and logged both heartbeat and breathing signals.

fMRI data processing and first level analysis

We pre-processed the functional and anatomical data utilizing SPM12 tools (Friston et al., 1994) and custom code written in MATLAB 2018b. For each participant, we established a unique coordinate system by positioning the origin of the anatomical image near the anterior commissure. The anatomical images were then divided into segments representing gray matter, white matter, cerebrospinal fluid (csf), and the skull. To account for head movement, functional images underwent a correction process based on the six-parameter rigid body transformation and were subsequently aligned with each participant's individual anatomical image. We utilized the average functional image combined with the outcomes of the anatomical segmentation to create a gray matter mask for functional images.

Using SPM12, we separately applied a General Linear Model (GLM) to the time series for each run. Both encoding and retrieval conditions were individually modeled as separate regressors. For the encoding conditions, we used a 7-second boxcar function that covered both the 6-second period of stimuli presentation and the subsequent 1-second delay. The retrieval conditions, on the other hand, were represented with a 7-second boxcar that spanned the response period. These boxcar functions were then convolved with a canonical hemodynamic response function (HRF). Rest was not modeled exclusively and served as the implicit baseline captured by the intercept term. The beta weights derived from the first-level GLM were normalized by dividing them with the residual-root-mean-square

image, providing normalized activity metrics for each voxel, condition, and run.

Cerebellar normalization

The cerebellum was isolated from the rest of the brain and segmented into white and gray matter using the Spatially Unbiased Infratentorial Template (SUIT) toolbox (Diedrichsen, 2006). In some instances, manual corrections were made post-segmentation. Using a non-linear deformation algorithm (Ashburner, 2007), cerebellar white and gray matter probabilistic maps were then transformed to align with the SUIT atlas space. This transformation was applied to both the anatomical images and the normalized beta weights obtained from the initial GLM. Before this normalization process, an isolation mask was utilized to discard the influence of neighboring inferior and occipital neocortical regions. For visual representation purposes, the SUIT toolbox was used to project the functional maps onto a flattened representation of the cerebellum (Diedrichsen and Zotow, 2015).

Neocortical normalization

For every participant, their anatomical image was processed to recreate the neocortical white matter and pial surfaces using Freesurfer (Fischl, 2012). Once reconstructed, these surfaces were expanded to a spherical shape and aligned with the fsLR 32k node template (Van Essen et al., 2011) using both a sulcal-depth map and local curvature. By averaging the activation values of voxels situated along the line connecting the respective vertices of the individual white matter and pial surface, the neocortical activity patterns were mapped onto these surfaces.

Region of interest (ROI) selection

We focused on the multi-demand network, which was identified using a cerebellum's data-driven parcellation, as described by Nettekoven et al., *In prep*. Comprising sub-regions (D1-D4), this network was delineated using a hierarchical clustering technique that ensured symmetry between the right and left hemispheres. To explore the functional topography, the multi-demand network was also subdivided into superior (located above the horizontal fissure) and inferior (below the horizontal fissure) sections.

To establish a one-to-one correspondence between cerebellar sub-regions in the multi-demand network and their counterparts in the neocortex, we utilized a functionally defined parcellation of the neocortex (Glasser et al., 2016). By employing this parcellation, a Winner-take-all (WTA) connectivity model was estimated at the group level. This was done by attributing the neocortical region, which had the strongest connectivity weight, to each designated cerebellar region of interest.

Connectivity model

To account for the potential convergence of neocortical inputs onto cerebellar circuits, we employed a task-invariant model of cortico-cerebellar connectivity (King et al., 2023). This model represents cerebellar voxel activity as a linear mix of neocortical inputs.

The model was developed on a public dataset encompassing two distinct task sets that broadly covered motor and cognitive domains (King et al., 2019). Each of these sets was executed in two sessions. Neocortical surfaces for participants were subdivided via an icosahedron parcellation, ranging from 80 to 1,848 parcels. Functional data within these parcels was averaged, culminating in a matrix of neocortical predictors serving as the model's input.

Three models, specifically Winner-takes-all, Lasso, and Ridge regression, were

honed to forecast cerebellar voxel activity in the SUIT atlas space based on the said inputs. The initial task set informed the connectivity weight estimations for every model (King et al., 2023), while the second task set (comprising multiple new tasks) functioned as a testbed for the trained models. Predictive accuracy of the model was measured via the Pearson correlation between observed and predicted voxel response profiles over tasks. For our study, the ridge-regression model featuring 1,848 neocortical predictors/parcels emerged as the top performer across participants. Connectivity weights for the group were calculated by averaging the best model's weights from all 24 participants.

Using these group connectivity weights, we predicted cerebellar activity in SUIT space, adapted to a 3mm isotropic resolution consistent with connectivity weight estimations. Neocortical activations were then averaged within each neocortical parcel, followed by multiplication with the group-averaged connectivity weights to derive predictions for every cerebellar voxel.

Similar to the approach in (King et al., 2023), we employed a crossed methodology: By dividing the dataset into odd and even runs, we predicted cerebellar activity patterns in half the data based on neocortical activity in the other half. This ensures accurate predictions are not merely artifacts of correlated noise processes across the neocortex and cerebellum regions (Buckner et al., 2011).

Given that our connectivity weights were extracted from a separate dataset with unique subjects and different SNR, we charted a linear regression line (without intercept) between observed cerebellar activations and model predictions. This line's slope compensates for SNR differences between datasets. Residuals derived from this regression were subsequently employed for cross-participant statistical testing.

Chapter 5

General Discussion

The primary goal of this PhD thesis was to reconsider the approach in studies of cerebellar function using fMRI. Our objective was not to try to explain cerebellar involvement in tasks with a single, universal function, rather we embraced an open-minded approach freeing ourselves from the confinement of identifying such an overarching transform.

In **Chapter 2**, we capitalized on what seemed to be a disadvantage in fMRI studies of cerebellar function: Cerebellar BOLD signal reflecting the incoming input from the neocortex. This rationalized modelling cerebellar activity as a function of cortical activity. We utilized a rich task battery to develop a **task-invariant** model that was able to generalize to unseen tasks. In the radical sense, the underlying intent of our efforts in this chapter was to render the field of cerebellar functional imaging obsolete: If our model had generalized perfectly to other tasks, there would be no need to image the cerebellum; Instead, the model could predict cerebellar activity based on the neocortical activity (King et al., 2023).

Despite the success of the model, there remained unexplained variances in the cerebellar data. It is reasonable to suggest that parts of the unexplained variances can be attributed to methodological limitations inherent in the model, and that further improvement would allow us to generate a task-invariant connectivity model that would predict the

activity in the cerebellum perfectly (up to the measurement uncertainty). In **Chapter 3**, however, we considered a more interesting, and functionally more relevant source for unexplained variance: the idea of **selective recruitment**, namely the task-dependent up- or down-regulation of the cortical input to the cerebellum. We posited that instances of up-regulations in input activity would serve as evidence that the cerebellum is especially important (relative to the neocortex) for the task in question.

To evaluate the effectiveness of our approach, we tested it within the motor domain. Drawing upon existing knowledge from patient studies, where specific cerebellar processes have been identified *a priori*, we manipulated the force and speed of alternating finger presses. In line with the symptoms observed in patients, we found that the cerebellum is selectively recruited for increasing speed but not force which effectively demonstrates the ability of our novel approach to discern cerebellar-specific processes.

Having validated our approach in motor domain, In **chapter 4** we utilized it to study the role of the cerebellum in the working memory domain. Using a digit span task that manipulated memory load and recall direction, we tested for selective recruitment of the cerebellar multi-demand network. We found that the cerebellar input was up-regulated when subjects were encoding 6 items in their memory. Contrary to results of patient studies, we found no significant differentiation of cerebellar involvement in backward recall.

The series of projects in this thesis collectively seek to tackle the methodological and interpretational challenges associated with fMRI studies of the cerebellum. We first utilized the cerebellar BOLD signal to create a model of cortico-cerebellar connectivity. With this model, not only we can estimate the input activity directed towards the cerebellum but also identify the neocortical regions that contribute to the input activity in a specific cerebellar region of interest. This provides us with a full picture of the cortico-cerebellar networks involved in motor behavior and cognition. This detailed understanding allows us to assess the relative dependence of a particular process on the cerebellum. We demonstrated the application of this analytical framework to the cognitive domain of working memory, revealing

the distinct role of the cerebellum in encoding items in memory.

5.1 A critique of the UCT approach in studies of cerebellar function

The Universal Cerebellar Transform (UCT) idea has been a pillar in the field of cerebellar research, inspiring numerous conceptual and computational interpretations of cerebellar function. The core of this idea is that, because the cerebellar micro-circuit is homogeneous across the entire cerebellar cortex, the structure plays a similar computational role in cognitive domains, such as working memory or language, as it does in the coordination of movement. In the subsequent sections, I will first explore the most prominent of these interpretations, review research outcomes, and lay out my critique concerning their limitations in delivering a comprehensive understanding of cerebellar function, with special consideration of the two tasks examined in this thesis. I will primarily concentrate on the concept of "internal models", which stands as the most widely accepted idea.

Mental calibration and dysmetria of thought

It is now well established that the deficits observed following cerebellar damage are not limited to motor domain. Indeed, individuals with cerebellar damage often exhibit deficits in executive, linguistic, and emotional tasks. Schmahmann (2004) proposed that the cerebellum fine-tunes cognitive processes in a similar manner to its role in motor control: it maintains behavior around a homeostatic balance, seamlessly and without conscious awareness. Its impaired function leads to disrupting this balance which in turn manifests itself as Cerebellar Cognitive Affective Syndrome (CCAS). This balancing mechanism inevitably requires error correction, a process repeatedly shown to involve the cerebellum.

In the finger tapping task, we only looked at correct trials to estimate cerebellar activations and yet we observed up-regulation of cerebellar input for speed. In the digit span task, we could not directly observe errors during the encoding phase. The most immediate proxy we have to errors during the encoding phase is retrieval error; these are errors that happen when retrieving items from memory. Even if we assume any error observed during retrieval is indicative of an encoding error, this idea predicts cerebellar engagement during both encoding and retrieval. In other words, we would expect to observe specially heightened activation not just during encoding, but also retrieval. On the contrary, we only found selective recruitment at load 6 during the encoding phase. Thus, for both tasks, it is uncertain if the cerebellum's involvement relates to correction mechanisms.

The Cerebellum as a chronometer

An alternative idea of a unified cerebellar function is that of a **"timing machine"**. Ivry (1997) proposed that the cerebellum is instrumental in both motor and perceptual tasks necessitating precise temporal representation. Instead of functioning as a single clock, Ivry and others have proposed that the cerebellum operates more like a vast set of interval timers, which assist in accurately coordinating complex temporal patterns essential for smooth and synchronized movements and cognitive processes (Mangels et al., 1998; Diedrichsen et al., 2003; Koch et al., 2009). The cerebellum is invoked whenever a task requires its timing function, but the exact neural components activated by it can vary based on the task's specifics.

In line with the "timing machine" hypothesis, the cerebellum has been suggested to aid in determining musical temporal patterns (Lebrun-Guillaud et al., 2008), with variations in its gray matter volume affecting an individual's ability to detect rhythm changes (Paquette et al., 2017). Additionally, experiments featuring finger-tapping tasks have revealed deficits in patients with cerebellar damage and activations in imaging studies of the cerebellum (see (Repp, 2005) for an overview). However, in other tasks, the necessity for precise timing

is less explicit. In our finger-tapping task, for instance, swift alternating finger movements necessitate accurate muscle coordination, but as no specific rhythm is imposed, it is unclear whether there is a need to estimate and apply timing intervals. Similarly, in the digit span task, no explicit timing requirement is enforced. Furthermore, it remains unclear how timing operations contribute to working memory processes.

Cerebellum as an internal model

Wolpert et al. (1998) suggests that the cerebellum can be regarded as an integral part of a feedback control system. This is illustrated in Figure 5.1 a) which outlines the fundamental elements of a general controlling system, namely: a controller (CT), an object under control (CO), a sensory system (SS), and an instructor (P) overseeing the controller. Feedback loops back to the controller via the SS, which consequently updated the command. The concept of an **internal model** emerges as a vital constituent of this feedback control system, serving to represent the external environment and facilitating both motor and cognitive functions (Ito, 2008; Wolpert et al., 1998). Essentially, the cerebellum, acting as an internal model, steps in to regulate the system in the presence of delayed sensory feedback, preventing the system from going into an unstable state.

The term "internal model" broadly encompasses two distinct types that outline how the cerebellum predicts and modulates behavior. In its role as a *forward model*, the cerebellum supports the controller - be it the motor cortex or prefrontal cortex - by utilizing an *efference copy*, a replica of the command issued by the controller. With this copy, the cerebellum can forecast the outcomes of a given command and relay it to the instructor, prompting an update of the instructing signal (Figure 5.1 b). Conversely, as an *inverse model*, the cerebellum deciphers the instructing signal, computes the requisite command to produce the intended outcome, and feeds this back to the controller (Figure 5.1 c). In either scenario, the overarching objective is to compensate for the inherent delay in the sensory system, ensuring fluid movements (or cognitive processes) in the presence of such delays.

In parallel, the cerebellum, functioning as an internal model, embodies two key concepts - prediction and error correction. A key operating principle of the cerebellum is making internal predictions about the state of the world, hence operating as a *prediction machine* (Hull, 2020; Wolpert et al., 1998; Ito, 1970, 1972). It can predict the results of commands (be it motor or cognitive). Subsequently, it compares the actual outcome of the command with its predictions (error). *Error correction* involves signaling errors via climbing fibers originating from the inferior olive. Feedback from the cerebellar cortex to the inferior olive, in turn, aims to minimize this error and achieve the desired outcome (Popa and Ebner, 2018).

One example of the error-corrective/predictive behavior of the cerebellum is during reaching movements with perturbations. You are reaching towards an object, while suddenly a force perpendicular to the trajectory of the hand is applied. In this case, an error signal is created. This error is compensated for by a corrective motion in the opposite direction of the applied force. It has been shown that in cerebellar degeneration patients these corrective behavior is reduced (Tseng et al., 2007), supposedly because the cerebellum does not make sensory predictions.

In the cognitive domain, the predictive ability of the cerebellum is often studied in an experiment by presenting words in a sentence and masking the last word. After a delay, the final word is presented. It sometimes violates the expectations of the participant and renders the full sentence meaningless. In particular, it has been shown that the cerebellar involvement in such tasks extends beyond the motor aspects of language. Rather, cerebellum is part of an internal model that aids in rendering a full meaningful sentence based on the initial context provided(D'Mello et al., 2017; Moberget and Ivry, 2016).

However, extending this behaviour to other tasks remains contentious. Is corrective action always necessary for tasks that involve the cerebellum? One could posit that the cerebellum steps in to refine behaviour towards perfect performance when feedback indicates an error. Yet, in our digit span task, the participants are not immediately aware of

the correct digit or that they have made an error during encoding; They will only become aware of error during retrieval when they have pressed the digit and observe the color-coded feedback (green for right, red for wrong). Therefore, it is not clear whether there is need for corrective behaviour during encoding of digits.

As for the cerebellar role in prediction, in the finger tapping task, the sensory predictions provided by the cerebellum enable the subject to tap with high speed by coordinating muscle contractions in a manner similar to the reaching task (Thach et al., 1992; Tseng et al., 2007; Izawa et al., 2012; Tsay et al., 2022). In the digit span task, however, we found selective recruitment for load 6 during encoding. It is not clear whether there is any predictive function needed during encoding of digits. How does prediction help with the processes during encoding and why specifically load 6? All in all, our results for the digit span task does not provide evidence supporting these hypothesized roles for the cerebellum.

If the cerebellum indeed applies a uniform transform across all tasks, identifying such a transform applicable across different domains is not straightforward. The core problem is to use one of the proposed theories for the UCT to make testable predictions for cognitive task conditions the cerebellum may and may not be involved in. Is it valid to attribute cerebellar activation seen in prediction or error correction tasks to these processes? Previous studies often show a confirmation bias, testing for prediction-related activity and indeed finding it in the cerebellum. These studies, however, usually do not consider alternative factors that also may cause cerebellar activation in the task.

The most significant question lies in distinguishing the predictions made by the cerebellum from those of the neocortex. This is particularly relevant because there is a growing preposition that the brain, as a whole, constantly predicts and updates its understanding of the surrounding world based on incoming sensory information (Friston and Kiebel, 2009; Keller and Mrsic-Flogel, 2018). Hence, limiting ourselves to searching for a single transform may not yield insightful results, as generating testable hypotheses

about a single function across different domains that can be distinguished from neocortical contributions is often challenging, and sometimes even untestable.

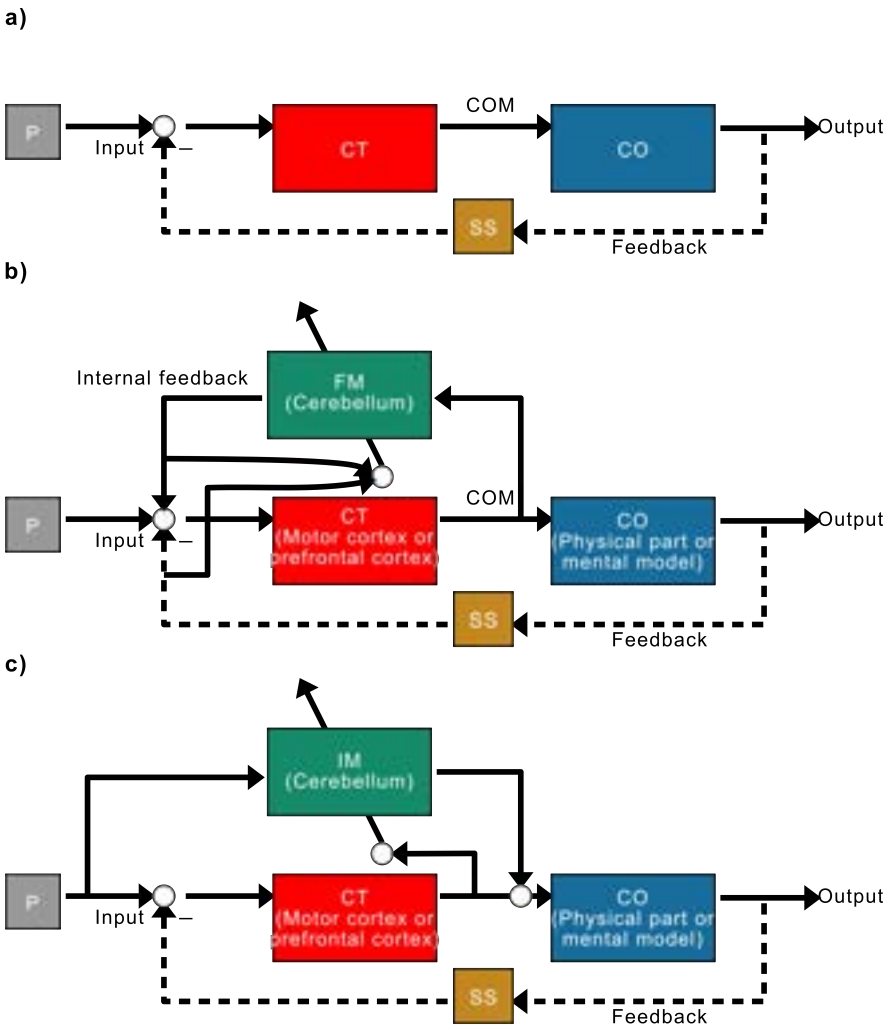

Figure 5.1: **Schematic of internal models**. Figure shows schematic diagrams of control systems. **a)** Shows a general control system that stabilizes based on feedback. **b)** Shows a control system that features a forward model. A copy of the controlling command goes to the cerebellum based on which it generates a prediction of the output. The prediction is then compared with the actual outcome (error). Consequently, the controlling command is refined so that the error is minimized. **c)** Shows a control system with the cerebellum as an inverse model. In this scenario, cerebellum generates a command to achieve the desired output. This command is then refined to make the actual outcome as close to the desired outcome as possible. Controller (CT), Controlled Object (CO), Sensory System (SS), Instructor (P), controlling command (COM), Forward Model (FM), Inverse Model (IM).

Figure adopted from Ito (2008)

5.1.1 Selective Recruitment: Unraveling the concept beyond the title

The cornerstone of this thesis is the concept of **selective recruitment**. In this section, we will first overview the main steps in the analysis, acknowledging one limitation, and explaining how we can still deduce specific cerebellar functions in spite of this limitation. Subsequently, we will deepen our exploration of selective recruitment by imagining an ideal scenario. This will help clarify statements such as "the cerebellum is selectively recruited in task A" and prevent potential mis/over-interpretations of the results.

Central to the idea of selective recruitment is the connectivity model, which aims to identify the neocortical regions supplying input to a particular cerebellar region. The model we developed is a heavily regularized regression model with regularization parameter of e^8 (For a detailed discussion on the importance of considering this model, see *The power of convergent mapping*). An outcome of this regularization is shrunken weights. As a consequence, the model predictions, which provide the comparison baseline to infer selective recruitment, end up on a scale roughly one-tenth the magnitude of the observed activation. This will render direct comparison impossible, since observed activations will consistently outweigh the predicted values.

To address this limitation, we utilize a linear regression. The residuals from this regression serve as a lens to discern selective recruitment. A residual near zero for a specific condition or task suggests that the observed activation mirrors a scaled prediction of the anticipated activation, signifying a linearly scaled input. Conversely, a substantial deviation from zero in the residual indicates a nuanced relationship. For such conditions, it denotes cerebellar-specific processing, suggesting the incoming input from the neocortex undergoes non-linear gating when distinct processing is necessitated.

To elucidate the notion of selective recruitment, envision an idealized scenario. Picture a flawless connectivity model detailing each cerebellar region's precise inputs from its corresponding neocortical areas; Imagine this model is free from the scaling issues previously highlighted. With this in place, comprehending questions like *which conditions engage these two structures equally? Which conditions are more relying on the cerebellum and which are more relying on the neocortex?* becomes more straightforward.

Conceptually, the interplay between the cerebellum and the neocortex is divided into two distinct zones, separated by a linear function. This linear function inherently signifies a condition's balanced reliance on both the cerebellum and the neocortex. Conditions situated above this function, and closer to the cerebellar axis, predominantly depend on the cerebellum. In other words, in these conditions, the cerebellum is more actively, or "selectively," recruited (refer to Figure 5.2). However, it is crucial to understand that the absence of cerebellar selective recruitment does not render the cerebellum inactive or irrelevant for the task. Given the comparative nature of this approach, it simply means the cerebellum is either engaged equivalently or to a lesser extent compared to the neocortex.

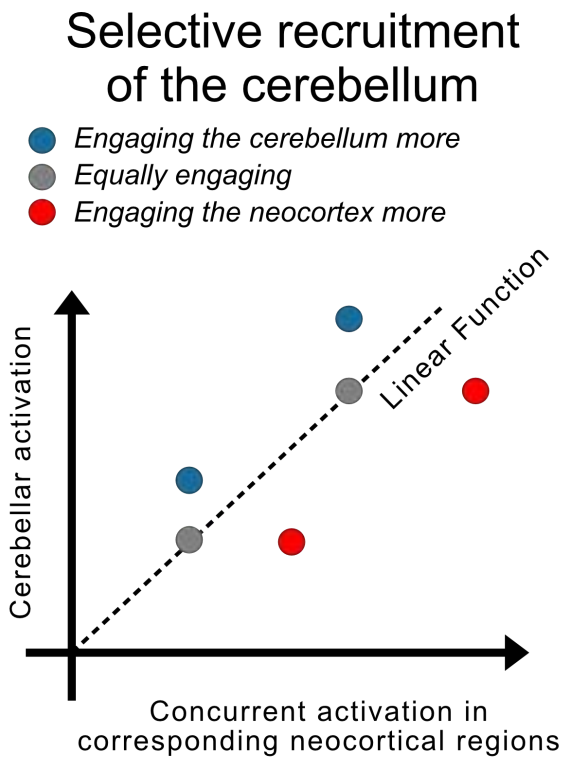

Figure 5.2: **Conceptualizing an ideal scenario in selective recruitment analysis**. In an optimal scenario, cerebellar activity can be contextualized against its corresponding neocortical activity. This interaction between the cerebellum and neocortex is categorized into three distinct zones: 1)The linear zone, suggesting an equal dependence on both the cerebellum and the neocortex. 2) The zone proximate to the cerebellar axis, indicating a specific reliance on the cerebellum, and 3) The zone near the neocortical axis, signifying a greater dependence on the neocortex. It is the processes that fall into the second zone, close to the cerebellar axis, that we describe as 'selectively recruiting' the cerebellum.

5.2 Selective Recruitment: strengths and limitations

This thesis presents a novel framework to study cerebellar function with fMRI. Rather than interpreting any BOLD activation in the cerebellum as a sign of its engagement in the task, we look for task-specific gating of input from the respective neocortical regions. In other words, we target specific cortico-cerebellar networks and look for specific cerebellar

contributions over and above the neocortex. This approach lays the groundwork for a more nuanced understanding of cerebellar functions. Naturally, like any method, it comes with its strengths and limitations. In the sections to follow, we will evaluate these in light of the two tasks we explored.

The power of convergent mapping

In Chapter 2, we introduced a connectivity model that emphasizes the value of recognizing varying degrees of input convergence across the cerebellum. Traditional models, which are grounded in a strict one-to-one topography (Buckner et al., 2011; Marek et al., 2018), can still allow for the inference of cerebellar selective recruitment. However, their representation of cerebellar inputs may not always be accurate. Take the motor network identified by Yeo et al. (2011) for instance. It captures the peak activation in the finger tapping task located in M1. When aligned with our connectivity model from Chapter 2, a significant overlap emerges between this network and regions having strong connectivity weights associated with the cerebellar ROI for the task (Figure 5.3 a). Yet, for the digit span task, high activations occur in neocortical regions outside the borders of Yeo et al. (2011)'s fronto-parietal network. This distinction is further reflected in the average connectivity weights from our model (Figure 5.3 b). Such findings emphasize that for certain tasks, a straightforward one-to-one mapping might overlook the full breadth of concurrent neocortical activation. This underscores the necessity of accounting for input convergence, especially when tasks engage the cognitive cerebellum.

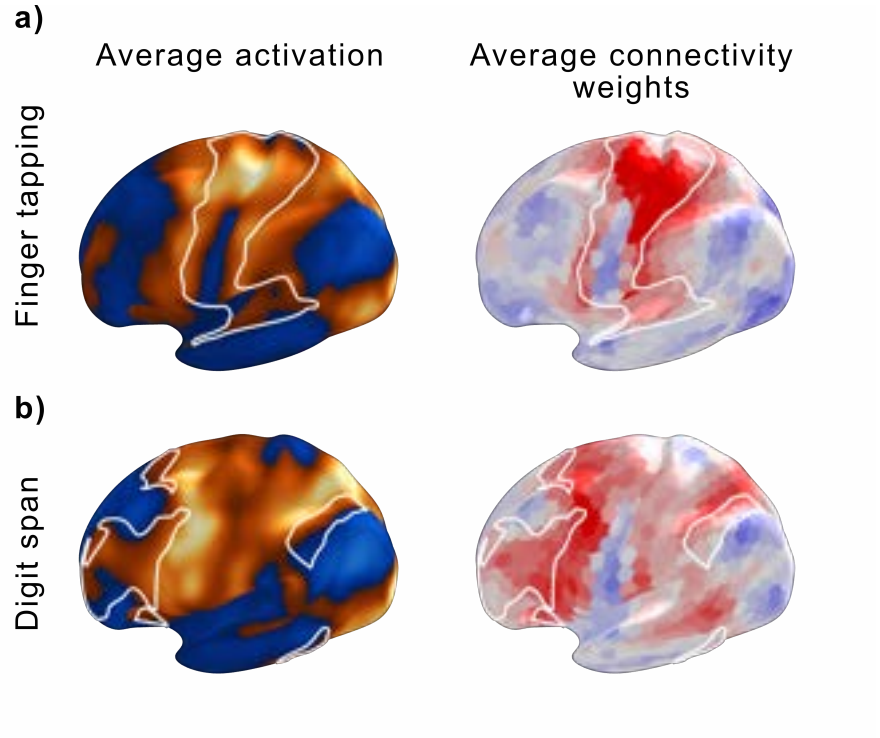

Figure 5.3: **Yeo parcellation on top of activation and connectivity weight map**. Given the tasks used, we selected the most relevant networks from Yeo parcellation (Yeo et al., 2011). **a)**Motor network for the finger tapping task and **b)**the fronto-parietal network for the digit span task are plotted in white solid outline on top of the average group activations and average connectivity weights for the selected cerebellar region in each task. As the figure shows, for the finger tapping task, the region with highest activation falls inside Yeo's motor network, although there are regions outside of this network that show high activations as well. This can be seen in the average group weights for the right hand area used for analysis of the finger tapping task. For the digit span task, however, most areas demonstrating high activations fall outside of the Yeo's network (Same for the average group connectivity weight.)

The Value of a Group-Based Task-Invariant Connectivity Model

We employed the multi-domain task battery (King et al., 2019) to create a **task-invariant** connectivity model as our comparison baseline for inferring selective recruitment. The primary rationale behind this choice was the battery included a wide range of tasks which

offers comprehensive coverage of both the cerebellum and neocortex. Nevertheless, it incorporated subjects distinct from those in our study. An alternative would have been to develop our comparison baseline, the connectivity model, using the task we were examining. For instance, when analyzing task-dependent gating in the finger tapping task, we could use data from participants performing that specific task to determine the connectivity weights. So, why did we opt against use of individual connectivity model, and what benefits could our chosen strategy of using a group-based model offer?

One advantage of this method is that it allows for the estimation of connectivity models on a per-subject basis. accounting for the considerable variability in the functional regions and their connections across individuals. However, a counterpoint to this advantage emerges when considering that both finger tapping and digit span tasks were specifically designed to target particular cortico-cerebellar networks, rendering the resulting models less likely to be task-invariant. In simpler terms, models constructed on the basis of a specific task may fail to effectively generalize to other tasks.

Figure 5.5 a illustrates a test case in which we employed ridge regression to estimate connectivity weights using two different datasets: WMFS (our tasks) and MDTB (multi-domain task battery). To assess the generalizability of these connectivity models to other datasets, we evaluated their performance on two fMRI task datasets: one focusing on the multi-demand network (Assem et al., 2022) and another aiming to reveal somatotopic motor maps within the cerebellum (Saadon-Grosman et al., 2022). The results show that the model trained on WMFS exhibits significantly lower predictive accuracy compared to the model trained on the MDTB dataset, for both the multi-demand and somatotopic datasets. In simpler terms, the model trained on WMFS uses a *narrow* task set, i.e. a task set that only targets specific cerebellar and neocortical regions, and hence fails to generalize effectively to other tasks. Consequently, it does not serve as a reliable task-invariant connectivity model, thus undermining the intended purpose of using the connectivity model.

Different strategies to refine the connectivity model

A quest for broader generalizability In the selective recruitment approach, we target variations in task activations unexplained by a task-invariant connectivity model. These unexplained variations can stem from various sources. Notably, the task-invariant model's limited adaptability to new tasks stands out. Although rich, the MDTB dataset used for developing the connectivity model might not aptly generalize to novel tasks. Thus, the incorporation of additional data might further enhance the model, providing a more precise baseline for comparison. One avenue for this enhancement involves crafting a framework to determine connectivity weights by integrating multiple task-based datasets.

One such framework can be to derive a group connectivity model for each dataset separately and subsequently unify these models by averaging their connectivity weights. A more complicated approach involves a Bayesian framework. This approach allows the fusion of connectivity models from various datasets, considering the uncertainty inherent in each connectivity weight. Such fusion is probabilistic: every weight from each dataset influences the final, amalgamated weight depending on its reliability. This Bayesian method's strength lies in its ability to weave in our prior knowledge. Interestingly, within this structure, datasets that don't entirely cover the cerebellum and neocortex can still be integrated. For regions marked by unreliable activity, the weights deduced will bear lower certainty. While these will have reduced influence during integration, they still play a part in shaping the eventual connectivity model.

Individual vs group connectivity model In inferring selective recruitment, our initial strategy was grounded in the formulation of a null hypothesis based on **group connectivity weights** rather than individual ones (see **The Value of a Group-Based Task-Invariant Connectivity Model**). Indeed, estimating an individual connectivity model in our study was limited by our use of *narrow* task sets, each tailored to engage a specific network exclusively: Motor network in th finger tapping task and Multi-demand network in the digit

span task. One solution to this limitation could be the introduction of a *connectivity localizer* which would entail participants performing a *wide task battery* similar to the one in MDTB. The primary goal of this data collection would pivot towards training, testing, and validation of individualized connectivity models to have a more accurate comparison baseline for inferring task-dependent selective recruitment (Figure 5.4).

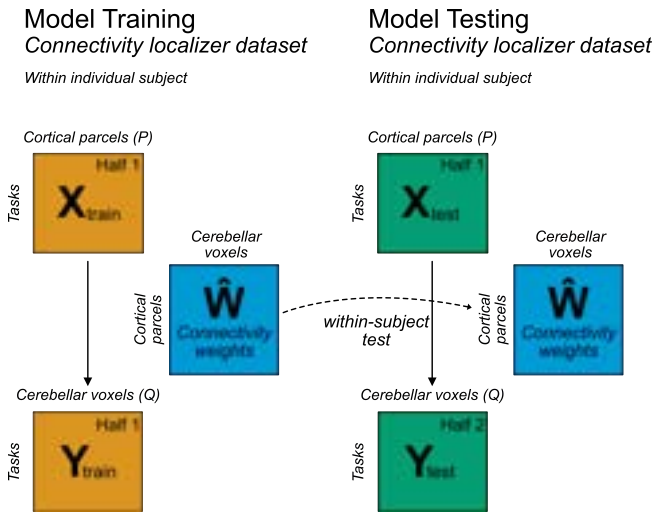

Figure 5.4: **Schematic of the alternative approach**. **a)** Each participant will perform a battery of tasks (similar to MDTB). This will serve as training and testing dataset to estimate the connectivity weights within each individual. With these connectivity weights tailored for each individual subject, we will be accounting for the individual differences when testing for selective recruitment.

As a preliminary test of this approach, we took advantage of the MDTB dataset wherein each participant performed two sets of tasks: set A and set B (King et al., 2019) to compare individual based models with group models. Within each individual, we used task set A as the *connectivity localizer* and evaluated the estimated model on task set B within the same subject. To get the group connectivity model, we adapted a leave-one-out approach: left one subject out and estimated the group connectivity weights by averaging over the weights of all the other subjects from task set A. This model was then evaluated on task set B of the left out subject. Figure 5.5 b shows the predictive accuracy of the individual

and group models estimated with this approach. Comparing the predictive accuracy of these two types of models revealed that the individual connectivity performs slightly better (Paired t-test, $t_2 3 = 2.22, p = 0.037$). Therefore, although a minor improvement, using the individual data is informative. To take advantage of both group and individual data, we can adopt a Bayesian framework approach similar to Zhi et al. (2023).

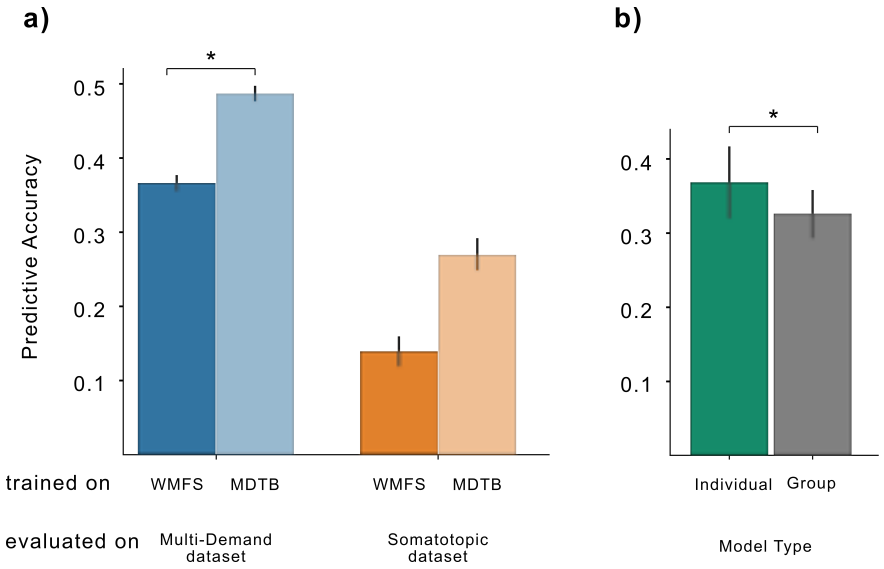

Figure 5.5: **Predictive accuracy of connectivity models**. **a)**We tested for the generalizability of two different models to new data. One model was trained on the MDTB dataset (King et al., 2019) and one was trained on WMFS (Shahshahani et al., *In prep*). To test for generalizability, the predictive accuracy of each model was calculated as the correlation between observed and predicted activity profiles in two new datasets: Multi-demand (Assem et al., 2022) and Somatotopic (Saadon-Grosman et al., 2022). The predictive accuracy of the model trained on MDTB is significantly higher than the model trained on WMFS for both testing datasets. **b)**Comparison of predictive accuracy between models trained on an individual and tested on the same individual or group connectivity models tested within individuals

5.3 Future directions in studies of cerebellar function

We have presented a model of cortico-cerebellar connectivity that could be utilized to study the interactions between the cerebral cortex and the cerebellum. We showed the utility of this connectivity model in studying cerebellar function through the lens of selective recruitment hypothesis. Our objective was to change the prevailing perspective on how cerebellar fMRI data should be interpreted.

While we have come a long way, our journey into understanding cerebellar functions is far from over. The tools we introduced in this thesis pave the way for future research into cerebellar function. Following this, I will elaborate on prospective research ideas that naturally extend from the work in this thesis.

5.3.1 Extension of selective recruitment to other tasks

Here, our exploration was limited to two tasks, neither of which wholly represent their respective domains. The finger-tapping task merely probed cerebellar engagement in alternating finger movements, leaving a range of other motor functions that potentially rely on cerebellar operations unexplored. Take motor planning for instance. Does the cerebellum have a role that goes beyond what the neocortex contributes in motor planning ? At what point during the planning of a movement does the cerebellum's role become significant? Is there a greater demand for cerebellar computations during real-time planning?

In the domain of working memory, we may extend our investigation to other processes potentially influenced by the cerebellum. For instance, does the cerebellum play a greater role in maintaining information in memory during periods when sensory-related information is absent, or is its engagement more pronounced when manipulating maintained information is necessary? In addition, deficits in cerebellar patients is limited to verbal

working memory tasks, with patients performance in spatial working memory comparable to healthy participants (Ravizza et al., 2006). Since verbal working memory is closely tied to the language domain, one important question is whether the cerebellar contribution to working memory is only through its involvement in language related processes.

To probe these questions, we can employ an array of tasks designed for different aspects of working memory such as n-back and sternberg, simple word reading, among others. The aim, in general, is to furnish a comprehensive collection of tasks that form a robust basis for examining the comparative engagement of the cerebellum across distinct processes. For instance, by comparing a condition that requires memorizing verbal information with a condition that requires simple word reading, we can distinguish between memory related and language related processes. More importantly, through use of the connectivity model we can put these activations in the context of neocortical activity and investigate whether for any of these conditions cerebellum is needed over and above the neocortex. The same design principles can be extended to the design of experiments aimed at studying cerebellar function in other domains such as motor planning and social cognition. Eventually, with careful design of experiments, we will have a fuller picture of cerebellar function.

5.3.2 Closing the circuit: incorporating other subcortical structures

Cerebellum forms known connections with other brain structures. Here, we only focused on a network with two components: the neocortex and the cerebellar cortex. But in fact, studies of cerebellar function as a part of a larger network will be incomplete unless we bring other components of the network into the picture. Notably, these include **Pontine nuclei** downstream from the neocortex, **Deep cerebellar nuclei** (DCN), particularly **Dentate nucleus**, and **Thalamus** upstream, going back to the neocortex, and **Inferior olive** which sends climbing fibers to influence activity of **Purkinje cells**. Additionally, cerebellum establishes direct connections (bypassing the neocortex) with the **Basal ganglia** (Bostan

and Strick, 2018). Imaging of these subcortical structures presents significant challenges, which might account for the less extensive study of these regions compared to the neocortex.

The first necessary step, therefore, is to determine whether we can acquire reliable signal in these structures using fMRI. While the Basal ganglia and Thalamus have been studied using fMRI, the Pontine, DCN, and Inferior olive have received less attention perhaps due to their anatomical location in the **Brainstem**. To address this, we have piloted a study using high-resolution 7 Tesla MRI. An ongoing challenge in this study, however, is to denoise the fMRI signal.

Particularly, denoising of signals from brainstem and cerebellar structures presents substantial challenges. Firstly, these structures, due to their small sizes compared to other brain structures, are challenging to distinguish, even with a 7 Tesla MRI. Secondly, their proximity to the neck renders signals from these regions more susceptible to motion artifacts triggered by swallowing, heartbeats, and minor head movements during scanning. Thirdly, these areas are located near the skull base, where the transition between bone, air, and brain tissue can result in magnetic field inhomogeneities, leading to signal loss or distortion in MRI images. Furthermore, their close proximity to air-filled cavities, such as the ear canals and sinuses, increases their sensitivity to magnetic susceptibility artifacts (Brooks et al., 2013; Beissner, 2015; van der Zwaag et al., 2015). Therefore, we have taken extensive measures to mitigate these effects by collecting respiratory and heart rate signals and meticulous noise removal practices.

Consider Pontine nuclei as an example and assume that we get reliable fMRI signal in these structures and we can detect information processing in these nuclei at the temporal resolutions available in fMRI. One plausible explanation for the nonlinear gating hypothesis is nonlinear gating occurring within Pontine nuclei. However, we can only substantiate such a claim if we acquire a more nuanced understanding of the functional divisions within these structures. This in itself, is an indication that Pontine nuclei are not simple relay stations and task-specific information processing is indeed happening in these structures. This

knowledge would also enable the formation of descriptive models that include the neocortex, Pontine nuclei, and cerebellar cortex. For instance, one such model could incorporate a nonlinear term that represents the potential complex computations within the Pontine nuclei. Therefore, knowledge of functional role of the Pontine nuclei is essential in studies of cerebellar function.

Furthermore, although we lack direct access to Purkinje cell activity through fMRI, if we can establish that the BOLD signal in the Dentate nucleus is neurally meaningful, we can access the immediate target of these cells. By having access to both the input and output of the cerebellar cortex, we can better model the transformations applied by the cerebellum in different domains which in turn enriches our knowledge of cerebellar function.

5.4 Conclusion

Overall, we regressed from the common approach in studies of cerebellar function. With a cortico-cerebellar connectivity model, we now have access to the neocortex-derived input, and can incorporate it in our evaluations. Our new approach allows us to study cerebellar function in many different cognitive domains, identifying the exact conditions that may require cerebellar processing in each domain. Instead of assuming a priori that these process can be easily summarized as a single universal transform, we believe it is essential to first do the careful empirical work of describing them, whether we can ultimately identify such a transform, or whether the cerebellar circuit fulfills inherently different functions in different domains, is an empirical question that we hopefully will be able to solve then.

Investigating different domains with our approach is like assembling bits and pieces of the puzzle of cerebellar function. It will bring us closer to a more comprehensive and nuanced understanding of cerebellar function. Only then we inch closer to determining whether a unitary transform indeed exists.

Bibliography

Alahmadi, A. A. S., Pardini, M., Samson, R. S., D'Angelo, E., Friston, K. J., Toosy, A. T., and Gandini Wheeler-Kingshott, C. A. M. (2015). Differential involvement of cortical and cerebellar areas using dominant and nondominant hands: An FMRI study. *Hum. Brain Mapp.*, 36(12):5079–5100.

Alahmadi, A. A. S., Samson, R. S., Gasston, D., Pardini, M., Friston, K. J., D'Angelo, E., Toosy, A. T., and Wheeler-Kingshott, C. A. M. (2016). Complex motor task associated with non-linear BOLD responses in cerebro-cortical areas and cerebellum. *Brain Struct. Funct.*, 221(5):2443–2458.

Albus, J. S. (1971). A theory of cerebellar function. *Math. Biosci.*, 10(1):25–61.

Allen, G., Buxton, R. B., Wong, E. C., and Courchesne, E. (1997). Attentional activation of the cerebellum independent of motor involvement. *Science*, 275(5308):1940–1943.

Arslan, S., Parisot, S., and Rueckert, D. (2015). Joint spectral decomposition for the parcellation of the human cerebral cortex using Resting-State fMRI. In *Information Processing in Medical Imaging*, pages 85–97. Springer International Publishing.

Ashburner, J. (2007). A fast diffeomorphic image registration algorithm. *Neuroimage*, 38(1):95–113.

Assem, M., Glasser, M. F., Van Essen, D. C., and Duncan, J. (2020). A Domain-General cognitive core defined in multimodally parcellated human cortex. *Cereb. Cortex*, 30(8):4361–4380.

Assem, M., Shashidhara, S., Glasser, M. F., and Duncan, J. (2022). Basis of executive functions in fine-grained architecture of cortical and subcortical human brain networks.

Attwell, D. and Iadecola, C. (2002). The neural basis of functional brain imaging signals. *Trends Neurosci.*, 25(12):621–625.

Azevedo, F. A. C., Carvalho, L. R. B., Grinberg, L. T., Farfel, J. M., Ferretti, R. E. L., Leite, R. E. P., Jacob Filho, W., Lent, R., and Herculano-Houzel, S. (2009). Equal numbers of neuronal and nonneuronal cells make the human brain an isometrically scaled-up primate brain. *J. Comp. Neurol.*, 513(5):532–541.

Balsters, J. H., Cussans, E., Diedrichsen, J., Phillips, K. A., Preuss, T. M., Rilling, J. K., and Ramnani, N. (2010). Evolution of the cerebellar cortex: the selective expansion of prefrontal-projecting cerebellar lobules. *Neuroimage*, 49(3):2045–2052.

Balsters, J. H., Whelan, C. D., Robertson, I. H., and Ramnani, N. (2013). Cerebellum and cognition: evidence for the encoding of higher order rules. *Cereb. Cortex*, 23(6):1433–1443.

Barton, R. A. and Venditti, C. (2014). Rapid evolution of the cerebellum in humans and other great apes. *Curr. Biol.*, 24(20):2440–2444.

Beissner, F. (2015). Functional MRI of the brainstem: Common problems and their solutions. *Clin. Neuroradiol.*, 25 Suppl 2:251–257.

Bell, C. C., Han, V., and Sawtell, N. B. (2008). Cerebellum-like structures and their implications for cerebellar function. *Annu. Rev. Neurosci.*, 31:1–24.

Bertolero, M. A., Yeo, B. T. T., and D'Esposito, M. (2015). The modular and integrative functional architecture of the human brain. *Proc. Natl. Acad. Sci. U. S. A.*, 112(49):E6798–807.

Bischoff-Grethe, A., Ivry, R. B., and Grafton, S. T. (2002). Cerebellar involvement in response reassignment rather than attention. *J. Neurosci.*, 22(2):546–553.

Bodranghien, F., Bastian, A., Casali, C., Hallett, M., Louis, E. D., Manto, M., Mariën, P., Nowak, D. A., Schmahmann, J. D., Serrao, M., Steiner, K. M., Strupp, M., Tilikete, C., Timmann, D., and van Dun, K. (2016). Consensus paper: Revisiting the symptoms and signs of cerebellar syndrome. *Cerebellum*, 15(3):369–391.

Bolceková, E., Mojzeš, M., Van Tran, Q., Kukal, J., Ostrý, S., Kulišťák, P., and Rusina, R. (2017). Cognitive impairment in cerebellar lesions: a logit model based on neuropsychological testing. *Cerebellum Ataxias*, 4:13.

Bostan, A. C. and Strick, P. L. (2018). The basal ganglia and the cerebellum: nodes in an integrated network. *Nat. Rev. Neurosci.*, 19(6):338–350.

Braitenberg, V. and Atwood, R. P. (1958). Morphological observations on the cerebellar cortex. *J. Comp. Neurol.*, 109(1):1–33.

Brandauer, B., Hermsdörfer, J., Geissendörfer, T., Schoch, B., Gizewski, E. R., and Timmann, D. (2012). Impaired and preserved aspects of independent finger control in patients with cerebellar damage. *J. Neurophysiol.*, 107(4):1080–1093.

Brodal, P. (1971). The corticopontine projection in the cat. II. the projection from the orbital gyrus. *J. Comp. Neurol.*, 142(2):141–151.

Brodal, P. (1978). The corticopontine projection in the rhesus monkey. origin and principles of organization. *Brain*, 101(2):251–283.

Brooks, J. C. W., Faull, O. K., Pattinson, K. T. S., and Jenkinson, M. (2013). Physiological noise in brainstem FMRI. *Front. Hum. Neurosci.*, 7:623.

Buckner, R. L. (2013). The cerebellum and cognitive function: 25 years of insight from anatomy and neuroimaging. *Neuron*, 80(3):807–815.

Buckner, R. L., Krienen, F. M., Castellanos, A., Diaz, J. C., and Yeo, B. T. T. (2011). The organization of the human cerebellum estimated by intrinsic functional connectivity. *J. Neurophysiol.*, 106(5):2322–2345.

Chen, S. H. A. and Desmond, J. E. (2005). Cerebrocerebellar networks during articulatory rehearsal and verbal working memory tasks. *Neuroimage*, 24(2):332–338.

Cole, M. W., Ito, T., Bassett, D. S., and Schultz, D. H. (2016). Activity flow over resting-state networks shapes cognitive task activations. *Nat. Neurosci.*, 19(12):1718–1726.

Cole, M. W., Ito, T., Cocuzza, C., and Sanchez-Romero, R. (2021). The functional relevance of Task-State functional connectivity. *J. Neurosci.*, 41(12):2684–2702.

D'Angelo, E. (2018). Physiology of the cerebellum. *Handb. Clin. Neurol.*, 154:85–108.

De Zeeuw, C. I., Lisberger, S. G., and Raymond, J. L. (2021). Diversity and dynamism in the cerebellum. *Nat. Neurosci.*, 24(2):160–167.

Desmond, J. E. and Fiez, J. A. (1998). Neuroimaging studies of the cerebellum: language, learning and memory. *Trends Cogn. Sci.*, 2(9):355–362.

Desmond, J. E., Gabrieli, J. D. E., Wagner, A. D., Ginier, B. L., and Glover, G. H. (1997). Lobular patterns of cerebellar activation in verbal Working-Memory and Finger-Tapping tasks as revealed by functional MRI. *J. Neurosci.*, 17(24):9675–9685.

Diedrichsen, J. (2006). A spatially unbiased atlas template of the human cerebellum. *Neuroimage*, 33(1):127–138.

Diedrichsen, J., Ivry, R. B., and Pressing, J. (2003). Cerebellar and basal ganglia contributions to interval timing. In Meck, W. H., editor, *Functional and neural mechanisms of interval timing , (pp*, volume 551, pages 457–483. CRC Press/Routledge/Taylor & Francis Group, xli, Boca Raton, FL, US.

Diedrichsen, J., King, M., Hernandez-Castillo, C., Sereno, M., and Ivry, R. B. (2019). Universal transform or multiple functionality? understanding the contribution of the human cerebellum across task domains. *Neuron*, 102(5):918–928.

Diedrichsen, J. and Zotow, E. (2015). Surface-Based display of Volume-Averaged cerebellar imaging data. *PLoS One*, 10(7):e0133402.

D'Mello, A. M., Gabrieli, J. D. E., and Nee, D. E. (2020). Evidence for hierarchical cognitive control in the human cerebellum. *Curr. Biol.*, 30(10):1881–1892.e3.

D'Mello, A. M., Turkeltaub, P. E., and Stoodley, C. J. (2017). Cerebellar tDCS modulates neural circuits during semantic prediction: A combined tDCS-fMRI study. *J. Neurosci.*, 37(6):1604–1613.

Dum, R. P. and Strick, P. L. (2003). An unfolded map of the cerebellar dentate nucleus and its projections to the cerebral cortex. *J. Neurophysiol.*, 89(1):634–639.

Fan, L., Li, H., Zhuo, J., Zhang, Y., Wang, J., Chen, L., Yang, Z., Chu, C., Xie, S., Laird, A. R., Fox, P. T., Eickhoff, S. B., Yu, C., and Jiang, T. (2016). The human brainnetome atlas: A new brain atlas based on connectional architecture. *Cereb. Cortex*, 26(8):3508–3526.

Fiez, J. A. (2016). The cerebellum and language: Persistent themes and findings. *Brain Lang.*, 161:1–3.

Fischl, B. (2012). FreeSurfer. *Neuroimage*, 62(2):774–781.

Fischl, B., Rajendran, N., Busa, E., Augustinack, J., Hinds, O., Yeo, B. T. T., Mohlberg, H., Amunts, K., and Zilles, K. (2008). Cortical folding patterns and predicting cytoarchitecture. *Cereb. Cortex*, 18(8):1973–1980.

Fonov, V., Evans, A. C., Botteron, K., Almli, C. R., McKinstry, R. C., Collins, D. L., and Brain Development Cooperative Group (2011). Unbiased average age-appropriate atlases for pediatric studies. *Neuroimage*, 54(1):313–327.

Friston, K. and Kiebel, S. (2009). Predictive coding under the free-energy principle. *Philos. Trans. R. Soc. Lond. B Biol. Sci.*, 364(1521):1211–1221.

Friston, K. J., Holmes, A. P., Worsley, K. J., Poline, J.-P., Frith, C. D., and Frackowiak, R. S. J. (1994). Statistical parametric maps in functional imaging: A general linear approach. *Hum. Brain Mapp.*, 2(4):189–210.

Gagliano, G., Monteverdi, A., Casali, S., Laforenza, U., and others (2022). Non-Linear frequency dependence of neurovascular coupling in the cerebellar cortex implies Vasodilation–Vasoconstriction competition. *Cells*.

Gatti, D., Vecchi, T., and Mazzoni, G. (2021). Cerebellum and semantic memory: A TMS study using the DRM paradigm. *Cortex*, 135:78–91.

Glasser, M. F., Coalson, T. S., Robinson, E. C., Hacker, C. D., Harwell, J., Yacoub, E., Ugurbil, K., Andersson, J., Beckmann, C. F., Jenkinson, M., Smith, S. M., and Van Essen, D. C. (2016). A multi-modal parcellation of human cerebral cortex. *Nature*, 536(7615):171–178.

Gordon, E. M., Laumann, T. O., Adeyemo, B., Huckins, J. F., Kelley, W. M., and Petersen, S. E. (2016). Generation and evaluation of a cortical area parcellation from Resting-State correlations. *Cereb. Cortex*, 26(1):288–303.

Guell, X., Schmahmann, J. D., Gabrieli, J. D. E., and Ghosh, S. S. (2018). Functional gradients of the cerebellum. *Elife*, 7:e36652.

Hallett, M., Berardelli, A., Matheson, J., Rothwell, J., and Marsden, C. D. (1991). Physiological analysis of simple rapid movements in patients with cerebellar deficits. *J. Neurol. Neurosurg. Psychiatry*, 54(2):124–133.

Henschke, J. U. and Pakan, J. M. P. (2020). Disynaptic cerebrocerebellar pathways originating from multiple functionally distinct cortical areas. *Elife*, 9:e59148.

Herculano-Houzel, S. (2009). The human brain in numbers: a linearly scaled-up primate brain. *Front. Hum. Neurosci.*, 3:31.

Hokkanen, L. S. K., Kauranen, V., Roine, R. O., Salonen, O., and Kotila, M. (2006). Subtle cognitive deficits after cerebellar infarcts. *Eur. J. Neurol.*, 13(2):161–170.

Holmes, G. (1939). THE CEREBELLUM OF MAN1. *Brain*, 62(1):1–30.

Howarth, C., Peppiatt-Wildman, C. M., and Attwell, D. (2010). The energy use associated with neural computation in the cerebellum. *J. Cereb. Blood Flow Metab.*, 30(2):403–414.

Huang, C.-C., Sugino, K., Shima, Y., Guo, C., Bai, S., Mensh, B. D., Nelson, S. B., and Hantman, A. W. (2013). Convergence of pontine and proprioceptive streams onto multimodal cerebellar granule cells. *Elife*, 2:e00400.

Hull, C. (2020). Prediction signals in the cerebellum: beyond supervised motor learning. *Elife*, 9.

Ito, M. (1970). Neurophysiological aspects of the cerebellar motor control system. *Int. J. Neurol.*, 7(2):162–176.

Ito, M. (1972). Neural design of the cerebellar motor control system. *Brain Res.*, 40(1):81–84.

Ito, M. (1989). Long-term depression. *Annu. Rev. Neurosci.*, 12:85–102.

Ito, M. (1993). Movement and thought: identical control mechanisms by the cerebellum. *Trends Neurosci.*, 16(11):448–450.

Ito, M. (2008). Control of mental activities by internal models in the cerebellum. *Nat. Rev. Neurosci.*, 9(4):304–313.

Ivry, R. (1997). Cerebellar timing systems. *Int. Rev. Neurobiol.*, 41:555–573.

Ivry, R. B. and Keele, S. W. (1989). Timing functions of the cerebellum. *J. Cogn. Neurosci.*, 1(2):136–152.

Izawa, J., Criscimagna-Hemminger, S. E., and Shadmehr, R. (2012). Cerebellar contributions to reach adaptation and learning sensory consequences of action. *J. Neurosci.*, 32(12):4230–4239.

Jäncke, L., Specht, K., Mirzazade, S., and Peters, M. (1999). The effect of finger-movement speed of the dominant and the subdominant hand on cerebellar activation: A functional magnetic resonance imaging study. *Neuroimage*, 9(5):497–507.

Ji, J. L., Spronk, M., Kulkarni, K., Repovš, G., Anticevic, A., and Cole, M. W. (2019). Mapping the human brain's cortical-subcortical functional network organization. *Neuroimage*, 185:35–57.

Keller, G. B. and Mrsic-Flogel, T. D. (2018). Predictive processing: A canonical cortical computation. *Neuron*, 100(2):424–435.

Kelly, R. M. and Strick, P. L. (2003). Cerebellar loops with motor cortex and prefrontal cortex of a nonhuman primate. *J. Neurosci.*, 23(23):8432–8444.

Kelly, R. M. and Strick, P. L. (2004). Macro-architecture of basal ganglia loops with the cerebral cortex: use of rabies virus to reveal multisynaptic circuits. *Prog. Brain Res.*, 143:449–459.

King, M., Hernandez-Castillo, C. R., Poldrack, R. A., Ivry, R. B., and Diedrichsen, J. (2019). Functional boundaries in the human cerebellum revealed by a multi-domain task battery. *Nat. Neurosci.*, 22(8):1371–1378.

King, M., Shahshahani, L., Ivry, R. B., and Diedrichsen, J. (2023). A task-general connectivity model reveals variation in convergence of cortical inputs to functional regions of the cerebellum. *Elife*, 12:e81511.

Kirschen, M. P., Davis-Ratner, M. S., Milner, M. W., Chen, S. H. A., Schraedley-Desmond, P., Fisher, P. G., and Desmond, J. E. (2008). Verbal memory impairments in children after cerebellar tumor resection. *Behav. Neurol.*, 20(1-2):39–53.

Koch, G., Oliveri, M., and Caltagirone, C. (2009). Neural networks engaged in milliseconds and seconds time processing: evidence from transcranial magnetic stimulation and

patients with cortical or subcortical dysfunction. *Philos. Trans. R. Soc. Lond. B Biol. Sci.*, 364(1525):1907–1918.

Kochiyama, T., Ogihara, N., Tanabe, H. C., Kondo, O., Amano, H., Hasegawa, K., Suzuki, H., Ponce de León, M. S., Zollikofer, C. P. E., Bastir, M., Stringer, C., Sadato, N., and Akazawa, T. (2018). Reconstructing the neanderthal brain using computational anatomy. *Sci. Rep.*, 8(1):1–9.

Krienen, F. M. and Buckner, R. L. (2009). Segregated fronto-cerebellar circuits revealed by intrinsic functional connectivity. *Cereb. Cortex*, 19(10):2485–2497.

Lebrun-Guillaud, G., Tillmann, B., and Justus, T. (2008). Perception of tonal and temporal structures in chord sequences by patients with cerebellar damage. *Music Percept.*, 25(4):271–283.

Leggio, M. G., Silveri, M. C., Petrosini, L., and Molinari, M. (2000). Phonological grouping is specifically affected in cerebellar patients: a verbal fluency study. *J. Neurol. Neurosurg. Psychiatry*, 69(1):102–106.

Leiner, H. C., Leiner, A. L., and Dow, R. S. (1986). Does the cerebellum contribute to mental skills? *Behav. Neurosci.*, 100(4):443–454.

Leiner, H. C., Leiner, A. L., and Dow, R. S. (1991). The human cerebro-cerebellar system: its computing, cognitive, and language skills. *Behav. Brain Res.*, 44(2):113–128.

Logothetis, N. K. (2003). The underpinnings of the BOLD functional magnetic resonance imaging signal. *J. Neurosci.*, 23(10):3963–3971.

Maex, R. and Schutter, E. D. (1998). Synchronization of golgi and granule cell firing in a detailed network model of the cerebellar granule cell layer. *J. Neurophysiol.*, 80(5):2521–2537.

Mai, N., Bolsinger, P., Avarello, M., Diener, H. C., and Dichgans, J. (1988). Control of isometric finger force in patients with cerebellar disease. *Brain*, 111 (Pt 5):973–998.

Mangels, J. A., Ivry, R. B., and Shimizu, N. (1998). Dissociable contributions of the prefrontal and neocerebellar cortex to time perception. *Cognitive Brain Research*, 7(1):15–39.

Mapelli, L., Gagliano, G., Soda, T., Laforenza, U., Moccia, F., and D'Angelo, E. U. (2017). Granular layer neurons control cerebellar neurovascular coupling through an NMDA Receptor/NO-Dependent system. *J. Neurosci.*, 37(5):1340–1351.

Marek, S., Siegel, J. S., Gordon, E. M., Raut, R. V., Gratton, C., Newbold, D. J., Ortega, M., Laumann, T. O., Adeyemo, B., Miller, D. B., Zheng, A., Lopez, K. C., Berg, J. J., Coalson, R. S., Nguyen, A. L., Dierker, D., Van, A. N., Hoyt, C. R., McDermott, K. B., Norris, S. A., Shimony, J. S., Snyder, A. Z., Nelson, S. M., Barch, D. M., Schlaggar, B. L., Raichle, M. E., Petersen, S. E., Greene, D. J., and Dosenbach, N. U. F. (2018). Spatial and temporal organization of the individual human cerebellum. *Neuron*, 100(4):977–993.e7.

Mariën, P. and Borgatti, R. (2018). Language and the cerebellum. *Handb. Clin. Neurol.*, 154:181–202.

Marr, D. (1969). A theory of cerebellar cortex. *J. Physiol.*, 202(2):437–470.

Marvel, C. L. and Desmond, J. E. (2010). Functional topography of the cerebellum in verbal working memory. *Neuropsychol. Rev.*, 20(3):271–279.

Mathiesen, C., Caesar, K., and Lauritzen, M. (2000). Temporal coupling between neuronal activity and blood flow in rat cerebellar cortex as indicated by field potential analysis. *J. Physiol.*, 523 Pt 1:235–246.

Mell, M. M., St-Yves, G., and Naselaris, T. (2021). Voxel-to-voxel predictive models reveal unexpected structure in unexplained variance. *Neuroimage*, 238:118266.

Miall, R. C., Weir, D. J., Wolpert, D. M., and Stein, J. F. (1993). Is the cerebellum a smith predictor? *J. Mot. Behav.*, 25(3):203–216.

Moberget, T. and Ivry, R. B. (2016). Cerebellar contributions to motor control and language comprehension: searching for common computational principles. *Ann. N. Y. Acad. Sci.*, 1369(1):154–171.

Murdoch, B. E. (2010). The cerebellum and language: historical perspective and review. *Cortex*, 46(7):858–868.

Ogawa, S., Lee, T. M., Kay, A. R., and Tank, D. W. (1990). Brain magnetic resonance imaging with contrast dependent on blood oxygenation. *Proc. Natl. Acad. Sci. U. S. A.*, 87(24):9868–9872.

O'Reilly, J. X., Beckmann, C. F., Tomassini, V., Ramnani, N., and Johansen-Berg, H. (2010). Distinct and overlapping functional zones in the cerebellum defined by resting state functional connectivity. *Cereb. Cortex*, 20(4):953–965.

Owen, A. M., McMillan, K. M., Laird, A. R., and Bullmore, E. (2005). N-back working memory paradigm: a meta-analysis of normative functional neuroimaging studies. *Hum. Brain Mapp.*, 25(1):46–59.

Paquette, S., Fujii, S., Li, H. C., and Schlaug, G. (2017). The cerebellum's contribution to beat interval discrimination. *Neuroimage*, 163:177–182.

Park, J., Phillips, J. W., Guo, J.-Z., Martin, K. A., Hantman, A. W., and Dudman, J. T. (2022). Motor cortical output for skilled forelimb movement is selectively distributed across projection neuron classes. *Science Advances*, 8(10):eabj5167.

Peterburs, J., Bellebaum, C., Koch, B., Schwarz, M., and Daum, I. (2010). Working memory and verbal fluency deficits following cerebellar lesions: relation to interindividual differences in patient variables. *Cerebellum*, 9(3):375–383.

Petersen, S. E., Fox, P. T., Posner, M. I., Mintun, M., and Raichle, M. E. (1989). Positron emission tomographic studies of the processing of singe words. *J. Cogn. Neurosci.*, 1(2):153–170.

Pisano, T. J., Dhanerawala, Z. M., Kislin, M., Bakshinskaya, D., Engel, E. A., Hansen, E. J., Hoag, A. T., Lee, J., de Oude, N. L., Venkataraju, K. U., Verpeut, J. L., Hoebeek, F. E., Richardson, B. D., Boele, H.-J., and Wang, S. S.-H. (2021). Homologous organization of cerebellar pathways to sensory, motor, and associative forebrain. *Cell Rep.*, 36(12):109721.

Pleger, B. and Timmann, D. (2018). The role of the human cerebellum in linguistic prediction, word generation and verbal working memory: evidence from brain imaging, non-invasive cerebellar stimulation and lesion studies. *Neuropsychologia*, 115:204–210.

Popa, L. S. and Ebner, T. J. (2018). Cerebellum, predictions and errors. *Front. Cell. Neurosci.*, 12:524.

Ravizza, S. M., McCormick, C. A., Schlerf, J. E., Justus, T., Ivry, R. B., and Fiez, J. A. (2006). Cerebellar damage produces selective deficits in verbal working memory. *Brain*, 129(Pt 2):306–320.

Repp, B. H. (2005). Sensorimotor synchronization: A review of the tapping literature. *Psychon. Bull. Rev.*, 12(6):969–992.

Saadon-Grosman, N., Angeli, P. A., DiNicola, L. M., and Buckner, R. L. (2022). A third somatomotor representation in the human cerebellum. *J. Neurophysiol.*, 128(4):1051–1073.

Schaefer, A., Kong, R., Gordon, E. M., Laumann, T. O., Zuo, X.-N., Holmes, A. J., Eickhoff, S. B., and Yeo, B. T. T. (2017). Local-Global parcellation of the human cerebral cortex from intrinsic functional connectivity MRI. *Cereb. Cortex*, 28(9):3095–3114.

Schmahmann, J. D. (2004). Disorders of the cerebellum: Ataxia, dysmetria of thought, and the cerebellar cognitive affective syndrome. *J. Nurse Pract.*, 16(3):367–378.

Schwarz, C., Möck, M., and Thier, P. (1997). Electrophysiological properties of rat pontine

nuclei neurons in vitro. i. membrane potentials and firing patterns. *J. Neurophysiol.*, 78(6):3323–3337.

Schwarz, C. and Thier, P. (1999). Binding of signals relevant for action: towards a hypothesis of the functional role of the pontine nuclei. *Trends Neurosci.*, 22(10):443–451.

Sereno, M. I., Diedrichsen, J., Tachrount, M., Testa-Silva, G., d'Arceuil, H., and Zeeuw, C. D. (2020). The human cerebellum has almost 80% of the surface area of the neocortex. *Proceedings of the National Academy of Sciences*, 117(32):19538–19543.

Shahshahani, L., King, M., Nettekoven, C., Ivry, R., and Diedrichsen, J. (2023). Selective recruitment: Evidence for task-dependent gating of inputs to the cerebellum.

Shen, X., Tokoglu, F., Papademetris, X., and Constable, R. T. (2013). Groupwise whole-brain parcellation from resting-state fMRI data for network node identification. *Neuroimage*, 82:403–415.

Snyder, S. H. (1992). Nitric oxide: first in a new class of neurotransmitters. *Science*, 257(5069):494–496.

Southam, E., Morris, R., and Garthwaite, J. (1992). Sources and targets of nitric oxide in rat cerebellum. *Neurosci. Lett.*, 137(2):241–244.

Spraker, M. B., Corcos, D. M., Kurani, A. S., Prodoehl, J., Swinnen, S. P., and Vaillancourt, D. E. (2012). Specific cerebellar regions are related to force amplitude and rate of force development. *Neuroimage*, 59(2):1647–1656.

Starowicz-Filip, A., Prochwicz, K., Kłosowska, J., Chrobak, A. A., Myszka, A., Bętkowska-Korpała, B., and Kwinta, B. (2021). Cerebellar functional lateralization from the perspective of clinical neuropsychology. *Front. Psychol.*, 12:775308.

Stoodley, C. J. (2012). The cerebellum and cognition: Evidence from functional imaging studies. *Cerebellum*, 11(2):352–365.

Stoodley, C. J., Valera, E. M., and Schmahmann, J. D. (2012). Functional topography of the cerebellum for motor and cognitive tasks: an fMRI study. *Neuroimage*, 59(2):1560–1570.

Strick, P. L., Dum, R. P., and Fiez, J. A. (2009). Cerebellum and nonmotor function. *Annu. Rev. Neurosci.*, 32:413–434.

Tavor, I., Parker Jones, O., Mars, R. B., Smith, S. M., Behrens, T. E., and Jbabdi, S. (2016). Task-free MRI predicts individual differences in brain activity during task performance. *Science*, 352(6282):216–220.

Thach, W. T., Goodkin, H. P., and Keating, J. G. (1992). The cerebellum and the adaptive coordination of movement. *Annu. Rev. Neurosci.*, 15:403–442.

Thalmann, M., Souza, A. S., and Oberauer, K. (2019). How does chunking help working memory? *J. Exp. Psychol. Learn. Mem. Cogn.*, 45(1):37–55.

Thomsen, K., Offenhauser, N., and Lauritzen, M. (2004). Principal neuron spiking: neither necessary nor sufficient for cerebral blood flow in rat cerebellum. *J. Physiol.*, 560(Pt 1):181–189.

Thomsen, K., Piilgaard, H., Gjedde, A., Bonvento, G., and Lauritzen, M. (2009). Principal cell spiking, postsynaptic excitation, and oxygen consumption in the rat cerebellar cortex. *J. Neurophysiol.*, 102(3):1503–1512.

Thürling, M., Hautzel, H., Küper, M., Stefanescu, M. R., Maderwald, S., Ladd, M. E., and Timmann, D. (2012). Involvement of the cerebellar cortex and nuclei in verbal and visuospatial working memory: a 7 T fMRI study. *Neuroimage*, 62(3):1537–1550.

Tibshirani, R. (1996). Regression shrinkage and selection via the lasso. *J. R. Stat. Soc. Series B Stat. Methodol.*, 58(1):267–288.

Tsay, J. S., Schuck, L., and Ivry, R. B. (2022). Cerebellar degeneration impairs strategy discovery but not strategy recall. *Cerebellum*.

Tseng, Y.-W., Diedrichsen, J., Krakauer, J. W., Shadmehr, R., and Bastian, A. J. (2007). Sensory prediction errors drive Cerebellum-Dependent adaptation of reaching. *J. Neurophysiol.*, 98(1):54–62.

van der Zwaag, W., Jorge, J., Butticaz, D., and Gruetter, R. (2015). Physiological noise in human cerebellar fMRI. *MAGMA*, 28(5):485–492.

Van Essen, D. C. (2002). Surface-based atlases of cerebellar cortex in the human, macaque, and mouse. *Ann. N. Y. Acad. Sci.*, 978:468–479.

Van Essen, D. C., Glasser, M. F., Dierker, D. L., Harwell, J., and Coalson, T. (2011). Parcellations and hemispheric asymmetries of human cerebral cortex analyzed on Surface-Based atlases. *Cereb. Cortex*, 22(10):2241–2262.

Van Overwalle, F., D'aes, T., and Mariën, P. (2015). Social cognition and the cerebellum: A meta-analytic connectivity analysis. *Hum. Brain Mapp.*, 36(12):5137–5154.

Vanlandewijck, M., He, L., Mäe, M. A., Andrae, J., Ando, K., Del Gaudio, F., Nahar, K., Lebouvier, T., Laviña, B., Gouveia, L., Sun, Y., Raschperger, E., Räsänen, M., Zarb, Y., Mochizuki, N., Keller, A., Lendahl, U., and Betsholtz, C. (2018). A molecular atlas of cell types and zonation in the brain vasculature. *Nature*, 554(7693):475–480.

Wolpert, D. M., Miall, R. C., and Kawato, M. (1998). Internal models in the cerebellum. *Trends Cogn. Sci.*, 2(9):338–347.

Yeo, B. T. T., Krienen, F. M., Chee, M. W. L., and Buckner, R. L. (2014). Estimates of segregation and overlap of functional connectivity networks in the human cerebral cortex. *Neuroimage*, 88:212–227.

Yeo, B. T. T., Krienen, F. M., Eickhoff, S. B., Yaakub, S. N., Fox, P. T., Buckner, R. L., Asplund, C. L., and Chee, M. W. L. (2015). Functional specialization and flexibility in human association cortex. *Cereb. Cortex*, 25(10):3654–3672.

Yeo, B. T. T., Krienen, F. M., Sepulcre, J., Sabuncu, M. R., Lashkari, D., Hollinshead, M., Roffman, J. L., Smoller, J. W., Zöllei, L., Polimeni, J. R., Fischl, B., Liu, H., and Buckner, R. L. (2011). The organization of the human cerebral cortex estimated by intrinsic functional connectivity. *J. Neurophysiol.*, 106(3):1125–1165.

Yousry, T. A., Schmid, U. D., Alkadhi, H., Schmidt, D., Peraud, A., Buettner, A., and Winkler, P. (1997). Localization of the motor hand area to a knob on the precentral gyrus. a new landmark. *Brain*, 120 (Pt 1):141–157.

Zhi, D., King, M., Hernandez-Castillo, C. R., and Diedrichsen, J. (2022). Evaluating brain parcellations using the distance-controlled boundary coefficient. *Hum. Brain Mapp.*

Zhi, D., Shahshahani, L., Nettekoven, C., Pinho, A. L., Bzdok, D., and Diedrichsen, J. (2023). A hierarchical bayesian brain parcellation framework for fusion of functional imaging datasets.